

PERKINS+WILL

Research Journal



2015 / VOL 07.02



www.perkinswill.com

SPECIAL ISSUE: FUTURE OF ARCHITECTURAL RESEARCH

ARCHITECTURAL RESEARCH CENTERS CONSORTIUM 2015 CONFERENCE

Editors: Ajla Aksamija, Ph.D., LEED AP BD+C, CDT and Kalpana Kuttaiah, Associate AIA, LEED AP BD+C

Journal Design & Layout: Kalpana Kuttaiah, Associate AIA, LEED AP BD+C

Acknowledgements: *We would like to extend our **APPRECIATION** to everyone who contributed to the research work and articles published within this journal.*

*We would like to extend our **VERY SPECIAL THANKS** to: Emily Gartland.*

Perkins+Will is an interdisciplinary design practice offering services in the areas of Architecture, Interior Design, Branded Environments, Planning + Strategies and Urban Design.

Copyright 2015 Perkins+Will

All rights reserved.

PERKINS+WILL

Research Journal

+ 2015 / VOL 07.02

JOURNAL OVERVIEW

The Perkins+Will Research Journal documents research relating to the architectural and design practice. Architectural design requires immense amounts of information for inspiration, creation, and construction of buildings. Considerations for sustainability, innovation, and high-performance designs lead the way of our practice where research is an integral part of the process. The themes included in this journal illustrate types of projects and inquiries undertaken at Perkins+Will and capture research questions, methodologies, and results of these inquiries.

The Perkins+Will Research Journal is a peer-reviewed research journal dedicated to documenting and presenting practice-related research associated with buildings and their environments. The unique aspect of this journal is that it conveys practice-oriented research aimed at supporting our teams.

This is the fourteenth issue of the Perkins+Will Research Journal. We welcome contributions for future issues.

RESEARCH AT PERKINS+WILL

Research is systematic investigation into existing knowledge in order to discover or revise facts or add to knowledge about a certain topic. In architectural design, we take an existing condition and improve upon it with our design solutions. During the design process we constantly gather and evaluate information from different sources and apply it to solve our design problems, thus creating new information and knowledge.

An important part of the research process is documentation and communication. We are sharing combined efforts and findings of Perkins+Will researchers and project teams within this journal.

Perkins+Will engages in the following areas of research:

- Market-sector related research
- Sustainable design
- Strategies for operational efficiency
- Advanced building technology and performance
- Design process benchmarking
- Carbon and energy analysis
- Organizational behavior

TABLE OF CONTENTS

JOURNAL OVERVIEW	Page 2
EDITORIAL	Page 4
01. DESIGNED FOR PERFORMANCE:		
Research Methods in a Collaborative Studio		
Rethinking Modern Curtain Walls		
Michael Gibson, Assoc. AIA, LEED AP	Page 7
02. OPTIMIZING SPATIAL ADJACENCIES USING		
EVOLUTIONARY PARAMETRIC TOOLS:		
Using Grasshopper and Galapagos to Analyze, Visualize,		
and Improve Complex Architectural Programming		
Christopher Boon		
Corey Griffin, Assoc. AIA		
Nicholas Papaefthimiou, AIA, LEED AP BD+C		
Jonah Ross		
Kip Storey	Page 25
03. URBAN MODELING WITH AGENT-BASED SYSTEM:		
Ming Tang, AIA, NCARB, LEED AP	Page 38
04. URBAN MICROCLIMATES AND ENERGY EFFICIENT BUILDINGS:		
Pravin Bhiwapurkar, PhD	Page 45
05. APPLES TO ORANGES:		
Comparing Building Materials Data		
Liane Hancock	Page 58
PEER REVIEWERS	Page 73
AUTHORS	Page 74

EDITORIAL

Special Issue: Future of Architectural Research

This special issue of Perkins+Will Research Journal is dedicated to the Architectural Research Centers Consortium (ARCC) 2015 Conference, with the theme “Future of Architectural Research”. The conference was organized by Dr. Ajla Aksamija (Perkins+Will/University of Massachusetts Amherst), Dr. John Haymaker (Perkins+Will), and Dr. Abbas Aminmansour (University of Illinois at Urbana-Champaign). It was held in Chicago, April 6-9, 2015. This was the first time that design practice and academic institutions were collaborating and organizing a conference dedicated to architectural research. The intention was to bring together researchers, design practitioners, faculty members, policy makers, educators, and students to discuss the latest achievements in architectural research and to bridge the gap between academic and practice-led research efforts.

Technological advancements, environmental considerations and concerns, complexity and requirements of today's design practices as well as challenging economic factors are some of the impending motives for bridging the gap between practice-led and academic research. Today, research is more important than ever and is becoming an integral component in the design practices. The conference addressed these aspects and intended to help define the future direction of architectural research.

Conference topics included:

- **Advanced Materials and Building Technologies:** new materials, their performance and applications in architectural design, experimental studies, building technologies, and implementations in current design projects.
- **Environmental, Energy, and Building Performance Factors:** environmental and energy aspects in buildings and cities, high-performance buildings.
- **Computational Design:** use of computational tools and approaches for design, BIM, parametric modeling, simulations and modeling, use of virtual reality for design.
- **Social and Behavioral Research:** buildings' use and operation, post-occupancy evaluations, and occupant satisfaction.
- **Building Types and Design Methods:** specific building types and their design methods.
- **Research in Practice:** new modes of research specifically suited for design practices, appropriate methods, and implementation of results.
- **Research and Education in Academia:** new modes of research in academic settings, integration of educational curricula, and research.

This conference included more than 120 papers and presentations from researchers and design practitioners. Research papers relating to extremely low-energy and net-zero energy buildings, building-scale and community resiliency, new materials and building technologies, advanced computational design methods, prototyping, and fabrication presented some of the emerging issues in architectural and design technologies. Social and behavioral research papers, which discuss occupants' psychological and physiological well-being as well as research modes and methods, identified important considerations and factors that influence the operational side of the built environment. [The proceedings book was published](#), which captured results of various research studies and projects presented at the conference.



This issue of the journal includes several selected articles that focus on diverse topics, such as collaboration between practice and an academic institution in researching curtain walls, data-driven urban modeling, development of a database for comparison of building materials data, use of parametric tools for architectural programming, and the effects of urban microclimates on buildings' energy consumption.

The intention of the conference was to increase visibility of current architectural research, practice-led and from the academy, and begin to form collaborative alliances that will result in wider implementation of research results, improved design practices and outcomes, increased funding opportunities for architectural research, and significant impacts on the society and built environment. The conference was successful in terms of bringing together practitioners, researchers, and faculty members, where new models of architectural research were discussed as well as potential modes of collaboration. Several future steps were identified as key aspects that need to be addressed: 1) formation of a consortium representing design practices that conduct architectural research and improved collaboration with academic institutions; 2) development of guidelines for best practices and research methods suitable for design professionals; 3) development of training and educational material for practitioners interested in architectural research; and 4) collaboration with academic institutions in forming new academic programs for practice-based research.

Ajla Aksamija, PhD, LEED AP BD+C, CDT
Kalpana Kuttaiah, Associate AIA, LEED AP BD+C

01.

DESIGNED FOR PERFORMANCE:

Research Methods in a Collaborative Studio Rethinking Modern Curtain Walls

Michael Gibson, Kansas State University, Assoc. AIA, LEED AP,

mdgibson@ksu.edu

ABSTRACT

The growing demand for high-performance buildings has pushed the architectural discipline to confront building performance as an integral part of design delivery, while increasing the necessity of collaboration between designers, building science experts, engineers, and manufacturers to find the best solutions to building performance challenges. At Kansas State University, a year-long research studio worked with professionals, consultants, and a major manufacturer of window systems to rethink modern curtain wall systems. Three experimental systems developed during the studio are summarized in this article along with data and observations showing their relative successes and shortcomings versus a contemporary high-performing curtain wall system. This article elaborates on methods employed in the studio including computer-based analysis and in-situ testing of full scale prototypes with emphasis on determining and comparing apparent thermal resistance calculated from observations. Lastly, some discussion is presented regarding how these methods and techniques could contribute to practice.

KEYWORDS: envelopes, performance, simulation, testing, prototyping

1.0 INTRODUCTION

Designing high-performance buildings requires architects to engage building science and manufacturing in a more direct way than in the recent past, where a handful of material properties were enough to inform decisions. Today, architects are poised to work with consultants, engineers, and manufacturers to improve solutions to building performance challenges. Coincidentally, architects are uniquely positioned to innovate in this area because the profession bridges between the technical aspects of building and the performance objectives driving projects. In the area of building skins, the intersection of technology and multivalent performance is particularly acute: skins have to resist heat flow, control moisture, shade the interior, provide views, resist wear and decay, and contribute to the identity of the building. Decisions with respect to the building skin are complex, often revealing gaps in the knowledge of how these building systems behave. Architects can do more than just identify these gaps – it is possible to use a foundation of building science knowledge, rigorous

research methods, and a collaborative approach to innovate in these areas.

This article summarizes work from a year-long architectural studio in the Department of Architecture at Kansas State University that engaged a team of practitioners from BNIM and PGAV (Kansas City architecture firms), outside engineers and specialist consultants, and a regional curtain wall manufacturer in a research and design project during the 2014-15 academic year. Students worked in teams in the fall of 2014 to develop experimental curtain wall systems intended to advance the thermal performance of today's best contemporary glass curtain wall systems, questioning material, environmental integration, and manufacturing implications of the systems they developed. In the studio, students were also introduced to a research approach based on building science concepts, experimental methods, simulation and analysis tools, and prototyping. The studio's work culminated with the live testing of their experimental systems, which they constructed at 1:1

scale and deployed in an instrumented test enclosure. In the spring of 2015, the students continued the work of the studio by designing a library branch: a realistic project where they further developed their experimental systems in detail (not discussed in this article). The collaborating architects, consultants, and manufacturer representatives provided feedback during both semesters. A more detailed discussion of the studio's work was previously published¹. This article examines the testing and analysis methods behind the work in greater detail, while restating and expanding earlier interpretations of how the three systems presented performed.

2.0 CURTAIN WALLS: PERFORMANCE CHALLENGES AND POTENTIAL SOLUTIONS

The performance associations of glass and aluminum curtain walls is certainly mixed today. Critics pan highly glazed buildings purported as “green” by their owners and designers, referring to the expectedly poor thermal performance of glass walls versus opaque construction depended on insulation products to reduce thermal transmission. The performance reality of large glass walls in green buildings is quickly changing, however. The best-performing glass systems achieving rated U-Values approaching 0.125 BTU/hr-ft²-°F, a level of thermal resistance on par with an insulated 2"x4" stud wall. Another widely misunderstood reality of curtain walls today is determining which components comprise the weak areas in the assembly. Decades ago, when thermally-broken metal framing became popular, the glass units were more challenging thermally. Yet glazing technologies (triple pane, argon-fill, low-E coated) can produce an insulated glass unit with a thermal resistance that can be many times greater than that of the frames. Curtain wall manufactures have thus invested heavily in producing the best insulated glass units possible. Yet the frames in curtain walls have remained unchanged for decades, descending nearly directly from profiles engineered in the mid-20th century and opened to free use when the intellectual property rights ceased in the 1980s. As a result, the frames remain as an important area for improving these systems.

Some of the biggest energy challenges with glass and aluminum curtain wall systems involve thermal performance. Thermal breaks reduce conduction, using new materials, such as polyamide that preserve the structural stability of the frames, but conduct heat much less

readily than aluminum. Gasketing and sealing further prevent conduction as well as provide the airtightness to reduce infiltration and exfiltration. Lastly, the system's real-life performance can be compromised by poor detailing and installation methods, which are usually not represented in a particular system's thermal ratings². Other energy challenges involve the production of high-quality glass and the demand for anodized coatings, which require high-quality “virgin” (unrecycled) aluminum.

2.1 Performance Advantages of Modern Curtain Walls

The advantages of these systems, however, are numerous. First, the systems are affordable, with a kit-of-parts erection process and clear expectations for performance (thermal and otherwise) when comparing to layered walls, such as veneer masonry that relies on complex, difficult-to-control, and difficult-to-inspect layers involving insulation, narrow air cavities, hangers, ties, and flashing. Secondly, curtain wall systems can also be very airtight in comparison to traditional fenestration systems where the layered envelope can be a challenge to seal. A recent assessment of the role of infiltration in energy use of commercial buildings developed a target infiltration rate used for energy models of 1.2 L/s-m² (0.24 cfm/ft²) @ 75 Pa (1.58 psi), based on modern construction data with a “best achievable” infiltration rate of 0.2 L/s-m² (0.04 cfm/ft²) @75 Pa (1.58 psi)³. Only six percent of a set of existing buildings tested met the target standard for infiltration³. The same study estimates that reducing infiltration rates in commercial buildings to the target rate would save 40 percent in natural gas and 25 percent in electrical energy in heating dominated climates. Consequently, the biggest infiltration problem areas in buildings comes from interfaces between fenestration and opaque walls, and one may surmise that buildings can be made tighter by avoiding the wall system of “punched” openings encouraged by prescriptive codes (and window-wall ratios) and use continuous systems where airtightness can be best maintained. The triple glazed curtain wall system available from the collaborating manufacture infiltrates at 0.06 cfm during a standard test at 6.24 psf; if the system could maintain such tightness continuously across an entire building envelope it could easily perform below the established targets^{3,1}.

[i] This comparison is based upon different tests (whole building infiltration versus assembly infiltration) and does not address the challenge of establishing continuity at floors, roofs, and other challenging areas, especially when required by tall buildings. Yet the potential for high-performing glazed curtain wall systems to outperform conventional layered walls is very strong when reduction of infiltration is considered.

3.0 STUDIO RESEARCH PROCESS AND METHODS

The studio's research model reflects aspects of several current research trends in academia and practice. The collaborating manufacturer in the project supported the students' research effort by providing materials and knowledge, but without a formal research stake in the project – similar to other open-ended “sponsored studios” taking place elsewhere in the academy. Yet, the studio sought to focus not just on experimentation, but also on advanced research tools and methods that could potentially bridge between the profession of architecture and performance-driven manufacturing. While taking inspiration from programs at other academic research centers, such as the Integrated Design Lab (University of Washington and University of Idaho) and High Performance Building Laboratory (Georgia Institute of Technology), the studio sought to demonstrate research process and outcomes that could be initiated and carried out in practice, instead of engaged in a specialized institution or lab. Considering this aim, the methods and tools of the studio are readily available to professionals at relatively low cost including widely available computer simulation software, but also the instrumentation used to perform in-situ testing. In summary, one might think of the student teams as design teams within any architect's office, given the latitude to study a particular performance problem involving a manufacturer, with architectural integration serving as a final objective. The trajectory of the students towards architectural integration played out in the studio with the students ultimately designing their experimental curtain wall systems into their design projects in the spring semester, where they finalized architectural detailing and worked their systems into their design concepts.

Beginning with a phase of background research and tours of the collaborating manufacturer's facility in Manhattan, Kansas, the students formed teams of three students each, for a total of five teams, and proceeded to develop experimental curtain wall systems offering improved thermal performance. The experimental systems were evaluated at each stage of development against

the manufacturer's 2.5-inch profile aluminum curtain wall system (referred to in the text as 250xpt), with polyamide thermal breaks and triple-glazed, argon-filled IGUs. Work began in a “what if” stage, where hypotheses were developed by the teams with respect to system performance and the physics of thermal efficiency, considering also material capabilities and structure.

3.1 Computer Simulation

Computer simulation was used in the earliest stages of experimental system development. Initially teams worked with THERM and WINDOW, two simulation programs developed by the Lawrence Berkeley National Laboratory, to analyze two-dimensional model sections. In this software, finite element analysis calculates multiple modes of heat transfer through the section, given prescribed environmental conditions at each side of the wall. Students used NRFC simulation configurations and boundary conditions to compare their systems' performance to the manufacturer's official NFRC certification models, as the National Fenestration Ratings Council (NFRC) uses this software in its certification process. Virtual testing at this stage also permitted student teams to easily test multiple configurations of their systems at one time, optimizing designs as they received feedback from the simulation programs, much like manufacturers do when developing new products. THERM and WINDOW models calculate thermal properties for an enclosure system, such as U-Value, Solar Heat Gain Coefficient, and Visible Transmittance; yet it is also important to understand how these thermal properties affect building performance when they contribute to overall building loads. In order to evaluate this impact, the studio used whole building energy simulations (carried out in Autodesk Ecotect) where a 24,000 square foot skin-load dominated office building was modeled according to IECC prescriptive guidelines. Set in Des Moines, Iowa (IECC Zone V) with 38 percent window-to-wall ratio and realistic internal and ventilation loads, these simulations showed how the experimental systems might improve overall building efficiency.



Figure 1: Image showing test structure and 1:1 scale prototypes constructed by the students for thermal testing.

3.2 Prototyping

The last phase of development involved the production of prototypes, built at 1:1 scale after the student teams had vetted their experimental systems via computer analysis. The first prototypes were “desktop models” that served as a proof-of-concept and helped students to understand the material and assembly implications of their proposals. The final prototypes built by the students were constructed to fill a 27 inch wide by 74 inch high opening in a specially constructed test enclosure (Figure 1). The large prototypes were intended first to demonstrate material and assembly concepts, but were also installed in the test enclosure so that real-world thermal performance could be evaluated alongside the manufacturer’s 250xpt curtain wall unit. Testing at this scale intended to test the typical, most frequently occurring joints in the curtain wall – though it may be mentioned that thermal transfer in curtain wall weak

points such as building corners and expansion zones was not part of the scope of prototyping and testing.

In order to fabricate the large mockups, the teams were forced to make substitutions in their materials and thus some difference would exist between the mock ups and the virtual tests conducted earlier. In the test enclosure, the curtain walls faced south with maximum solar exposure, with the remaining walls of the test enclosure were composed of 3.5 inch structural insulated panels with an additional 0.75 inches of polystyrene insulation over the exterior (see notes for more information on test house construction) with all joints double sealed with foil tape. Lastly, a thermostatically controlled electric heating unit was used during tests to heat the interior of the roughly 1000 cubic foot volume (16’ x 8’ x 8’), using a low velocity fan and directed away from any of the prototypes and temperature sampling sites. Testing in the enclosure during the winter of 2014-15 involved a

number of experiments where temperatures at specific points on the prototypes were monitored as well as a series of infiltration tests to measure air leakage through the prototypes.

3.3 Testing Apparent Thermal Resistance

The goal of monitoring temperatures in the prototypes was to compare the apparent thermal resistance of six systems at similar locations in the glass units and center mullions. It is important to emphasize the distinction between apparent thermal resistance and resistance (i.e. R-Value) calculated by computer simulation or provided in material ratings, the latter two being somewhat idealized. It was expected that the apparent resistance of the systems would be different from those calculated by THERM and WINDOW, although the relative order or

performance (most to least thermal resistance) would persist in the live tests. Additionally, the studio's tests referenced ASTM standards related to measuring temperature (ASTM C1046-95) and determining heat flux from in-situ data (ASTM C1155-95) in some respects, but could not follow the standards set in ASTM C1155-95) for calculating thermal resistance because of the lack of heat flux sensors among the instruments used^{4,5}. Further discussion of heat flux sensors is made in the notes; one of the attempts of the research was to use easier-to-acquire temperature data without heat flux meters to calculate apparent thermal resistance. The validity of this method is certainly open for interpretation and more work is needed to establish the accuracy of using only temperature data to evaluate building components in-situ^{ii,iii}.

[ii] The test enclosure was constructed using aluminum structural components and enclosed using 3.5in SIP panels with polyurethane insulating cores. With an additional 0.75 inches of continuous insulation the envelope was increased to a thermal resistance of R 28.3 ft²·°F·hr/Btu. Interfaces between structure and envelope panels used gaskets that were compressed as panels were bolted together. All gaps were taped and any accessible gaps were filled with loose foam and backer rod. Prototypes were installed over steel sill flashing and were separated by a two inch of extruded polystyrene (0.75 inchs of expanded polystyrene at the edges), and all gaps were sealed with backer rod and silicon caulk.

[iii] Data collected during thermal tests referenced ASTM C1046-95 (2013) and ASTM C1155-95 (2013), but as noted did not use heat flux sensors to measure heat flux. A single heat flux sensor would provide a precise measure of heat flux (q) for any given temperature sampling site, and the resistance of the envelope (R_{env}) could be solved with only the observed interior and exterior surface temperatures at that site. However, heat flux sensors are many times more expensive than thermocouples, and data acquisition required to log these sensors is also more expensive and challenging, involving signal processing at the microvolt scale. For the experimental setup used in the studio, where fourteen individual sampling sites were monitored on both inside and out, using so many heat flux sensors was not possible. It may be possible in the future to use one heat flux sensor and some process of interpolation to make resistance calculations more accurate for multiple locations, but this methodology requires further evaluation. Research on how to conduct in-situ thermal resistance tests economically (i.e. by students and designers) is ongoing.

Temperatures from the thermocouples were recorded at five second intervals using synchronized data acquisition and a laptop during tests^{iv}, and the tests were conducted for several hours without disturbance, focusing on nighttime periods with cold temperatures and minimal wind with the heat source's thermostat set at point at 68°F. Thermography was used during the tests to supplement the temperature data points. The manufacturer's system had corresponding (normally aligned) interior and exterior thermocouple sites on the center of its lower glass pane and the center of its middle mullion. The five systems were similarly instrumented so that side-by-side comparisons could be made with the manufacturer's system. Lastly, interior air temperature was recorded at three mid-height locations in the enclosure along with exterior air temperature.

Calculating the apparent thermal resistance of the test units was accomplished with the equations below, derived from the principle of thermal resistance networks. In Eq.1, it is presented that given steady state conditions, absent thermal storage, heat flow conducting through the envelope assemblies equals the heat flowing into the assembly via convection and radiation (also noted in Figure 2). These heat flows can be represented in terms of resistances (in ft²-h-°F/Btu units) and related temperature differentials (ΔT in °F).

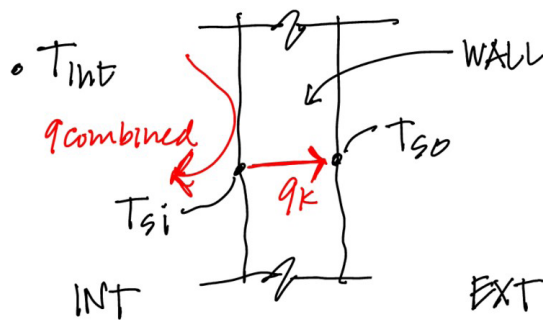


Figure 2: Diagram showing temperature sampling points used to calculate apparent envelope resistance.

Eq. 1

$$\frac{(T_{int} - T_{si})}{R_{conv+rad}} = \frac{(T_{si} - T_{so})}{R_{envp}}$$

Where: T_{int} = interior ambient temperature

T_{si} = envelope surface temperature, interior

T_{so} = envelope surface temperature, exterior

$R_{conv+rad}$ = convective and radiative resistance, combined

R_{envp} = envelope conductive resistance

The resistance network equation can be then rearranged to solve for envelope conductive resistance, as shown in Eq. 2.

Eq. 2

$$R_{envp} = \frac{(T_{si} - T_{so}) (R_{conv+rad})}{(T_{int} - T_{si})}$$

The components of Eq. 2 demonstrate the environmental parameters required to calculate envelope conductive resistance: a stable interior temperature, the corresponding interior and exterior surface temperatures, and the combined convective and radiative resistance for the interior environment. Note that exterior air temperature is not required in this equation, though in testing, exterior temperature was logged to ensure that for a given segment of time exterior air temperatures remained stable to maintain relatively steady state heat loss. It may also be noted that $(T_{int} - T_{si})$, the difference between interior ambient temperature and interior envelope surface temperature, is a factor (mathematically) in the calculation of envelope resistance. In lieu of calculating this resistance, the relative magnitude of various observed temperature differentials correlates closely to the calculated resistance, although only calculated resistance is presented in the results (Table 2).

Surface temperatures T_{si} and T_{so} were taken directly from thermocouple data sampled every 10 seconds. The interior temperature, T_{int} , was established as the average value from three locations within the enclosure. Temperatures from these three points remained very close throughout the tests, to around 0.5 °F, although due to the nature of the heating source, temperatures would

[iv] Thermocouples were adhered to surfaces using aluminum tape spray-painted either black or white to reduce the effects of radiant heat loss on local temperatures, and thermal imagery confirmed temperature uniformity around thermocouple locations during testing. Data acquisition devices recorded synchronized data from all channels on a laptop computer at five second intervals. Individual thermocouples were calibrated using ice point calibration prior to testing, and a specific correction applied to every thermocouple according to this calibration. The heater was directed away from the curtain wall prototypes in the interior and because of the small size of the heater, forced convection had a negligible effect on the individual prototypes and sensors.

rise and fall at intervals (typically 30 to 40 minutes, changing dependent on the exterior temperature). This is a departure from typical test enclosures that would have constant temperature control rather than on/off cycling. As a result of these temperature cycles, and the variation in response at the various thermocouple sites, calculations presented used the most local interior air temperature to a given surface temperature sampling site, and instantaneous resistances were calculated and then averaged for a two minute period. The criteria for setting this period involved identifying a two-minute period (containing 12 temperature samples) within the off cycle of the heating system, a time period most closely representing steady state heat loss through the envelope (Figure 5). Three two minute intervals were analyzed in this way, and the resulting resistances were averaged to determine an average R_{envp} value for each sampling site (Table 2).

Having thus far established the methods and intent of collecting temperature samples, the question of heat transfer at the interior envelope surface must be addressed. Recalling Eq. 1 and Eq. 2, $R_{conv+rad}$ is the resistance of the air at the surface of the interior envelope where heat is being transferred from the air to the envelope wall. For the purposes of the experiments, this resistance factor accounts for convection and some amount of radiation, although radiative transfer in the test enclosure is minimized due to the reflective interior surfaces of the enclosure walls^v. The resistance factor $R_{conv+rad}$ is the inverse of the combined coefficient of convection and radiation (h_{conv} with units Btu/ft²-h-F) and plays a critical role in determining the apparent resistance of an enclosure is quite critical, while these values under ambient indoor conditions can vary widely. Indoor values for h_{conv} may fall roughly between 1 and 5 Btu/ft²-h-F as a textbook reference, however, in precise scientific experiments requiring this value the experimenter is typically obliged to determine the value of h_{conv} by in situ observation, under the exact conditions of the planned experiment. While some part of h_{conv} can be attributed to the surface characteristics of the materials upon which the air is convecting, it should be emphasized that this is a property of the air and the surrounding environment. Thus in the case of the test enclosure, a generalized h_{conv} value may reasonably apply to all of the heat transfer cases in the envelope because each temperature sampling sites involve similar, adjacent surfaces.

If the experimental methods included heat flux sensors, the need to calculate h_{conv} would be moot because the sensors would yield instantaneous heat flux (heat transfer rates) and, along with the same temperature values discussed above, the resistance of the wall could be calculated without further effort. In the absence of heat flux sensors, h_{conv} must be determined another way. Coincidentally, the need to “fill in” this information is a major stumbling block in the effort to directly glean information on thermal resistance from only temperature data. For example, a previous study used systematically attained thermography to calculate the in-situ apparent R-value of complex wall systems, after they had been executed⁶. The study remarked at the disparity between very low apparent R-values calculated by field measurements versus the R-value determined by computer analysis; yet this methodology (referenced from sources in the thermography field) used an h_{conv} of 1.471 Btu/ft²-h-F ($R_{conv+rad}$ of 0.68 Btu/ft²-h-F), a value taken from standard air film resistances cited by ASHRAE⁶. While the goals of the Payette study are insightful – to better understand the relationship between heat transfer and architectural detailing – using a generic air film resistance intended for another purpose (determining assembly R-values by summation) is problematic when calculating for observed conditions where the air film and convection coefficient may be very different. Moreover, standards set in simulation software such as THERM (also used in⁶) apply much lower rates for the convection coefficient (for metal window frames, an h_{conv} of 0.549 Btu/ft²-h-F and for glass surfaces an h_{conv} of 0.375 Btu/ft²-h-F). Lower convection coefficients suggest a reduction in heat transfer by convection, so it is no wonder THERM results and calculations using the generic number do not agree.

After temperature data was initially collected, the combined coefficient for convection and radiation was determined experimentally by conducting a series of tests in the test environment. An aluminum bar of known physical and dimensional properties was heated and cooled, with intervals in between to allow the bar to reach equilibrium with the environment of the test enclosure. Conditions during the tests approximated the interior conditions during earlier thermal testing (an interior temperature in the mid-60s F), but the heating system was not operated during these tests. A thermocouple was mounted to the aluminum bar and a second thermocouple was suspended a few inches

[v] Radiation would be an increased factor if surface temperatures in the environment would be greatly different. However, temperatures were within a rather tight range. Also, the surfaces that would exchange the most heat by radiation would be normal to the prototypes on the interior and the foil-faced surfaces of the SIPs would also greatly reduce radiative heat transfer.

from its surface. Each test began outside the enclosure, where the bar was either heated by a heat gun or chilled in an ice bath and then quickly brought into the test enclosure and positioned. Temperature readings of the bar were logged every second until the bar reached the temperature of the surrounding environment. Analyzing the drop in temperature across a given timestep throughout warming or cooling of the bar was then used to calculate the time constant of convective heat transfer. The following equation (Eq. 3) was used to determine the time constant from temperature data, a process referenced in⁷:

Eq. 3

$$\Delta T(t) = \Delta T_o e^{-t/\tau}$$

Where: $\Delta T(t)$ = difference in temperature at time increment t
 ΔT_o = initial temperature difference at $t=0$
 t = time increment
 τ = time constant
 e = Euler's number

Using Microsoft Excel, temperature drops across time steps of 30 secs were plotted, and an exponential function ($y=Ae^{-B/x}$) was graphed to the plot^{vi}. The inverse of the constant in the resultant function established an approximation for the time constant τ . Two cooling off and two warming up tests were conducted, and the time constant calculated for each of the four tests. Having determined the time constant, it was then possible to calculate h_{conv} using Eq. 4 and the known material and geometric properties of the aluminum bar. It should be noted that the data analyzed to determine the time constant was using 30-second steps; this requires a conversion factor of 120 in introducing the time constant to Eq. 4 where the final units of h_{conv} use hours. The tests to establish the time constant and coefficient of

convection and radiation thus yielded the values shown in Table 1, with close agreement among the four tests in arriving at a suitable value for h_{conv} . The values for h_{conv} could then be used in Eq. 2 to calculate the apparent thermal resistance of the assemblies, understanding that the inverse of h_{conv} is equivalent to $R_{conv+rad}$. It may be noted that the average value of 2.81 Btu/ft²-h-F for h_{conv} is within the expected range of 1 to 5 Btu/ft²-h-F, although it is a higher rate of convection (i.e. less resistance) than those discussed from THERM parameters and from typical values attributed to interior air films when considering R-Value summations.

Eq. 4

$$h_{conv} = \frac{m c}{\tau A}$$

Where: m = mass of the aluminum plate
 c = specific heat of the aluminum alloy
 τ = time constant, converted to hours
 A = surface area of the aluminum plate exposed to convection

Table 1: Thermal constant values (τ) and the resultant values for h_{conv} calculated from experiments in the test enclosure. These values were used, along with temperature data, to calculate apparent R-values for the assemblies tested.

	τ (30 sec)	h_{conv} Btu/ft ² .h.F
Cooling Test A	9.3	2.67
Cooling Test B	8.5	2.95
Heating Test A	8.7	2.87
Heating Test B	9.1	2.75
	h_{conv} average	2.81

[vi] The graphs in Figure 3 show plots that were used to calculate a value for combined convective and radiative heat transfer (h_{conv}) at the interior wall of the prototypes. A bar of aluminum was either heated or cooled above ambient temperature, and its heating or cooling to equilibrium was recorded in five second intervals while it was inside the enclosure. A temperature difference (the Y axis) for time steps of 30 seconds was then calculated from these heating or cooling curves in order to determine the thermal constant for heat loss and gain in the test enclosure environment. The exponential equation fit to each plot was used to determine the time constant, according to Eq. 3. Heating up of the aluminum from a cooler temperature is the most difficult process to measure because of the fast response of the aluminum – however this was done to demonstrate that the thermal constant applies to both heating and cooling.

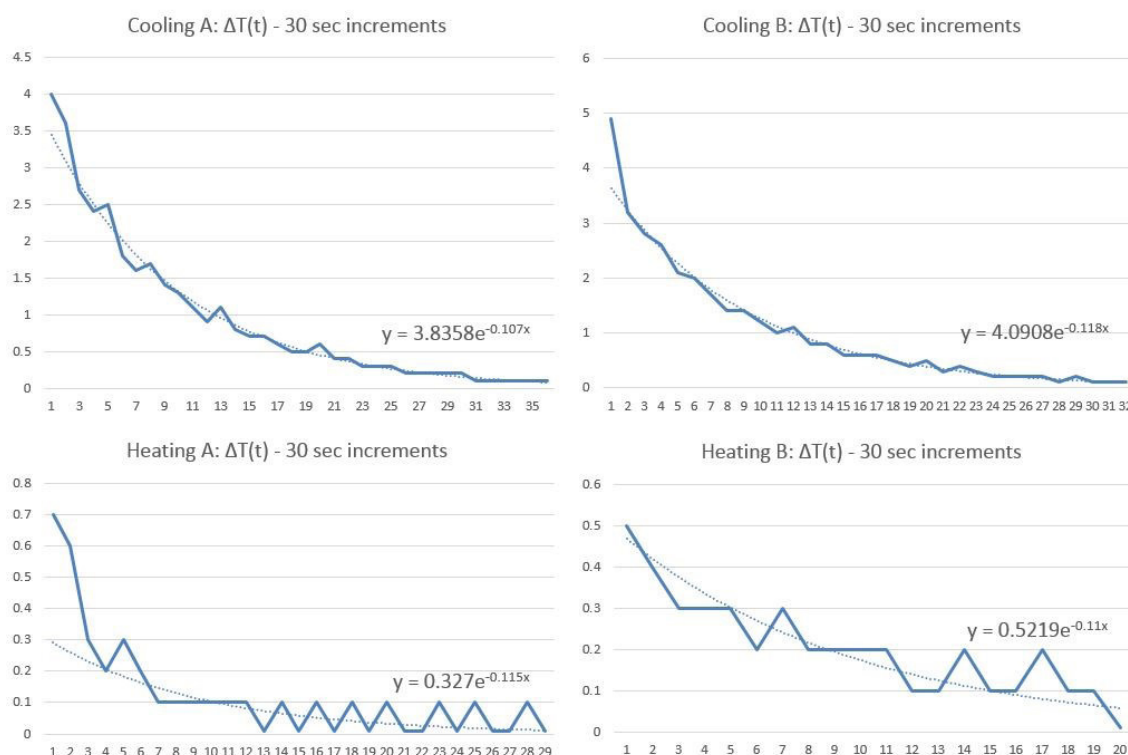


Figure 3: Temperature difference (the Y axis) for time steps of 30 seconds, plotted from tests showing the heating and cooling of an aluminum bar within the test enclosure environment.

3.4 Testing Infiltration

In addition to monitoring temperature data to calculate envelope resistance, tests were also conducted to measure infiltration (air leakage rate) for each prototype at -50 Pa and -75 Pa depressurization. Testing used a micro-controlled blower door kit, with the blower unit mated directly to the test enclosure. Masking of the prototypes involved applying masking tape to the perimeter shim area of each curtain wall prototype to exclude these gaps from the infiltration tests, given that the subject of the tests were the tightness of the glazing-to-frame interfaces within the prototypes. Thus infiltration results would represent the systems' deployment as a continuous, stick-built curtain wall system rather

than a unit inserted into a wall. Masking and testing protocols referenced ASTM E783-02, using heavy poly sheet to seal off surfaces that were not part of the subject area for a given test⁸. The poly sheet also provided visible verification of negative pressurization within the test enclosure. The first infiltration test masked off all of the prototype systems using poly sheet; this initial test determined a baseline infiltration rate for the enclosure minus the prototype systems. Individual infiltration tests could then be carried out for the prototypes simply by unmasking them one at a time. Further discussion regarding the setup of the infiltration tests is discussed below^{vii}.

[vii] Infiltration tests referenced ASTM E783-02 (2010)⁸. Following this standard, "extraneous" gaps around each prototype were masked using masking tape to ensure only internal air leakage (around IGUs and in between frame connections) were measured. When a prototype was being tested, the other five prototypes were covered with five mil polyethylene sheet, taped to the exterior of the glass units. Data was recorded after the polyethylene sheet was "sucked" to the surface of the other prototypes, indicating complete negative pressure was achieved inside the test enclosure. Testing used a duct testing apparatus joined directly to the test enclosure, and tests were conducted at -50 Pa and -75 Pa and used an average of three 120-second averaged recorded by the testing instrument.

4.0 EXPERIMENTAL SYSTEMS AND FINDINGS

Fabricating and testing the prototypes at full scale was important in understanding their viability against real-world conditions and concerns. Three experimental systems along with the base system from the manufacturer are compared in this article, with their conceptual bases and findings from simulation and testing discussed.

4.1 Base System: 250xpt System from Collaborating Manufacture

The system provided uses aluminum frame with an internal polyamide thermal break to fully isolate the exterior pressure plate and cap from the interior frame (Figure 4). The glazing unit used was a triple glazed, argon-filled IGU with Low-E glass and structural silicone spacers and a factory edge seal, installed with EPDM gaskets on interior and exterior in the curtain wall frame (Figure 1). Joints in the assembly of the frame were friction-fit with factory-supplied hardware and further sealed with silicone. This system is the manufacturer's best performing curtain wall product, with performance on par with other top-of-the-line glass curtain walls. It should be noted that the base system was assembled in the factory by an experienced fenestration contractor as part of a demonstration organized for the students, while the experimental systems were devised in part or wholly in the college shop.

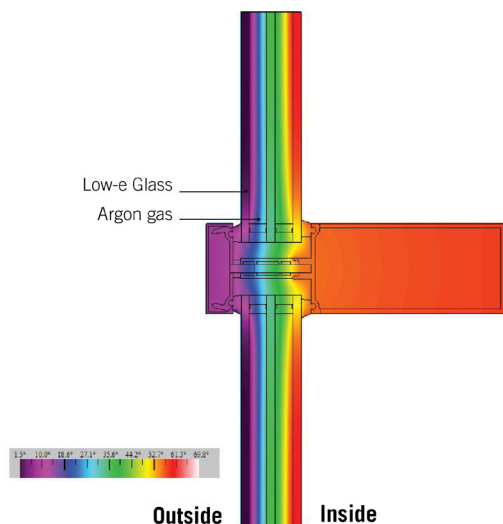


Figure 4: The collaborating manufacturer's 250xpt system with triple glazing and thermal break.

The manufacturer's system is also discussed in some detail along with the other systems, but testing yielded impressive results in both apparent thermal resistance and air leakage. With respect to apparent thermal resistance (Table 3), the glass was within 50 percent of the calculate R-Value from THERM (Table 2) with the value of h_{conv} likely part of the discrepancy. The sampling point of the frame yielded a higher than expected local resistance in the center of the frame, although R-Values from THERM account for the total values along the profile. In terms of apparent resistance, the 250xpt's triple glass unit also performed very closely to the students' System B (Composite Node) that used a deep, insulated airspace with two multiwall polycarbonate skins (each rated at R-2.5). In infiltration tests, leakage in the manufacturer's unit was nearly immeasurable at -50 Pa, bettering all the students' prototypes that used stick-built assembly techniques (Table 4). It may also be remarked that if the 250xpt's tested -75 Pa infiltration rate (0.06 cfm/ft²) could be maintained across an entire building envelope, it would well exceed the "best achievable" tightness (0.04 cfm/ft² @75 Pa)³. In sum, the manufacturer's system set a high performance bar for the student systems.

4.2 System A: Structural Spacer in Insulated Glass Units - Developed by: Tyler Countess, Hanh Phung, Samantha Wai

This system was developed by a team that acknowledged a conventional curtain wall frame is not used to its full structural capacity in the horizontal direction, merely transferring loads from the glass to the higher-loaded vertical mullions. The team also recognized that curtain wall frames have lower thermal resistances than modern IGUs, so eliminating any framing in the overall system would increase its thermal resistance. In response the team integrated a horizontal steel member within the top and bottom of the IGU that served both structurally and as a spacer (Figure 4). The spacer designed by the team is capable of spanning six inches in a 24 ft². IGU according to structural calculations for resisting dead load and wind loads and given the allowable deflections in the glass and adhesives. Two internal films within the slightly wider glass unit restrict convection. Computer simulations were carried out with the IGU using an argon fill and Low-E films, while the prototype constructed by the team was filled with air and used uncoated Mylar films. Vertical framing in the system used a shelf bracket to transfer loads from the now-structural IGUs to frame, while using conventional pressure plates and covers to complete the installation. A compressible foam gasket and silicon seals the hori-

horizontal joints between IGUs resulting in a visible joint of only about 1/4 inch.

Virtual testing in THERM indicated an increase in thermal resistance of 59 percent compared to the base system, a significant improvement (Table 2). It appears that much of this improvement comes from an elimination of surface area at the frame where mullions have been eliminated. Though the thermal resistance at the structural space actually decreases, this is locally a much smaller area for heat transfer than the conventional mullion. Improved thermal properties were then simulated with whole building energy modeling (Autodesk Ecotect) in a 24,000 ft² commercial building. In comparative simulations, combined HVAC energy usage was reduced by 17 percent using this system versus a high-performing double glazed system. Secondly, the research team also used Ecotect to simulate the improvements to daylight factor offered by their system versus the base system; in a room with a 2:1 depth to height ratio, daylight factor increased 20 percent.

In prototype testing, the system performed quite well despite some compromises in the prototype materials: namely in the improvised IGU, which used uncoated Mylar rather than a low-E coated film, and also used air in glass unit rather than argon. Despite these compromises the glazing unit performed very closely to the manufacturer's base unit, with apparent thermal resistance slightly increased over the 250xpt mockup. Although apparent resistance at the center joint was much less than the 250xpt's center mullion, thermography confirmed that areas of increased transfer at structural mullion were much more isolated: a similar comparison as that drawn from THERM modeling. As an estimation, the observed resistances (Table 3) can be multiplied by the profile length of these two joints: the 250xpt's would conduct at 0.40 Btu/h per foot of mullion ($R-2.18 \times 10.5''$ of profile), while the structural mullion would conduct at merely 0.28 Btu/h per foot of joint ($R0.45 \times 1.5''$ of profile). While not measured, light admittance and view through the small prototype was increased notably in comparison to the more bulky conventional center mullion in the manufacturer's unit.



Figure 5: System A prototypes and thermal simulation.

During infiltration testing, the prototype suffered from assembly shortcomings in the glazing unit seals and Mylar interlayers, yet the system was tighter than the test enclosure (Table 4) and did not appear to leak through the horizontal joint. Industrial assembly methods would certainly improve the infiltration resistance of this system.

4.3 System B: Composite Node System - Developed by: Brian Conklin, Nick Nelson, Dylan Rupar

A team of students developed the composite node system in response to two strategies. First, the team adopted low cost, thermally insulating multiwall polycarbonate as an exterior and interior skin, separated by a framing system that would allow for a deep cavity of translucent polymer fiber insulation to increase overall thermal resistance. The second development in the system involved the frame itself. Rather than using a

10 inch deep aluminum profile, the team devised a system consisting of interior and exterior “rails” that could receive either polycarbonate or conventional IGUs and could be finished with conventional pressure plates and caps. Nodes of low conductivity laminated wood intermittently tie the rails together and connect the system back to building structure. Weather stripping, mechanically installed pressure plates, and conventional sealants complete the air and water barrier on the exterior face, with the interior wall left unsealed to allow periodic equalization of vapor from within the wall cavity.

One of the most important implications of this system is that aluminum is used in an advantageous manner: it remains an easy-to-erect system of components yet thermal conduction is reduced and the amount of aluminum overall is reduced. Further, the system could use more affordable non-appearance grade coatings for the rails, allowing with it the use of recycled aluminum instead of virgin aluminum.

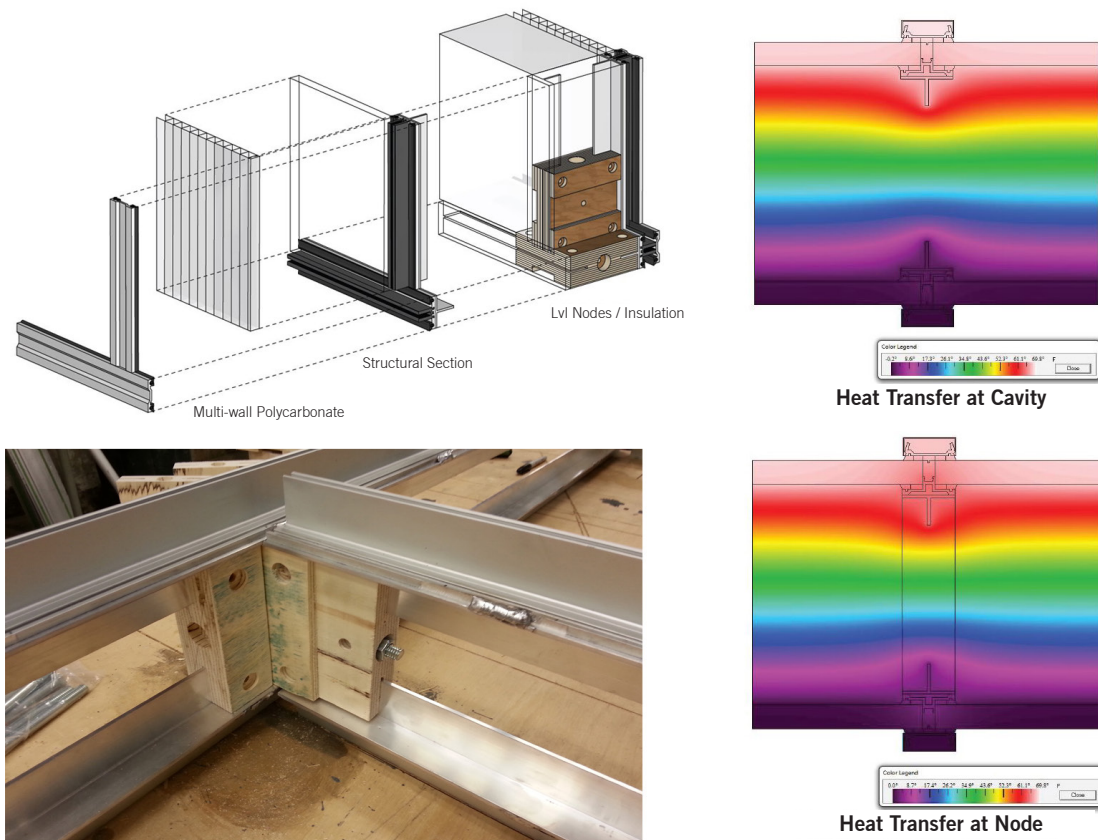


Figure 6: System B diagrams and thermal simulations.

Simulations in THERM show that thermal resistance of the infill system with a six inch deep cavity would increase by a minimum of 65 percent at node connections to a maximum of 84 percent in the cavity areas of the system (Table 2). Whole building energy simulations were then used to compare performance of the 24000 ft² test building using this system versus the manufacturer's base system. With an aggregated U-Value for a composite wall of 20 percent glazing and 80 percent polycarbonate infill, building HVAC energy usage is reduced by 20 percent. The team also conducted several daylight simulations using Radiance to evaluate the impact of their system for daylight diffusion, distribution, and glare prevention.

Refinement of the team's node and raid system was aided by prototyping during the design process and aluminum rails in the final 1:1 prototype were improvised by welding standard curtain wall parts to aluminum "T" sections to create the system's cross profile. The nodes were milled and machined from laminated composite wood using CNC equipment and the final design used universal nodes (i.e. all node connections were made with the same components). The team's IGU, caps, pressure plates, and weatherstripping were provided by the manufacturer. Multiwall polycarbonate was sourced by the team from a local hardware store and the system substituted loose polyester fiber for translucent insulation batting for the cavities, the latter reducing the thermal resistance of the system. The system performed well in live testing, with higher apparent thermal resistance in the frames and polycarbonate than the manufacturer's system, although the margins were slimmer than expected from THERM tests (Table 3). In summary, the testing of the prototype confirmed expectations from computer simulations and showed that the main strategies of the system to reduce thermal transmission were working as expected. Infiltration tests were telling as well, with infiltration rates much lower than the SIP envelope of the test enclosure and lower than other groups' prototypes (Table 4). While not as tight as the manufacturer's system, this prototype had many more parts and opportunities for leakage and yet still performed well, demonstrating that the system's depth and double wall construction could pay off with airtightness and excellent thermal resistance.

4.4 System C: Structural Foam Composite -

Developed by: Kate Gutierrez, Kristina Johnson, Jenelle Tennigkeit

The final system discussed in this article was developed by a group interested in unitized curtain walls and

non-linear construction, versus stick systems that are assembled in the field from separate frame and glazing components. The group reasoned that framing systems were a liability for glass curtain wall systems, and often these facades were not entirely clear glass anyway with many installations using opaque, spandrel glass units. The solution devised by the group was to eliminate the aluminum framing altogether, replacing the glass support system with structural foam panels where glass units would be directly glazed using silicon adhesive. With a thin exterior skin of fiber-reinforced composite, the team calculated that IGUs of 50 ft² or more could be supported within a foam panel spanning floor to floor. Such foam panels can reduce the weight of conventional glass and infill panel systems by 60 percent, reducing construction equipment requirements and emissions in transportation. Details developed with the system included a concept for using cam locks to realize a tight seal against the building and adjacent panels to reduce infiltration, and a lapped interface between glass and panel that would maximize sightlines while reducing sharp thermal gradients that could result in condensation. Devised to demonstrate the concept of an "active Z-axis", the 1:1 prototype was CNC milled with a faceted profile facing the exterior: a strategy that could be applied in real applications to increase the structural rigidity, control surface runoff, or provide light control.

In the computer simulations (Table 1) and in live testing, this system showed a high degree of thermal resistance, as expected from the depth and foam composition of the panel. Given the relatively low thermal gradient, and the high resistance of the panel, the calculated thermal resistance was also the most inconsistent across the three testing intervals. Coincidentally the glass IGU, a double-glazed Low-E unit, recorded colder temperatures than any other glass surfaces during testing, perhaps because its recessed position in the deep panel where a cold pocket of air could develop. Whole building energy simulations using the 24,000 ft² base building, with an aggregate U-Value for a composite wall of 25 percent glazing and 75 percent opaque infill, showed a potential reduction in HVAC energy usage is reduced by 12 percent. The performance of this team's system is highly design-dependent and in a building where the spatial and functional impact of the wall is favored over glazing, greater energy reductions could be realized. Predictably, the monolithic nature of this system performed well in infiltration tests, showing no measured leakage at -50 Pa (Table 4) and only minor leakage at -75 Pa.



Figure 7: System C prototype and thermal simulation.

Table 2: Thermal performance of the tested systems versus the manufacturer's triple-glazed system, as tested using THERM and WINDOW software with NFRC testing parameters applied.

Comparison of Thermal Performance: THERM and WINDOW Simulations w/ NFRC Guidelines		
System	Window Assembly U-Value, Glass and Frame, Btu/h-ft ² -	Infill System U-Value, Btu/h-ft ² -F
Mfr's 250xpt	0.29	N/A
System A: Structural Spacer	0.128	N/A
System B: Composite Node	0.29	0.11 (node intersections) 0.05 (max, cavity ctr)
System C: Foam Composite	0.29	0.025

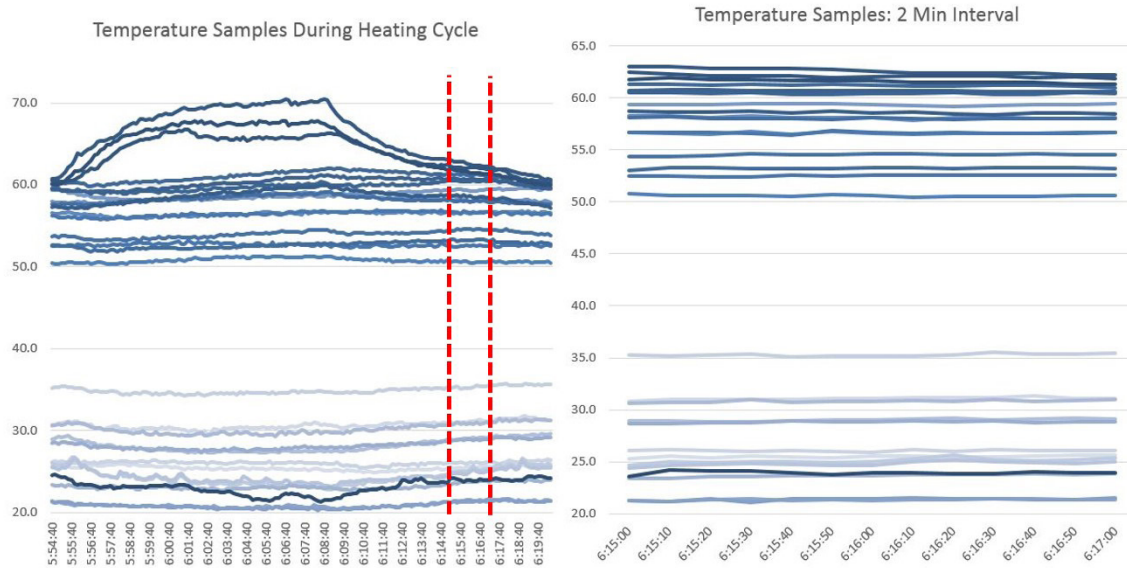


Figure 8: An example of temperature plots from prototyping testing, part of three separate tests conducted over periods of several hours to multiple days. At left shows temperatures through a single heating interval of approximately 25 minutes, with the top three plots representing interior air temperature, and the lowest plots exterior surface temperatures. The section of data yielding the two-minute interval is demarked between vertical lines. At right is the two-minute interval used for calculating apparent thermal resistance of the various systems, showing conditions close to steady-state during the interval.

Table 3: Apparent envelope resistance of the tested assemblies. Testing intervals (A, B, and C) of 120 seconds were taken from three respective tests. Apparent resistance was calculated using Eq. 2.

Apparent Envelope Resistance, R_{env} h.ft².F/Btu

	Ave, Interval A	Ave, Interval B	Ave, Interval C	Ave, Total
Center of Middle Mullion				
Mfr's 250xpt (Mullion)	2.20	2.19	2.15	2.18
System A - Structural Spacer (IGU at Spacer)	0.46	0.44	0.45	0.45
System B - Composite Node (Mullion)	2.67	2.53	2.56	2.58
System C - Foam Composite (Solid)	28.92	23.65	16.44	23.00
Center of Lower Panel				
Mfr's 250xpt (Glass)	3.59	3.76	3.75	3.70
System A - Structural Spacer (Glass)	1.74	1.74	1.82	1.77
System B - Composite Node (Polycarbonate)	3.77	4.05	3.56	3.79
System C - Foam Composite (Solid)	13.19	16.94	9.98	13.37

Table 4: Infiltration tests conducted for each system. The baseline infiltration rate of the test enclosure represents the rate of the entire envelope of enclosure with the tested systems masked. Negative pressures of 50 pascals and 75 pascals correspond to common depressurization values used in building commissioning.

Infiltration Tests

Configuration tested	@-50 Pa	@-75Pa	CFM/ft ² @ -50Pa	CFM/ft ² @ -75Pa
All systems masked - baseline	199.9	259.0	0.39	0.51
Mfr's 250xpt	0.1	0.9	0.04	0.06
System A: Structural Spacer	4.6	6.9	0.30	0.45
System B: Composite Node	2.6	4.3	0.17	0.28
System C: Foam Composite	0.0	2.1	0.00	0.13

*The area of each system tested for infiltration was 15.47 square feet. The total surface area of the test enclosure, minus the area of the systems, was approximately 512 square feet.

5.0 CONCLUSION

Research applications involving the test enclosure is continuing at Kansas State in the Department of Architecture, with a new project involving a new system. With this new project, some improvements to data collection and analysis will be attempted^{viii}, specifically to improve prototype comparisons that are dependent on stable environmental conditions in the enclosure. Clearly for thermal resistance, the apparent thermal resistance measured in these in-situ tests will never perfectly match the ratings derived from controlled laboratory testing, it is anticipated that improvements to the experimental set up and methods will yield observations with more confidence and closer to expected values. Yet, despite discrepancies between apparent thermal resistances and simulated resistances, the experiments using the test enclosure yielded insightful results that were useful in making comparisons from system to system.

A larger goal of the work is thus to develop and perfect methods that are rigorous, in the sense of ASTM standard methods, yet can be achieved by designers

and professionals – architecture students and architects interested in design and not just engineering conclusions – without highly technical laboratories. While there are challenges in achieving the testing rigor of ASTM standard methods, those cited in this article are methods proven for in-situ conditions, rather than labs, and we can use them as a starting point for practice-friendly methods, as long as these methods are based on sound building science fundamentals. For example, calculating an apparent convection coefficient (h_{conv}) is perhaps a painful process, but a more informed approach than using a generic textbook value. As architects increasingly gain access to evaluation tools, such as simulation software and instruments like thermal cameras, adequate building science knowledge and rigor in methodology are critical in realizing the benefits of these tools to design.

Overall, the process of prototyping and experimentation resulted in a comprehensive knowledge of the thermal performance of curtain wall assembly systems, and how they could be improved. The first realization from the studio's testing was that the manufacturer's 250xpt

[viii] Several improvements will improve future experiments. The biggest improvement is expected to come from adding an always-on heating system that can control the interior temperature without cycling. This will stabilize interior temperatures near a steady state, and make localized air temperatures near sampling points more consistent. Secondly, adding more thermocouple channels will allow air temperatures to be taken closer to the sampling points, perhaps one air temperature reading for every interior surface temperature reading. The reality is that in an environment, air temperatures can be very dynamic and variations of a few degrees have a large impact on heat flow. Introducing one or several heat flux sensors into the experiments is also planned, though the hope is that accuracy can be improved with a thermocouple based method that is more affordable and easier to manage.

system is indeed quite remarkable at resisting thermal flows, setting a challenging bar for the students' systems to exceed. For example, System B (Composite Node), with a deep insulated airspace and two layers of multiwall polycarbonate, might be picked to easily surpass the 250xpt with its glass and conventional framing system; however, the performance of the two systems were very close. The airtightness of the 250xpt was also impressive, showing how a controlled, industrialized system can meet its performance objectives when it is assembled and installed correctly. Given the performance capability of modern curtain wall systems, these systems can be logically integrated, rather than avoided as a liability, for innovative low-energy buildings. Some important performance advantages were demonstrated by the student systems, as discussed already. With some improvements to prototypes, performance could increase further towards the outcomes predicted by computer analysis, this would include using the same simulated materials and profiles (and specifically, materials with available reference properties) in the prototypes and improving student fabrication skills to level out the impact of construction and installation quality. Additionally, the three student systems would show an even greater degree of advantage if they were compared to code-minimum curtain wall systems, instead of the "green flagship" system represented by the 250xpt. While economics was not a part of the studios' analysis of experimental systems, any of these three systems could arguably be manufactured affordably and reasonably, possibly even as an initial trial emerging from direct collaboration between manufacturer, architect, and consultants.

While the process of prototyping and testing (including the computer tools and analytical methods) in this project came from an academically-based research effort, this process could also take place as part of real world practice. As discussed earlier, architecture firms are acquiring tools for evaluation and have the ability to use methodical analysis to better inform design decisions. Builders already build 1:1 prototypes for architects for some level of aesthetic, quality, or water testing: certainly these prototypes could be used for thermal and infiltration testing. With commissioning and other performance-related imperatives becoming more common, it is evident that testing prototypes is advantageous, rather than the final product where failure is costly.

Lastly, the role of curtain wall manufacturers in assembling products from an amalgam of proprietary materials from other manufacturers is worth highlighting from the

studio's work. It may seem remote that a manufacturer adopt a system whose disparate material components must come from several different outside sources, like the Composite Node System discussed in this article. Yet this is exactly what curtain wall manufacturers do: they do not handle raw materials to make anything, but purchase component materials from other sources to produce a finished product including glass, aluminum profiles, gaskets, thermal breaks, coatings, spandrel infill materials, integrated shading devices, and many other individual components are sourced from others to create a "product" for any given manufacturer. Thus it might be argued that the next horizon in high-performing curtain wall systems are simply new, better performing composites of existing components.

Acknowledgements

The author would like to thank Manko Window Systems and Kevin Dix, PE and Vice President of Manko, for generously working through the process of inquiry, design, and prototyping with the student teams involved in this research and for providing the glazing components and glass for the prototypes.

Brian McKinney and Nadav Bittan, of BNIM architects in Kansas City, and Rick Shladweiler of PGAV architects in Kansas City also contributed their time and collaborative efforts for crits and reviews during the research process.

This research work was also sponsored by an NCARB Award for the Integration of Practice and Education. Funding from the award was used almost entirely for materials to build the test enclosure, for student prototypes, and for new equipment that supported this research.

Lastly, the author is indebted to the extensive efforts of the students involved, acknowledging the enthusiasm, curiosity, knowledge base, and persistence that is needed to bring serious research into the design studio. The participating students were: Brian Conklin, Tyler Countess, Kate Gutierrez, Kristy Johnson, Cameron Marshall, Jose Martinez-Giron, Nick Nelson, Nathan Niewald, Alex Otto, Kevin Perks, Hanh Phung, Dylan Rugar, Lawrence Tan, Jenelle Tennigkeit, and Sammi Wai. The author would also like to thank the Department of Architecture and the College of Architecture, Planning, and Design for the opportunity to teach this funded studio.

REFERENCES

- [1] Gibson, M. D., (2015). "Designed for Performance: A Collaborative Research Studio Rethinks Glass Curtain Wall Systems", *Future of Architectural Research -- Proceedings of the ARCC 2015 Research Conference*, Aksamija, A., Haymaker, J. and Aminmansour, A., eds.: Chicago, IL, April 6 – 9.
- [2] Boyle, B. J., Runkle, J., and Ziegler, R., (2013). "Achieving Tight Buildings through Building Envelope Commissioning", *Proceedings of the 3rd AIVC Airtightness Workshop*, Washington DC, April 18-19.
- [3] Emmerich, S., McDowell, T., and Anis, W., (2005). "Investigation of the Impact of Commercial Building Envelope Airtightness on HVAC Energy Use", National Institute of Science and Technology.
- [4] ASTM C1046-95, (2013). Standard Practice for In-Situ Measurement of Heat Flux and Temperature on Building Envelope Components, West Conshohocken, PA: ASTM International.
- [5] ASTM C1155-95, (2013). Standard Practice for Determining Thermal Resistance of Building Envelope Components from the In-Situ Data, West Conshohocken, PA: ASTM International.
- [6] Love, A., and Klee, C., (2014). "Thermal Bridging: Observed Impacts and Proposed Improvement for Common Conditions", *Proceedings of BEST4 Conference Building Enclosure Science & Technology*, Kansas City, MO, Retrieved from <http://www.brikbases.org/content/thermal-bridging-observed-impacts-and-proposed-improvement-common-conditions> on 7/25/2015.
- [7] Conti, R., Gallitto, A., and Fiordilino, E., (2014). "Measurement of the Convective Heat-Transfer Coefficient", arXiv; Cornell University Library Database, Retrieved from <http://arxiv.org/pdf/1401.0270.pdf> on 6/10/2015.
- [8] ASTM E783-02, (2010). Standard Test Method for Field Measurement of Air Leakage Through Installed Exterior Windows and Doors, West Conshohocken, PA: ASTM International.

02.

OPTIMIZING SPATIAL ADJACENCIES USING EVOLUTIONARY PARAMETRIC TOOLS: *Using Grasshopper and Galapagos to Analyze, Visualize, and Improve Complex Architectural Programming*

Christopher Boon, Portland State University, christopher.a.boon@gmail.com

Corey Griffin, Assoc. AIA, Portland State University, cgriffin@pdx.edu

**Nicholas Papaefthimious, AIA, LEED AP BD+C,
ZGF Architects LLP,** nicholas.papaefthimiou@zgf.com

Jonah Ross, ZGF Architects LLP, jonah.ross@zgf.com

Kip Storey, ZGF Architects LLP, kip.storey@zgf.com

ABSTRACT

This article documents the use of Grasshopper and Galapagos (Rhino plugins) as analytical tools to graphically represent and optimize the adjacency requirements in programmatic spaces. The resulting three-dimensional spatial diagrams are evaluated based on evolutionary fitness, which within this research context is defined as minimizing the numerical value of the total distance of all interconnected programmatic elements. This approach offers a unique system of analysis that can create an extensive range of otherwise unexplored solutions to space planning when faced with complex adjacency requirements and a large number of programmatic elements. The Grasshopper script is a significant leap forward over existing research in this area, with the ability for users to define an irregular shaped site boundary, input multiple stories, relate program elements to external adjacencies (views, parking, etc.) and handle an unlimited number of program elements. Consequently, the resulting script can be used as an aid in the schematic design of buildings that have inherently complex programmatic relationships. This article uses a three-story hospital on a sloping site with fifty program elements to demonstrate the efficacy of this approach.

KEYWORDS: space layout planning, parametric design, genetic algorithms

1.0 INTRODUCTION

Parametric tools for architectural design have advanced significantly since the advent of “blob architecture” at Columbia University and as seen in the work of Greg Lynn, Michael McInturf, and Douglas Garofalo in the mid-1990s¹. The early computer software tools used by architects during this time including Maya and CATIA, allowed for the design and construction of complex forms not previously possible. Due to the perception that these new forms were little more than willful sculptures that performed poorly², the pejorative term “blobitecture” was coined³.

Despite these inauspicious beginnings, academics and practicing architects realized that the implications for parametric design are larger than generating unusual forms. In the past two decades, parametric tools have been used to enhance the design process, allowing architects to iterate more quickly and focus on optimizing the performance of a building. These optimizations have focused on topics as varied as reducing energy use⁴, improving the flow of passengers in an airport⁵, and the topic of this article – space layout planning⁶. Before discussing the use of evolutionary design tools in space planning in more depth, we will first outline the development of parametric design and genetic algorithms.

1.1 Parametric Design

Scholarly articles on parametric design first appear in the 1950s and 60s, focusing on the design of rockets and airplanes^{7,8}, and therefore it should be no surprise that the early proponents of parametric design in architecture used software originally developed for airplane design. In one of the first articles to discuss the impact of parametric modeling on architecture, Roller (1991) discusses the way specific information storage – parametric information – in combination with the construction process has the potential to capture a true version of design intent, while the benefits of iterative variation in the design process are examined⁹. Motta (1999) focuses on computer-aided, intelligent modeling systems, illustrating their widespread application and value as tools that have the potential for reuse. A series of precedents in parametric design highlight the importance of establishing a workflow that produces useful results in this field¹⁰. More recently, Woodbury (2010) summarizes the role of parametric modeling in architectural design, “rather than the designer creating the design solution (by direct manipulation) as in conventional design tool, the idea is that the designer first establishes the relationships by which parts connect, builds up a design using these relationships and modifies the relationships by observing and selecting from the results produced”¹¹. He breaks down the essential components of parametric modeling, including geometry, programming, and patterns.

During conceptual and schematic design stages, much of what is explored involves theoretical concepts. The work is expressed diagrammatically. If the concept can be distilled into numerical parameters, then it is possible to use parametric modeling. This type of analysis allows designers to explore a much wider range of options in a much shorter timeframe. This article explores the ability of evolutionary parametric modeling as a space planning diagram-building tool. For a building to be efficient, it must meet the needs of its occupants. The needs of the occupants are determined during the design process by a complex relationship of programmatic and physical adjacencies. These spaces and their adjacencies can be measured and converted as numeric values, which in turn allow them to be turned into parameters to be manipulated.

1.2 Genetic Algorithms and Evolutionary Design

The field of biology, and more specifically evolutionary developmental biology, has studied the relationship between evolution and form for living organisms for decades. This work is best summarized by Thompson

(1942) and more recently by Carroll (2005)^{12,13} and highlights the breadth and depth of research in evolutionary “design” in biology over architecture. Fogel (1966) and Holland (1975) were two of the first authors to apply evolutionary design to artificial systems, introducing the concept of genetic algorithms to model evolution^{14,15}. Goldberg (1989) popularized the use of genetic algorithms as general function optimizers for other sciences and engineering¹⁶. Lenski et al. (1999) explore the ability of digital models to evolve like organisms in nature¹⁷. Through experimentation, they attempt to find the best possible way to create a digital genome as well as how influences in nature, such as mutation, can affect the population. The authors use diagrams to help explain the methods that can achieve the fittest results.

Frazer (1995) provides an overview of early work applying genetic algorithms to architecture, adopting nature’s processes of evolution to the design of buildings¹⁸. Applying genetic algorithms for generative design and structural form finding, Hensel et al. (2010) and Weinstock (2010) focus on the concept of emergence as the main process for evolutionary design, “emergence is... a central concept of biomimetics, in which biological structures are analyzed and understood as material hierarchies self-organized into structures that are achieved by a bottom up process of self-assembly from which their properties and performances emerge”^{19, 20}. Frazer, Hensel, and Weinstock all emphasize the role of biomimicry in their work over using genetic algorithms as optimization engines to solve complex, multi-objective problems as seen in computer science and engineering. Weng et al. (2014) summarize the history and use of genetic algorithms in optimizing the form of buildings with an emphasis on reducing energy use⁴.

1.3 Previous Visual, Parametric Tools for Space Planning

Several academic researchers have looked at generating algorithms for computer optimized space planning over the last fifteen years²¹⁻²⁸. Dutta and Sarthak (2011) provide a summary of this line of research⁶. This academic research focuses largely on the computer programming and mathematics behind the genetic algorithms and optimizations developed. However, more practical applications are needed, especially in visualizations for these space planning algorithms or “tools”. Visual tools are necessary in order to communicate the results of space planning with a variety of stakeholders and allows for architects to quickly assess the merits of a given scheme.

Architecture firms have been developing space planning visualization and optimization tools using Grasshopper. LMN has used detailed sets of spreadsheets to create architectural geometry based on programmatic relationships^{29,30}. The tool arranges program elements based on relationships marked within the information on the spreadsheets and translates this information into individual spaces that organize themselves according to user defined hierarchies. This parametric tool is limited in that it is primarily used for visualizing program spaces with no algorithm for optimizing adjacencies or even generating a spatial layout. NBBJ developed a tool that allows designers to quickly organize and visual architectural programs in three dimensions³¹. The project uses spring physics to create gravity between the various elements, which are represented by spherical volumes, to optimize adjacencies. This tool is very limited and requires significant input on the part of the user to transform the results of the spring physics into an architectural space layout plan. However, similar research using Newtonian gravitational models has been recently published by academic researchers at the Vienna University of Technology²⁸. Unfortunately, neither LMN or NBBJ have written peer-reviewed articles about their work in this field. This is likely due to the desire to keep research confidential that gives the firms an edge when competing with other firms for projects or simply the lack of resources to pursue peer-reviewed research.

1.4 Goals for a New Optimization Tool

This article explores the utilization of Grasshopper (a Rhino plugin) as an analytical tool to graphically represent a three-dimensional analysis of adjacency requirements in space layout planning. As much space planning in architecture firms is based on past experience with similar building types and a limited number of iterations, this research explores new ways of using evolutionary design to improve floor-plan layouts for complex programs, such as hospitals, and provide potential solutions that the architect would not have discovered otherwise. Using an adjacency matrix and list of program spaces as the input, the Grasshopper script developed in this research uses the “evolutionary solver” Galapagos to minimize the distance between programmatic elements that need to be adjacent and creates three-dimensional diagrams. As a brute force iterative process, the genetic algorithm can work away at a space layout problem without further user input until a certain amount of time has elapsed or the fitness plateaus. This type of approach offers a unique system of analysis that can create an extensive range of unique and otherwise unexplored solutions when faced with problems in developing complex order for spatial relationships.

2.0 METHODOLOGY

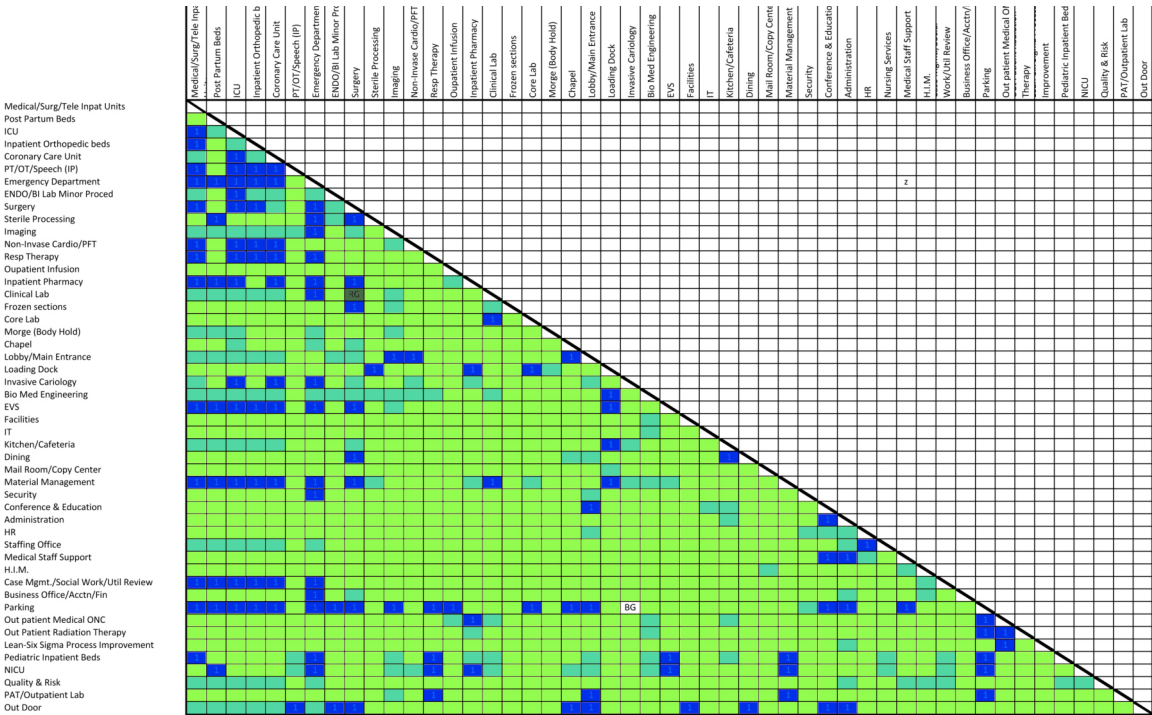
2.1. Design Directive

Programming for complex buildings, such as a health care facility, is a difficult job. This is due to the high level of complexity in spatial relationships and high number of programmatic elements. A hospital also requires a high level of efficiency, due to the nature of its function in society.

ZGF Architects LLC (ZGF) has significant experience designing hospitals. With this expertise, one can rely on client interviews and intuition to achieve efficiency in spatial relationships – grouping elements that need to

be adjacent and minimizing the travel distance between them. At the beginning of this research project, ZGF was in process of designing a hospital and there were program adjacency charts generated at client meetings and these resources were made available as sample test figures (Table 1). The numbers on the charts represent the various needs of the client. At meetings, the design team and clients develop a matrix of all the discrete programmatic elements. The matrix forms a hierarchy of space in terms of priority and ranks the adjacency requirement of each element in relation to all other elements in the chart. A space like the emergency room would take priority over the gift shop for example, and the two have no adjacency need.

Table 1: This matrix shows the various programmatic elements for a hospital and the relationship with others. There are three different levels of importance indicated by tones.



2.2. Tool Development and Geometry

The definition begins by input of some simple geometric parameters, thereby establishing the programmatic volumes that will be used in the iterative process. These first steps are the customizable portions of the tool. Each unique architectural situation requires some unique combination of factors that this research attempts to address to some extent in terms of spatial proxemics. The potential floor plan space is all that is actually drawn by the user. The ground floor of the building or site outline is first drawn and then additional floors can be added of any shape. Floor to ceiling height is adjustable. Any number of floors is allowed and there can be multiple sites separated from one another. Any shape can be used to describe the boundary conditions. The tool will automatically fill in the shapes with a three dimensional, rectilinear grid that can also be adjusted as desired.

The geometry all occurs within a three dimensional grid. This begins to describe a geometric system. All of the cells in the grid are marked with a single point. These points are all contained in a cloud. Each programmatic element is also built around a single point (Figure 1).

The programmatic central points are here referred to as "origins". Within the list of programs, there exists an explicit hierarchy. That is to say, the first program on the list dominates the second, which dominates the third and so on. The first program is placed in the grid by selecting one of the points in the cloud. The selected point becomes the center of the mass, which forms as a pixelated sphere around that point (Figure 2). Once a program occupies a space, all points within it are subtracted from the cloud. The next program repeats the process until all the programs are massed out. The proximity is determined by measuring the distance between origin points. The relationships are weighted in terms of their needs by multiplying the distances by various factors, the higher priority the adjacency need, the higher the multiplication factor. This multiplication factor can also be negative to repel program elements that need to be isolated from one another. The algorithm calculates the total value of all relationships by performing mass addition. This figure is the fitness score. The evolutionary process tries to minimize this number as much as possible. The idea is that a lower score creates a closer proximity and a more effectively adjacent situation.

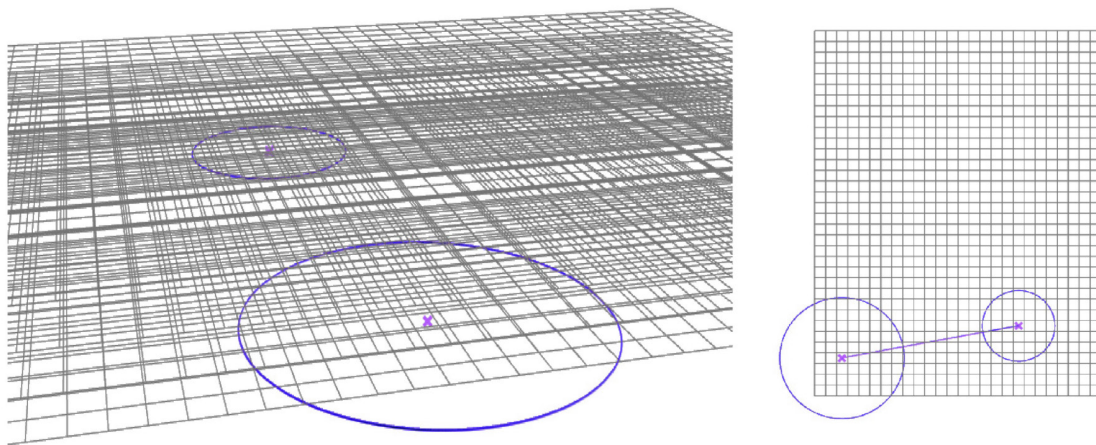


Figure 1: Screenshots showing the origin points selected in the grid and the relative floor area.

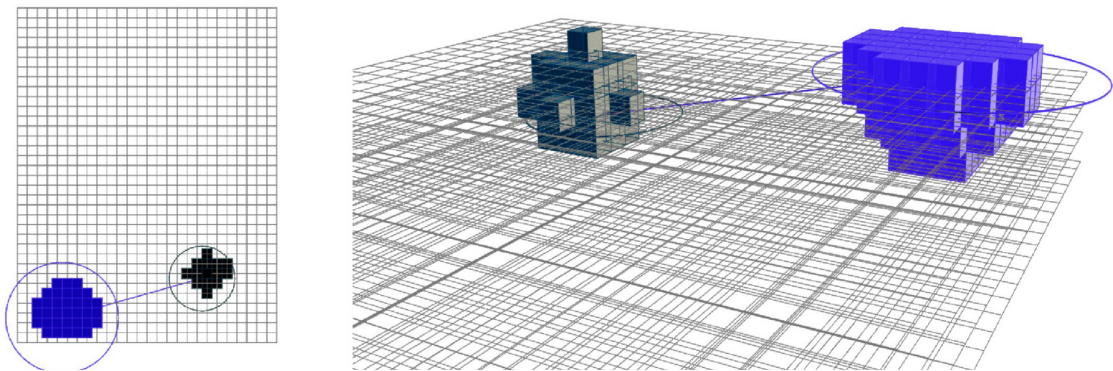


Figure 2: Areas are translated into “pixelated spheres”.

To create the evolutionary element in the process, the computer is allowed to manipulate all the origin points to create iterations. The point cloud within the shell is a list, and Galapagos can iterate using the sliders connected to that list.

2.3. Tool Demonstration and Steps

A series of generic tests help to demonstrate how the system works and where it needs refinement. This test

was run with nine programmatic elements. Those are broken into three groups represented by different colors (yellow, magenta, and cyan). Each group member wants to be adjacent to the others in the same group. The site outline for this experiment is for square blocks. There are four floors to be occupied. The Grasshopper definition (Figure 3) is implemented using the steps outlined in Table 2 and described in more detail below.

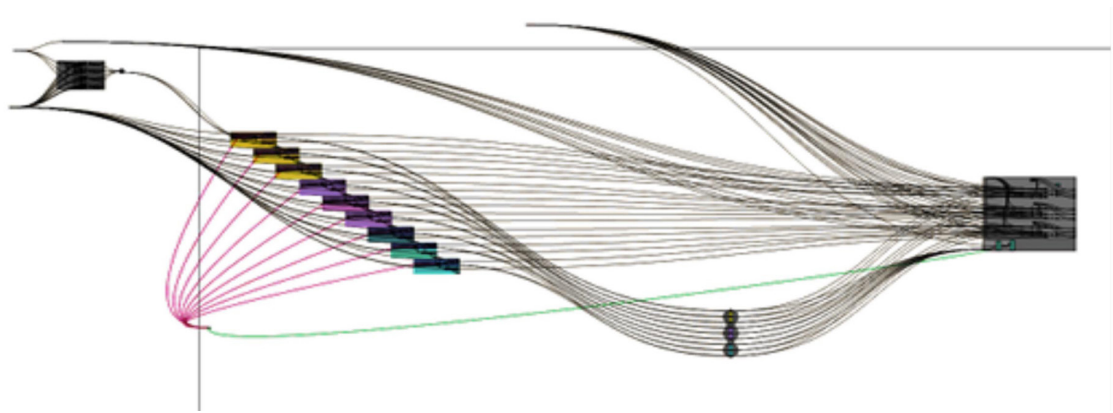


Figure 3: Grasshopper definition, screenshot where color represent program groupings.

Table 2: Diagram outlining the software programs and steps used to generate adjacency diagrams.



Optimizing Spatial Adjacencies Using Evolutionary Parametric Tools

Step 1: Establish site-specific initial geometry and offset levels

The starting parameters are customizable. The user sets up a grid that the spaces are built within. The number of cells and size of cells can be set to a specific coarseness. The program can also build the grid inside of a two-dimensional site outline to accommodate non-rectilinear sites. To account for multiple levels the grid can be offset vertically any number of times and the floor-to-floor height is adjustable (Figure 4).

Step 2: Assign hierarchy of spaces with list order

When the program activates, the order of the list of program elements is the order of importance. The first element in the list is ranked as the most important. This hierarchy is applied when spaces are divided and re-assigned giving priority to the most important program elements.

Step 3: Input square footage and set initial locations for each program element

The square footage for each space is set using a slider in the Grasshopper definition. The various program elements are assigned an initial origin point in the grid for a starting location. This point is center of the pixelated sphere, which represents a program element in the definition.

Step 4: Generate adjacency lines between program elements

The definition creates a line connecting the origin points for every adjacency requirement. A lower value indicates a closer proximity and more optimized adjacency. The definition adds up the total distance of all adjacency lines, which can be weighted to create greater attraction or repulsion in order to prioritize certain adjacencies over others or ensure two program elements are isolated from one another. The Galapagos evolutionary solver will try to minimize this total distance to improve fitness.

Step 5: Run Galapagos and record visualization of every iteration

The Galapagos “genome” is solely made of the origin location sliders, which allows it to rearrange the location of the program elements within the grid in order to improve fitness by creating the lowest total adjacency line distance (Figure 5). The areas inside the program circles are translated into pixels on the grid and extruded into three-dimensional volumes by the Grasshopper definition. All iterations are recorded in sequence along with their fitness score. The results (Figure 6) can be exported as an animation.



Figure 4: Point cloud formation, derived from initial geometry: site outlines and offset floors.

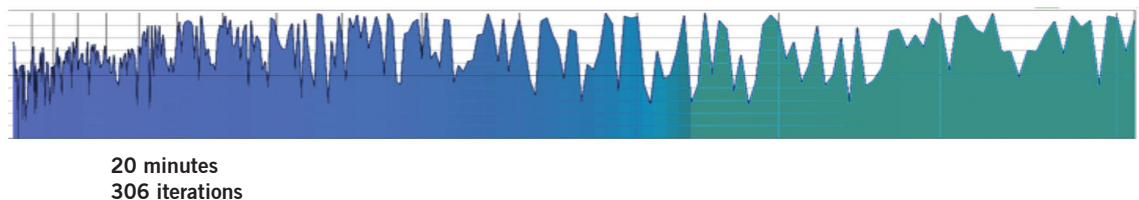


Figure 4: Point cloud formation, derived from initial geometry: site outlines and offset floors.

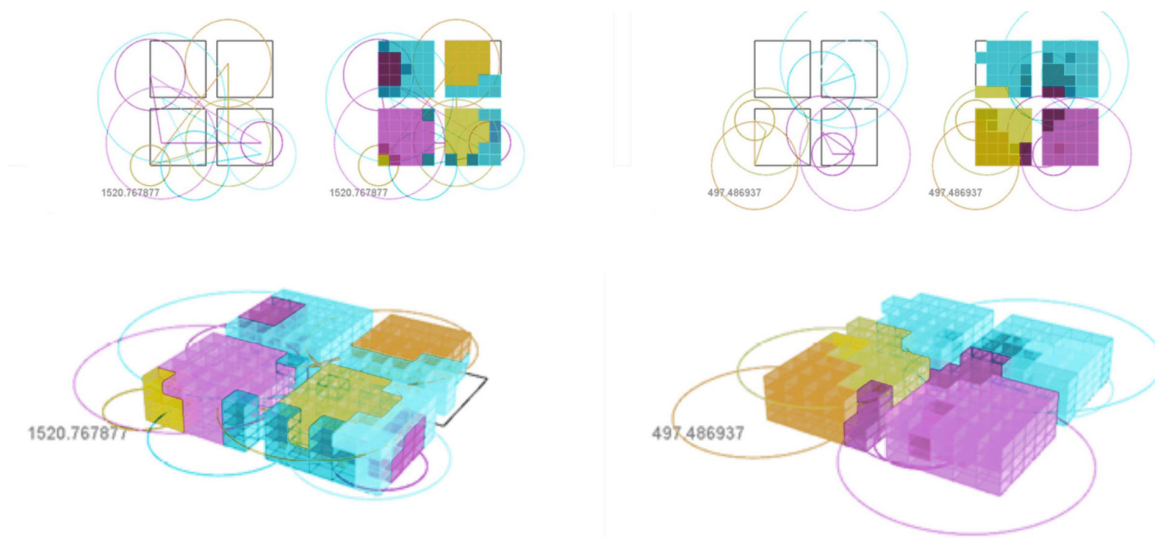


Figure 6: Least fit result (left) and most fit result (right).

3.0 CASE STUDY

Using thirty-six program elements (Figure 7) and the adjacency matrix for an actual hospital project (Table 1), a hypothetical sloping site with an irregular outline

and a three story building height was chosen to test the Evolutionary Parametric Program Adjacency Script (EP-PAS).

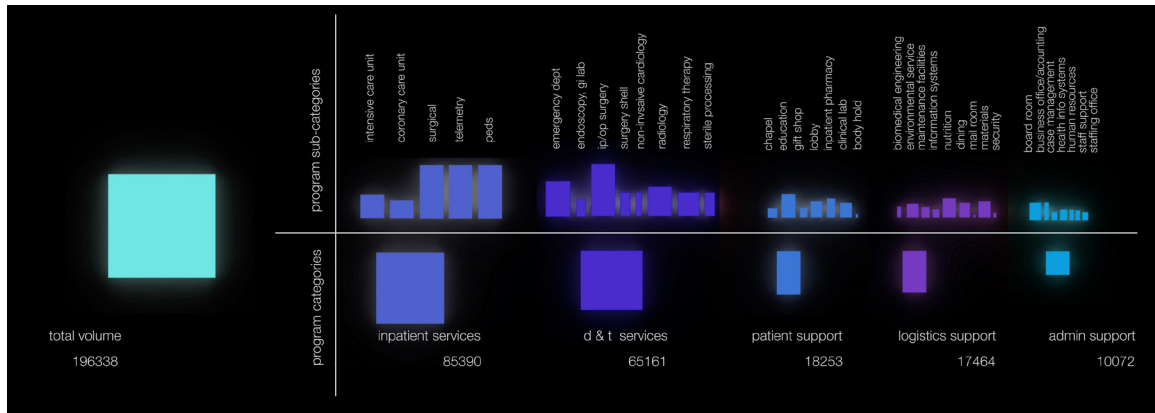


Figure 7: Program elements and relative square footages for a hospital.

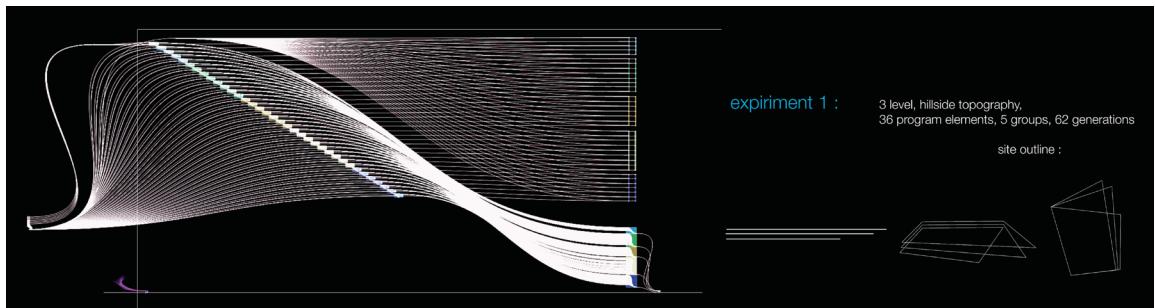


Figure 8: Grasshopper definition (left) and site constraints (right).

Optimizing Spatial Adjacencies Using Evolutionary Parametric Tools

3.1. Script Deployed

Figures 8-11 depict the Grasshopper definition for this specific set of programs and adjacencies as well as

the resulting Galapagos generated iterations, using the steps outlined in Section 2.2.

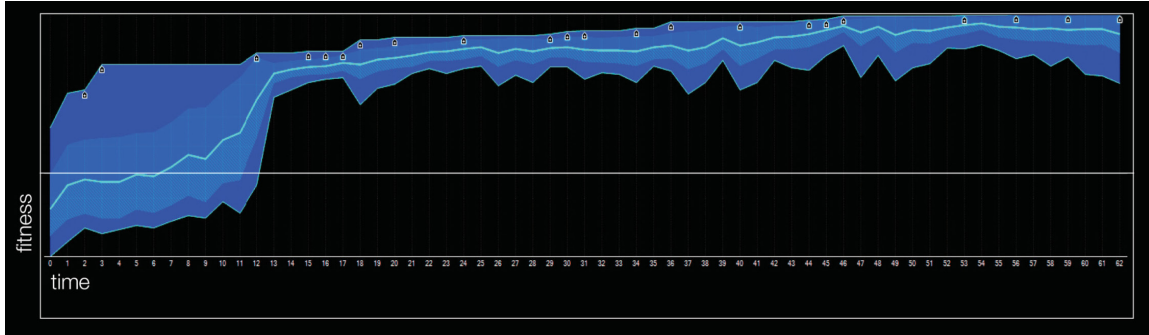


Figure 9: Graph depicts fitness variation (y) over generation number (x), where 62 generations took eight hours to compute.

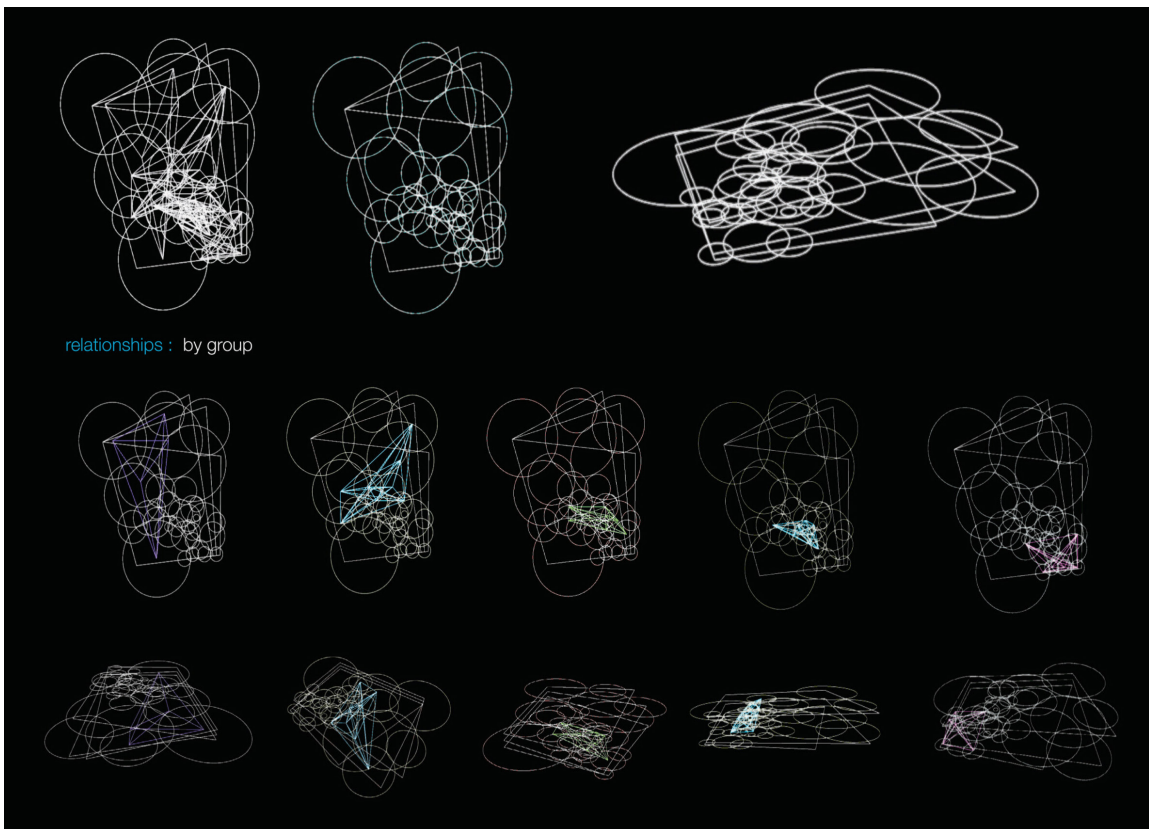


Figure 10: Generations, highlighting the geometries and distances used to optimize adjacencies and relationships by program type ("group").

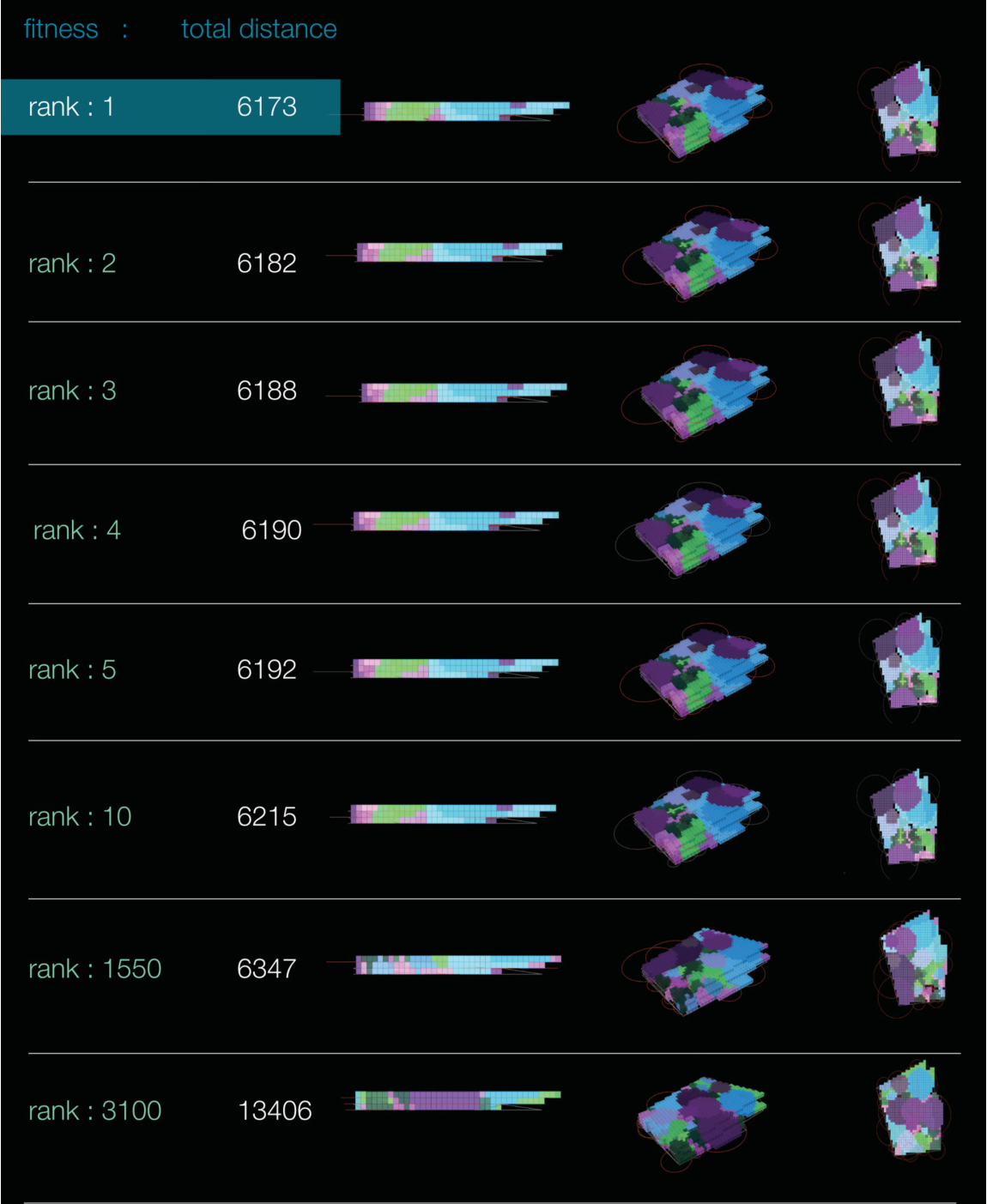


Figure 11: Least fit result (bottom) and most fit result (top) in section, isometric and plan.

3.2. Case Study Discussion

The script can run indefinitely, although it reaches a point where the results show no serious improvement in fitness. At these points it is best to either stop the process and take best result, or continue by restarting the process and hope for a different type of mutation to take hold of the evolutionary direction. There are clearly many ways to achieve similar results within the structure of the parametric tools, so this is just one solution to a problem. Better definitions are ones that can accomplish complex moves within a few commands, this makes the load on the computer exponentially lighter and therefore it produces more results and is easier to use. In this particular example, the most significant improvement in fitness occurred by the 13th iteration (Figure 9), with only slight improvements in fitness over the next 50 iterations. Despite these small improvements in fitness, these last 50 iterations could still be valuable to the architect as they highlight a variety of solutions that are similar in performance rather than one “right” or best answer.

There are several limitations to this script. This script currently treats program elements as three dimensional and does spread program elements over multiple floors during the optimization process. For many program elements, this situation is likely not ideal. Further development of the script would be necessary to put boundaries on programs that need to be located on the same story – slowing down each iteration. As outlined in the Methodology section, this script uses a cumulative total distance taken between each program element and attempts to minimize it as the definition of fitness or optimization. This could lead to iterations where there is one long and inefficient relationship compensated by other tightly packed elements. This possible iteration could rank better than one where all elements are equidistant from each other. It is necessary and - given the graphic outputs of the script – possible for the user to manually check for these types of situations and rule out iterations that have obvious inefficiencies. The authors would encourage users of this script to look at iterations with similar fitness scores to see which result would work best with other architectural constraints not currently accommodated in this research.

The advantages of this script, particularly with respect to healthcare, are that the program elements must be prioritized when the script is generated. This allows critical spatial relationships to be built into the script to avoid impractical solutions. For example, the emergency room can be placed near a particular parking lot or driveway to ensure quick access rather than allow-

ing the script to place the emergency room on the third floor even though that might be the most “fit” location for it in terms of adjacencies. Other anchors can be programmed to ensure particular views or orientations as needed. Another advantage is that programs that cannot be adjacent to one another for reasons of noise or contamination can be given a negative value for distance in the algorithm to reward the script for placing those elements further apart. The major advantage in using this script for space planning layout in healthcare is the fact that a large number of program elements and adjacencies are required in contemporary healthcare. It would be challenging during conceptual design to iterate space planning layouts more than a few times manually, given this complexity and potentially better layouts could be missed.

4.0 CONCLUSION

The Grasshopper/Galapagos script presented in this article is best applied to projects with complex programs with multiple adjacency requirements in early design phases. It can give designers data to inform their process and ultimately justify their decisions to clients who want to see a more data-driven or evidence-based approached to architectural design. The adaptability of the tool is critical to its usefulness. It has been simplified in terms of the scripting to a large degree, but could perhaps still be refined to produce faster results. One observation from the experiments, however, is that the best way to save time is by sacrificing certain amounts of flexibility. The more customizable the tool becomes, the more complex the calculation. A downside to this flexibility is that the user must use the Grasshopper interface to input the program elements. It would be ideal for non-Grasshopper users to be able to use the script as a tool by inputting an excel spreadsheet of program elements and their required adjacencies. This is one future line of development for this project.

Creating the range for the results is the task of the designer, and the narrower the range, the more meaningful results are. In other words, narrowing the field where variables can occur creates more pertinent results. The end results of this definition are diagrammatic, so they serve as a source of information that can be observed as a metric then incorporated into design. It could be expanded into a more literal space, with doors and windows, and the results could become more directly applicable to building design in the later stages. There will always be limitations in using genetic algorithms to optimize space planning layouts or any other criteria. In the case of using Grasshopper with Galapagos, this comes in the necessary simplification of complex relationships

into a single number to be maximized or minimized. For example, instead of total cumulative distance as a measure of fitness and proxy for optimized adjacency, this research could have used an average distance or ratio of shortest to longest distance. The authors specifically chose cumulative distance to allow for the repulsion of elements that need separation that would be more difficult to account for in averages and ratios. Still, this single number as an adjacency proxy can be misleading when not taken into consideration with the other architectural criteria that must be considered when organizing spaces in a building.

The introduction of the evolutionary process is extremely useful in creating iterative design tools. It should be noted these are tools, not an artificial intelligence created to replace architects or their decision making. These evolutionary design tools will only be as good as the user who programs the scripts and adjacency information generated in collaboration with the building's users. Consequently, computer programming should already be a skill in demand in architectural practice. Thankfully, visual programming tools that work in tandem with drafting programs make the learning and integration of parametric design and genetic algorithms more rapid. After being skillfully designed and programmed by the user, genetic algorithms are a way in which computer can independently process time consuming iterative work. The ideal situation for the tool involves a combination of parametric operations with evolutionary solving. The evolutionary modeling methods discussed in this article could be used on a much wider range of situations. This research explored adjacency, but any parameter or combination of parameters could be driving the model process including daylighting, structural efficiency, thermal comfort, and energy use, and many academics and professionals are already working on these types of tools. As a diagramming tool, parametric engines allow designers to start their process from an informed standpoint. The authors believe these methods are sound, but it will take further tests that at the very least are compared to the results of humans attempting the same optimization without the assistance of genetic algorithms.

Acknowledgments

The authors would like to thank the Van Evera and Janet M. Bailey Fund of the Oregon Community Foundation for supporting the graduate seminars in which this research was conducted. The authors would also like to thank ZGF Architects for their collaboration on this research.

REFERENCES

- [1] Sterling, B., (2009). "Blobitecture and Parametrics", *Wired*, July 23.
- [2] Silber, J., (2007). *Architecture of the Absurd: How "Genius" Disfigured a Practical Art*, New York, NY: Quantuck Lane Press.
- [3] Safire, W., (2002). "On Language: Defenestration", *New York Times*, December 1.
- [4] Weng, Z., Ramallo-González, A. P., and Coley, D. A., (2014). "The Practical Optimization of Complex Architectural Forms", *Building Simulation*, Vol. 8, No. 3, pp. 307-322.
- [5] Sitek, M., and Masły, D., (2014). "Parametric Design of Airport Passenger Service Areas", *Advances in Human Factors and Sustainable Infrastructure: Proceedings of the AHFE 2014 Conference*, pp.138-146.
- [6] Dutta, K., and Sarthak, S., (2011). "Architectural Space Planning Using Evolutionary Computing Approaches: A Review", *Artificial Intelligence Review*, Vol. 36, No. 4, pp. 311-321.
- [7] Harriman, T. J., (1958). "Technical Management of Missile Systems", *Engineering Management, IRE Transactions*, Vol. 4, pp. 133-135.
- [8] Swihart, J., and Wimpres, J., (1964). "Influence of Aerodynamic Research on the Performance of Supersonic Airplanes", *Journal of Aircraft*, Vol. 1, No. 2, pp. 71-76.
- [9] Roller, D., (1991). "An Approach to Computer-Aided Parametric Design", *Computer-Aided Design*, Vol. 23, No. 5, pp. 385-391.
- [10] Motta, E., (1999). *Reusable Components for Knowledge Modeling: Case Studies in Parametric Design Problem Solving*, Amsterdam, The Netherlands: IOS Press.
- [11] Woodbury, R., (2010). *Elements of Parametric Design*, New York, NY: Routledge.
- [12] Thompson, D., (1942). *On Growth and Form*, Cambridge, UK: The University Press.
- [13] Carroll, S., (2005). *Endless Forms Most Beautiful: The New Science of Evo Devo and the Making of the Animal Kingdom*, New York, NY: Norton.

- [14] Fogel, L., (1966). *Artificial Intelligence through Simulated Evolution*, New York, NY: Wiley.
- [15] Holland, J., (1975). *Adaptation in Natural and Artificial Systems: An Introductory Analysis with Applications to Biology, Control and Artificial Intelligence*, Ann Arbor, MI: The University of Michigan Press.
- [16] Goldberg, D., (1989). *Genetic Algorithms in Search, Optimization, and Machine Learning*, Reading, UK: Addison-Wesley.
- [17] Lenski, R.E., Ofira, C., Collier T.C., and Adami, C., (1999). "Genome Complexity, Robustness and Genetic Interaction in Digital Organisms", *Nature*, Vol 400, pp. 661-664.
- [18] Frazer, J., (1995). *An Evolutionary Architecture*, London, UK: Architectural Association.
- [19] Hensel, M., Menges, A., and Weinstock, M., (2010). *Emergent Technologies and Design*, New York, NY: Routledge.
- [20] Weinstock, M., (2010). *The Architecture of Emergence: The Evolution of Form in Nature and Civilisation*, New York, NY: Wiley.
- [21] Gero, J. S., and Kazakov, V. A., (1998). "Evolving Design Genes in Space Layout Planning Problems", *Artificial Intelligence in Engineering*, Vol. 12, No. 3, pp. 163-176.
- [22] Jo, J. H., and Gero, J. S., (1998). "Space Layout Planning Using an Evolutionary Approach", *Artificial Intelligence in Engineering*, Vol. 12, No. 3, pp. 149-162.
- [23] Michalek, J., Choudhary, R., and Papalambros, P., (2002). "Architectural Layout Design Optimization", *Engineering Optimization*, Vol. 34, No. 5, pp. 461-484.
- [24] Azadivar, F., and Wang, J., (2000). "Facility Layout Optimization Using Simulation and Genetic Algorithms", *International Journal of Production Research*, Vol. 38, No. 17, pp. 4369-4383.
- [25] Medjdoub, B., and Yannou, B., (2000). "Separating Topology and Geometry in Space Planning", *Computer-Aided Design*, Vol. 32, No. 1, pp. 39-61.
- [26] Wong, S. S., and Chan, K. C., (2009). "EvoArch: An Evolutionary Algorithm for Architectural Layout Design", *Computer-Aided Design*, Vol. 41, No. 9, pp. 649-667.
- [27] Zawidzki, M., Tateyama, K., and Nishikawa, I., (2011). "The Constraints Satisfaction Problem Approach in the Design of an Architectural Functional Layout", *Engineering Optimization*, Vol. 43, No. 9, pp. 943-966.
- [28] Lorenz, W. E., Bicher, M., and Wurzer, G., (2015). "Adjacency in Hospital Planning", *Mathematical Modeling*, Vol. 8, No. 1, pp. 862-867.
- [29] Scrawford, S., (2010). "Grasshopper Space Planner", Retrieved from <http://lmnts.lmnarchitects.com/parametrics/grasshopper-space-planner/> on 1/18/2015.
- [30] Scrawford, S., (2013). "Update to GH Graphic Programming Tool", Retrieved from <http://lmnarchitects.com/tech-studio/parametrics/graphic-programming-round3/> on 7/24/2015.
- [31] Syp, M., (2010). "Architecture: Realtime Physics for Space Planning", Retrieved from <http://vimeo.com/15563685> on 3/3/2015.

03.

URBAN MODELING WITH AGENT-BASED SYSTEM:

Ming Tang, AIA, NCARB, LEED AP, University of Cincinnati, tangmg@ucmail.uc.edu

ABSTRACT

This article describes research on using local interactions to generate intricate global patterns and emergent urban forms. An agent-based system (ABS) is used to optimize an urban network and construct the micro-level complexity within a simulated urban environment. The author focuses on how agent-driven emergent patterns can evolve during the simulation in response to the “hidden hand” of macro-level goals. The research extends to the agents’ interactions driven by a set of rules and external forces. An evaluation method is investigated by combining network optimization with the space syntax. The multi-phase approach starts with defining the self-organizing system, which is created by optimizing its topology with ABS. A macro-level “attraction map” is generated based on the space syntax analysis, where the map is used to control various construction operations of an urban model.

KEYWORDS: self-organizing, agent-based system, space syntax, bottom-up, emergent

1.0 INTRODUCTION: AGENT-BASED SYSTEM

An agent-based system (ABS) consists of numerous agents, which follow simple localized rules to interact with an environment, thereby formulating a complex system. Since Craig Reynolds’ artificial “bodies” and flock simulation, the concept of the ABS has been widely used in computer science, biology, and social science, such as swarm intelligence, decentralized social networks simulation, and economic growth modeling. ABS consists of interacting rule-based agents that can create real-world-like complexity. In urban modeling, agents can be defined as autonomous “physical or social” entities or objects that act independently of one another¹. The autonomous agent can represent humans, animals, robots, plants or artificial lives. As the essential element in an ABS, the most popular behavior of an agent is movement. The movements are usually based on simple rules, such as separation, alignment, and cohesion. Computer scripts can be used to simu-

late agent’s velocity, maximum force, the range of vision, and other properties (Figure 1). This autonomous, bottom-up approach is most practical for movement-related analysis. For instance, ABS has been widely used to simulate the behavior of crowds, where the agents’ movements are computed based on the interactions between them as well as the interactions with the environment.

In recent years, ABS has become an integrated analysis and evaluative process to assist architectural and urban design. Some of the emerging aspects in practice involve using ABS to generate complex self-organizing systems and geometries that respond to the interactions of elements and external forces. An agent can represent various architectural entities ranging from panels, rooms, and even abstract building program. ABS allows complex systems to emerge from the simple interaction among agents. Each agent can “sense” its neighbors

and “react” to them by modifying its location, shape or other attributes. For instance, Ehsan Baharlou and Achim Menges used ABS to compute the topology of a tessellated pattern across a complex surface². Li Biao used ABS to optimize the locations of skyscrapers to maximize their views and solar exposure³. ABS for urban design is also established in the same relational model and computational strategy. Some of the rigorous methods in the urban design practice involve using ABS to generate micro level self-organizing urban forms that respond to the top-down rules and traditional planning methods. The ABS approach can be found in large urban design projects, such as the context-aware multi-agent system for urban infrastructure by David Gerber⁴, and path optimization system in the Kartal Pendik urban design project by Zaha Hadid Architects. ABS also inspired Jeff Jones’ unconventional computing using the slime mold *Physarum polycephalum* to construct the natural multi-agent computational model⁵.

2.0 METHOD

Our research investigated the agent as the physical entity within the field of urban design. It focused on the agent’s properties used to respond to external changes, specifically how the agents can “sense” and “act” to form a bottom-up system. We studied the self-organizing behavior research from Kokkugia, agent and cells method by Batty as well as the wet grid by Frei Otto. The investigation focused on the movement based urban network, which was simulated through ABS and evaluated by the space syntax method.

2.1 Phase I: Movement Network

Our process began with a straight network, which was constructed based on the desired movement among a group of spatial nodes. This approach used the bottom-up interaction of individual agents to respond to other agents within the system. First, a group of spatial nodes were woven into a network in Autodesk Maya program.

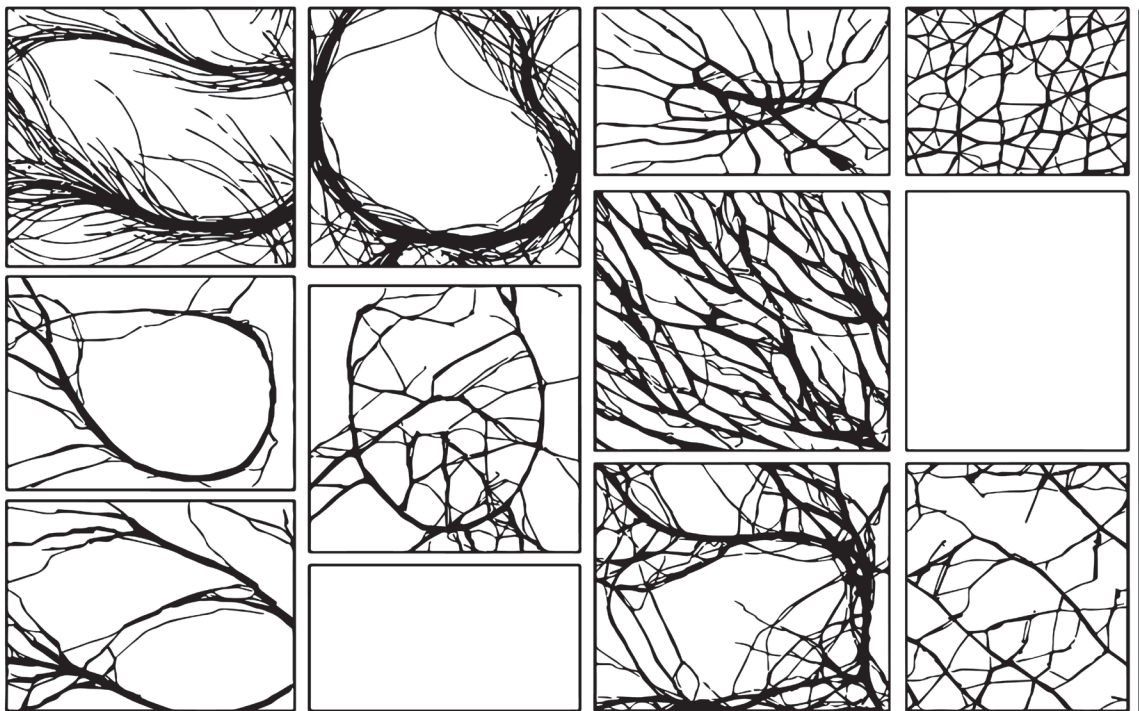


Figure 1: ABS movement network by processing.

Once the respective nodes were identified, the straight paths connected those nodes and formed an intersecting network (Figure 2: Row 1). The initial network was optimized using Frei Otto's wet grid method, which is a physics-based analog model. Instead of a simple "dumb" static network, each Control Vertex (CV) along a path became an active agent driven by the physics engine in Maya. The agent interacted with other CVs from neighboring lines based on the proximity, attraction, and collision. Maya Nucleus engine optimized the movement network based on the proximity and interaction of agents. The virtual environment was formed by a series of static collision objects including buildings and none-destructive topographic boundaries. As a reactive agent, every CV along a path was analyzed in its rela-

tionship to other CVs within the system. With ABS, the autonomous "action" of each path lied within modifying its CV point based on the repulsion or attraction to neighboring agents in addition to the environment itself. Over a period, a path organization was automatically formed as the agents stop and remain their positions.

With the external forces and interaction among agents, the autonomous "action" of each agent lied within modifying its movement based on the repulsion or attraction to neighboring agents in addition to the environment itself. A complex movement organization was automatically formed over time. Visually, the agents' trails appeared to be bent, deformed, and merged into one another based on their contextual relationships.

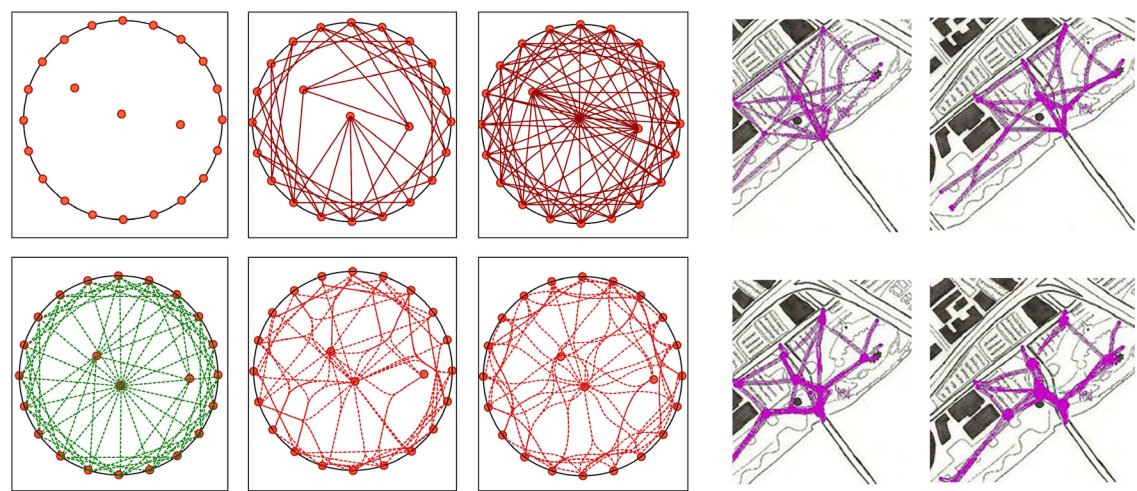


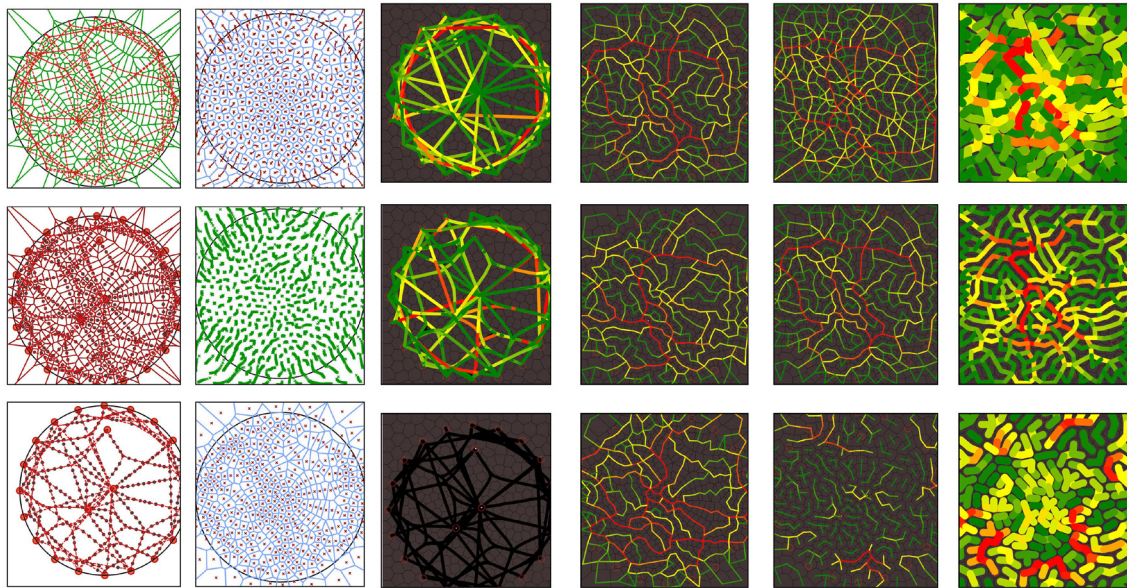
Figure 2: Row-1: Initial straight network. Row-2: Optimized Network.

2.2 Phase II: Blocks and Spatial Accessibility

Space syntax is a powerful method to study movement patterns and accessibility. A street is computed as a line, and open environment is calculated as a cluster of “cells” in space syntax. By using various spatial analysis tools, the accessibility of cells and lines can be measured. These simulated results are generated to measure spatial integration, accessibility, and other circulation related values. These qualitative values extracted from space syntax analysis can be combined with other data for further computation. We used Grasshopper script to apply the space syntax as a quick evaluation method to the self-organizing pattern generated in the first phase. The result was then translated into a raster

image, named “attraction map” representing the overall spatial accessibility. The raster image was combined with other maps and used later in Phase III to drive the urban form generation (Figure 3).

In this stage, the urban blocks were generated by the abstract self-organizing movement pattern from Phase I. We defined a block as a “placeholder” with an index value projected back to the attraction map. A Grasshopper script was used to extract the “attraction” value based on the index of each block.



2.3 Phase III: Urban Modeling

Besides the accessibility values from space syntax, various assumption data were added to the “attraction map” to represent development intensity, Floor Area Ratio (FAR), zoning, and other planning related quantitative attributes. These data were represented as various maps and combined with appropriate weight values. Each block can “read” its corresponding data

from a particular map and use the values to construct an urban model. For example, a building type map was created to control the building type. A building height map was used to control the levels of each building. A means-of-transit map was used to indicate the car usage. These maps guided the placement of buildings, green space, parks, and automatically filled blocks. The overlaid external data were understood as the changing

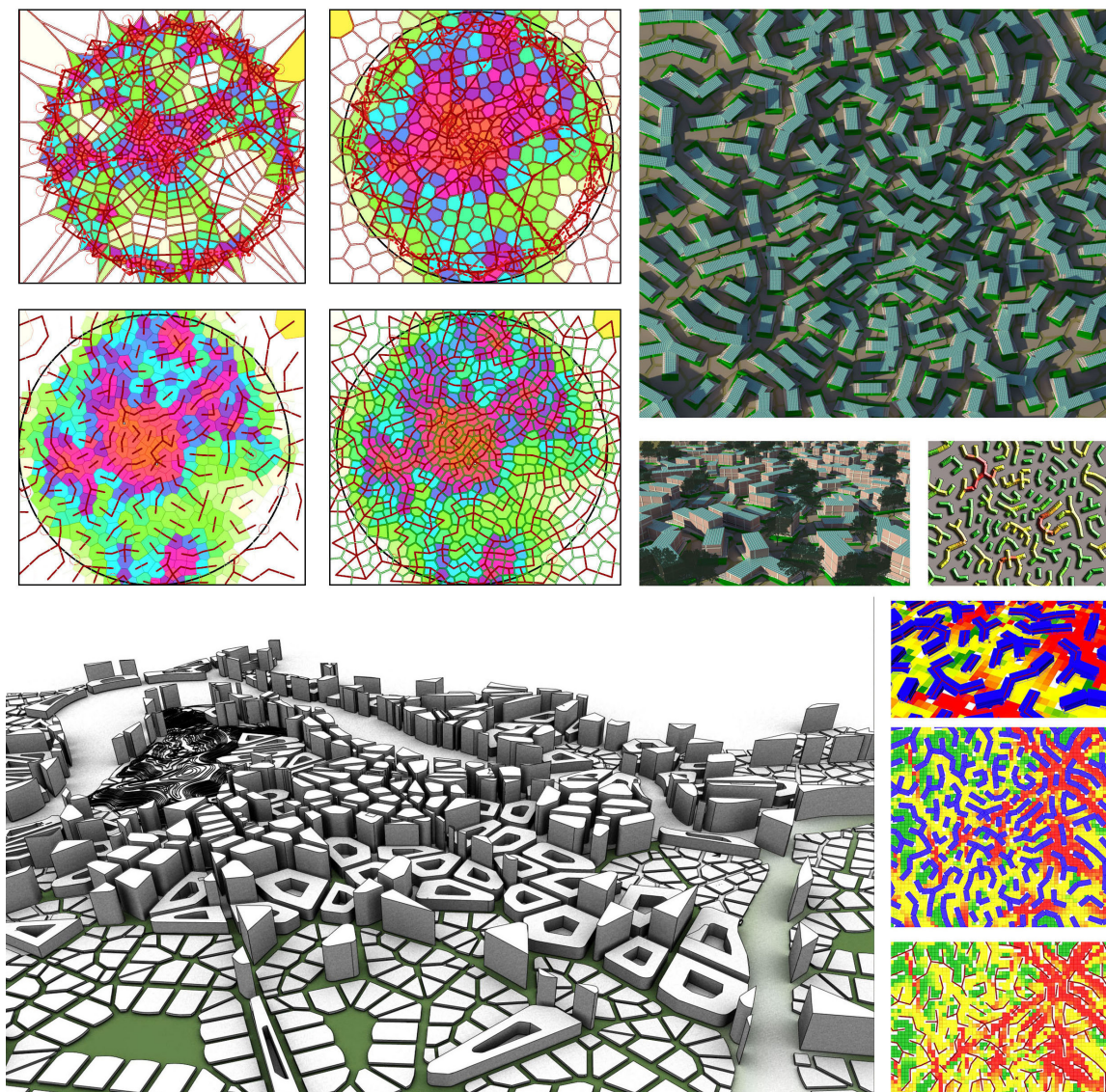


Figure 4: Phase III. An urban model constructed from 2D maps. Grasshopper script was used to populate various building types into the blocks.

scenarios over time. Similar to the design iterations, a large-scale urban model was constructed with flexible parameters of operation. Each scenario includes a set of changing variables. By changing values through a slider, an urban model simulated the growth from one scenario to another scenario.

3.0 PROJECTS APPLICATION

We applied the three-phase method to an urban design project sponsored by the municipal planning institute in Huanyuankou (HYK), Dalian, China. We were commissioned to design a 2,000,000 square meter district as a central hub and public space in the HYK economic zone, Dalian, China. Together with the multi-purpose buildings, the project required a mixed-use central business district blend with residential, commercial, business, tourism, and education programs. In our proposal, the idea of “slow life” and “slow movement” was realized by introducing bottom-up, self-organizing pedestrian network based on the existing attractions such as natural landscape, landmarks, and commercial centers. The three-phase ABS method was executed and produced organic movement pattern on top of the

existing recliner infrastructure. This new superimposed movement network serves as the stimuli to rebuilt vacant lots and relinks various green corridors back to the natural landscape. The self-organizing pattern and conceptual model were further developed by architects, urban designers, and planners to fit the local context and program needs.

We applied the network optimization and space syntax to create the attraction map. An intricate order of urban pattern emerged based on the microscale interactions among agents. Multiple Voronoi shaped blocks automatically adopted a set of rules based on both bottom-up movements as well as the top-down planning methods. The self-organizing pattern of the movement network emerged based on the connection between proposed landmarks and the proximity to the existing natural landscape. A microstructure oriented land use map as well as a transportation system for pedestrian and bike were achieved through ABS and space syntax. Then the traditional planning method was used to drive the further design decisions (Figure 5).

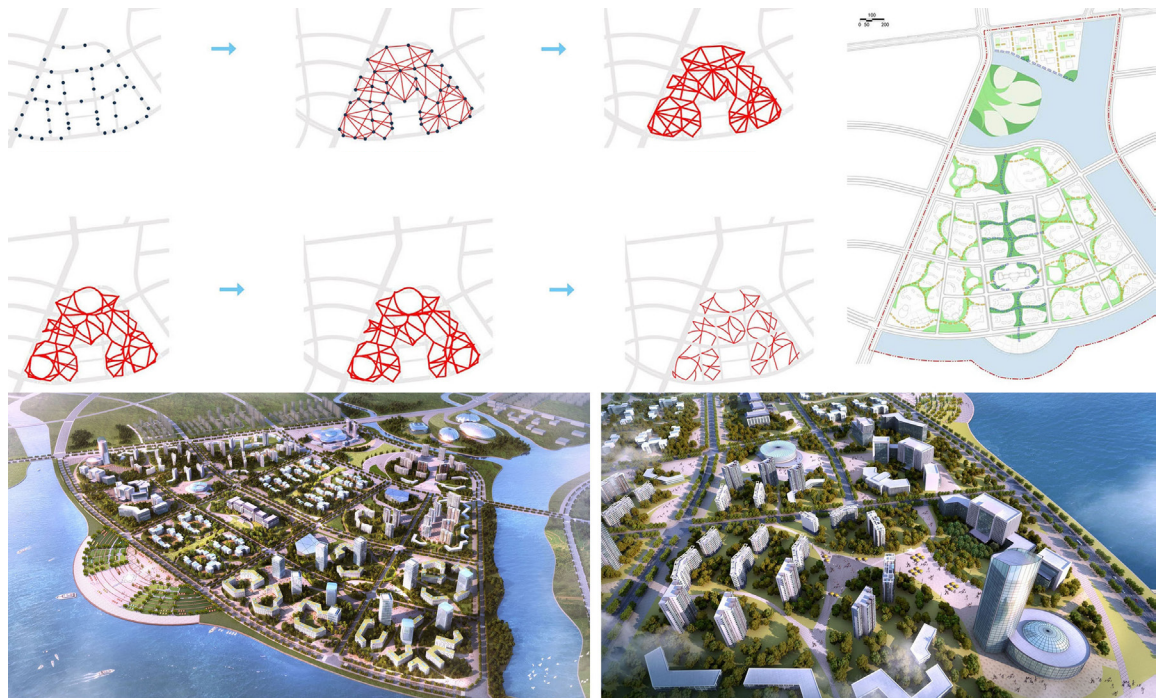


Figure 5: HYK district. To investigate the pedestrian movement in a complex spatial configuration, we evaluated and optimized the self-organizing pattern developed in ABS.

4.0 CONCLUSION

The research investigated how to integrate ABS into the urban design process and evaluate the result with space syntax. Compared with traditional top-down planning, this new method does not operate at the global level. It relies on the emergent properties and local interactions among agents. Together with traditional humanistic evaluation and ABS, a new relationship of designer and design agent has been forged. Within the process of ABS, the design is a result of the interaction between agents and their environment and the modulation of agents' behaviors within external rules. Our new ABS produced measurable improvement in the design. For instance, the ABS optimized curved network increased only three percent of traveling time compared to the original straight network. However, by joining and modifying paths into a new network, the overall length of the network was reduced by 43 percent. The optimization is significant for saving construction cost. In the HYK project in China, we applied ABS for path optimization. The initial straight network was generated by connecting existing urban nodes. We optimized the network to reduce the overall network length. The wet grid was used to create the pedestrian paths, bike route as well as the recreational areas. For the individual curved path, the traveling time was increased only three percent compared to the original straight path. The overall network construction length was reduced 35 percent - 45 percent compared to the straight network.

However, this method is not appropriate for the vehicular-based transportation design due to the small intersection angles. The optimized network is often irregular and different from the typical urban grid. Because the ABS is generated as a highly abstract in the micro level, we have to combine ABS with other transportation planning methods to construct a practical urban model in the later process. This post process can lead to confusion of the design logic and violate the early abstract model. The value of early ABS and the self-organizing solution was undermined.

There are other limitations in this method. The optimized network was evaluated by space syntax to facilitate design decisions such as land use, FAR, and development intensity. The one-way linear data flow was from ABS to space syntax, and eventually to the development intensity and land use. The early stage micro level ABS was isolated from the influence of space syntax evaluation. In an ideal situation, the space syntax analysis should be able to affect the ABS and serve as a feedback loop in a non-linear fashion. We are cur-

rently experimenting the genetic algorithm in Galapagos to integrate space syntax into the path optimization process. We are also investigating on importing geographic information system (GIS) data and other geospatial related "big data" into the "attraction map." The goal is to create a virtual urban laboratory allowing designers to manipulate environmental conditions and behaviors of artificial agents and test various design theories in both micro and macro levels.

Acknowledgments

The author would like to acknowledge the following individuals for their contributions: Dallas Puckett, Derek Morphew, James DiMeolo, Yiren Weng, Trey Meyer, Boer Deng, Guande Wu, Ladan Zarabadi, Xinhao Wang, Christopher Auffrey, Mingming Lu, Arefi Mahyar, Zhou Yang and the design team from Dalian Dushifazhan Institute in China.

REFERENCES

- [1] Batty, M., (2007). *Cities and Complexity, Understanding Cities with Cellular Automata, Agent-Based Models, and Fractals*. Cambridge, MA: MIT Press. pp. 210.
- [2] Baharlou, E, and Menges, A., (2013). "Generative Agent-Based Design Computation: Integrating Material Formation and Construction Constraints", *Proceedings of the 2013 Ecaade Conference*. pp. 165-174.
- [3] Biao, L., Rong, L., Kai, X., Chang, L., and Qin, C., (2008). "A Generative Tool Based on Multi-Agent System: Algorithm of 'HighFAR' and Its Computer Programming", *Proceedings of the 2008 CAADRIA Conference*. pp. 335-342.
- [4] Gerber, D. and Lopex, R., (2014). "Context-Aware Multi-Agent Systems", *Proceedings of the 2014 ACA-DIA Conference*. pp. 153-162.
- [5] Jones, J., and Adamatzky, A., (2014). "Computation of the Traveling Salesman Problem by a Shrinking Blob", *Natural Computing*, Vol. 12, pp. 1-16.

04.

URBAN MICROCLIMATES AND ENERGY EFFICIENT BUILDINGS

Pravin Bhiwapurkar, PhD, University of Cincinnati, pravin.bhiwapurkar@uc.edu

ABSTRACT

The challenges of a warm climate on urban buildings' energy needs for space conditioning are discussed by assessing the impact of intra-urban microclimatic changes, also called urban heat islands (UHI). This article analyzes the results of a simulation study on the energy consumption required for heating and cooling a small office building within five intra-urban microclimatic conditions of the Chicago metropolitan area. The study simulated a small office building per ASHRAE Standard 90.1-2013 with a whole-building energy simulation program and weather files that accounted for climatic changes due to urban development and synoptic weather conditions for selected locations. The results confirm that heating load decreases and cooling load and overheating hours increase as the office location moves from rural (less developed) to urban (developed) sites. However, these changes are influenced by the location's distance from downtown and from Lake Michigan. The article shows that prominent intra-urban climatic variations are an important factor affecting energy performance, examines detailed results for a typical small office located within the intra-urban climatic zones of the metropolitan area, and argues for the necessity of considering using weather files based on urban microclimates in designing buildings to safeguard their efficiency in the future.

KEYWORDS: lake effect, wind, cloud cover, solar radiation, heating and cooling energy

1.0 INTRODUCTION

Urban areas' climates are modified by high rates of urbanization resulting from drastic demographic, economic, and land use changes¹. These modifications include increasing temperature and changing wind speeds, precipitation patterns, cloud cover, and solar irradiance. The most significant modification is the creation of urban heat islands (UHI), a term that refers to elevated temperatures over urban (developed) areas compared to rural (less developed) areas. UHIs are commonly studied under calm wind conditions during sunny days and have been found to be more prominent during nighttime, when wind speed is relatively lower than during the day. Paved urban surfaces and their configurations—for example, streets, sidewalks, parking lots, and buildings—are crucial in the formation of UHI because they absorb heat during the day and release it during the night. The lack of vegetation also reduces evapotranspiration. When studied using satellite thermal infrared images, surface heat islands are more prominent where the albedo and emissivity properties of paved urban surfaces are often intensified; vertical

surfaces are often ignored². The role that vertical urban surfaces, such as building facades, plays within dense urban environments is measured by Sky View Factor (SVF), which looks at the surface exposure to the sky that influences surface thermal balance^{3,4}. In addition, the geography, topography, large bodies of water, land use, population density, and physical layout of the urban area all influence UHI⁵. Rapidly expanding urban boundaries constantly modify the rural landscape; the nature of the constantly evolving urban landscape also varies with land-use and land-cover changes. Furthermore, the increasing anthropogenic heat contribution of the urban environment is significant^{6,7} and includes waste heat from buildings, industries, and transportation⁷. Therefore, this article focuses on the need to recognize the broader and more complicated range of intra-urban climatic conditions that influence building heating and cooling demand. The goal is to inform engineers and architects about lake effects—wind, cloud cover, and solar radiation—so that buildings will be designed to be more energy efficient.

UHI modify microclimatic conditions, increase air pollution⁸, and exacerbate heat waves in urban areas⁶. Heat-related fatalities are observed globally⁹; in particular, the 1995-96 Chicago heat wave and the 2003 European heat wave are most reported in the literature. While the frequency of heat waves is increasing, mortality rates are decreasing where the use of air conditioners is prevalent¹⁰⁻¹². The increased use of air conditioners to counterbalance this warming effect subsequently increases buildings' waste heat contribution and adds warmth to the urban environment. Although warm urban conditions reduce buildings' heating energy needs, they increase cooling energy needs. Internal heat load-dominated buildings operated during the daytime, like office buildings, are significantly affected. Therefore, UHI increases summertime peak electric demand that adds to the burden on the existing power infrastructure and increases greenhouse-gas emissions. However, the variation in peak demand within metropolitan areas is less recognized and this study investigates such variations within its microclimates.

Most UHI studies on building energy needs present air temperature as the climatic variable for energy impact and suggest increasing vegetation and albedo of pavements and roofs for energy savings¹³. Studies have also reported on the impact of air temperature and relative humidity on heating and cooling energy needs¹⁴. The wind speed is often associated with nighttime UHI, which prevents transportation of urban heat absorbed during the daytime by urban thermal mass, allowing it to rise above the city. Thermal properties of paved surfaces and their spatial organization within urban form¹⁵ is critical for nighttime urban cooling. Buildings in warming climate benefit from night flushing and it is a suggested energy-saving strategy for office buildings¹⁶. However, variation in climatic elements within metropolitan area due to physical development and lake effect are less studied. For example, daytime and nighttime UHI variation, especially in the case of the Chicago metropolitan area, is not well established and has yet to show promising evidences¹⁷. Also, UHI studies are often reported during clear sky conditions with low wind speed; however, both of these conditions constantly change throughout the year.

To account for the combined influence of the urban environment and climate on building space-conditioning energy practices, especially in view of the synoptic weather conditions of the Great Lakes region, this article seeks answers to the following questions using average

climatic data over a 30-year period (1980-2010) recorded in Typical Meteorological Year-3 format:

- Do intra-urban or microclimatic variations exist in the study area and how do they vary seasonally?
- How do intra-urban microclimatic changes influence peak building energy use and peak demand?

2.0 METHODS AND MATERIAL

2.1 Context

The Chicago metropolitan area lies on the flat Lake Michigan plain (41°52' north and 87°37' west) with minimal elevation changes of 176.5 meters (579 feet) to 205.1 meters (673 feet) above sea level. Chicago has a humid continental climate, with an average mean air temperature from May to September of 25.9°C (1961–1990). In July and August, prevailing west-southwest (240°) winds average 13.2 km/h (8.2 mph) (1981–2010), transporting in warm humid air from the central and southern plains¹⁸. Tree cover plays an important role in moderating air temperatures in the region and the city of Chicago had an average tree canopy of 11 percent. Chicago falls within ASHRAE climatic zone 5A (cold and humid) and “Dfa”, humid continental (hot summer, cold winter, no dry season, latitude 30-60°N) per Köppen climate classification. While the 2010 population of the Chicago-Joliet-Naperville metropolitan statistical area was 9,461,105, the population of the city of Chicago was 2,695,598 per US Census. In 2010, Chicago had an average population density of 45.7 persons per ha (18.1 persons per acre) within the city limits. Researchers suggest that Chicago's current UHI patterns are likely to intensify with a warming climate and further urbanization in the region. This will significantly alter Chicago's micro-climate and increase its vulnerability to ecological and financial risks¹⁹.

UHI effect is typically studied under calm wind conditions on clear, sunny days (Figure 1), in which urban heat rises above the built environment and raises the air temperature of the downtown area. However, the Chicago heat island often appears in the western suburbs, not in the downtown area²⁰. The lake wind influences the transport of urban heat over the West Side development (Figure 2a). Gray and Finster reported an average about 3 to 5°F temperature gradient between Lisle (located between 2 and 5 in Figure 2) and downtown Chicago in the summer months (June through August) from 1992 to 1996²⁰.

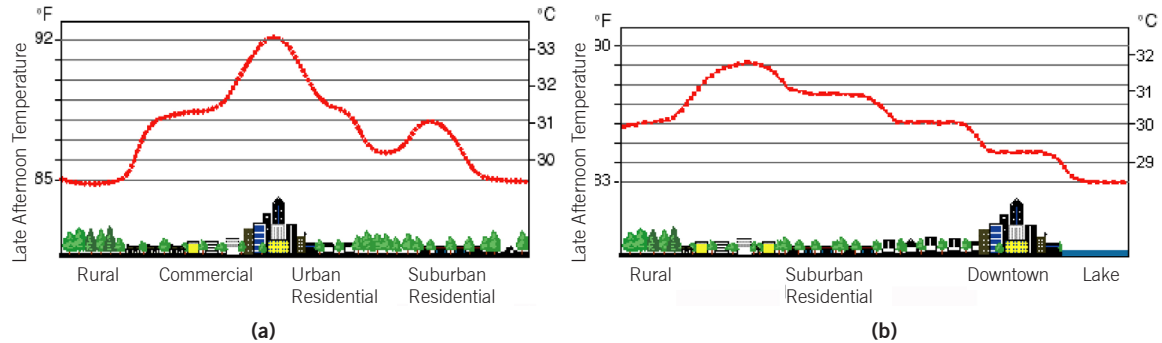


Figure 1: (a) Typical urban heat island profile under calm wind conditions and (b) Chicago's heat island profile²⁰.

2.2 Climatic Data: Sources and Suitability

The weather stations monitored by the National Climatic Data Center (NCDC) are selected for investigating climatic variations in the Chicago metropolitan area for quality purposes (Figure 2). These stations are located at varying distances from Lake Michigan: Waukegan is 3.37 miles away, Midway 9 miles, O'Hare 13.5 miles, DuPage 31.5 miles, and Aurora 45 miles. The hourly

climatic data obtained from these five weather stations in TMY-3 format are suitable for this study because they reflect the combined influence of land-use/land-cover changes, related anthropogenic heat from buildings, transportation and automobiles, and the lake effect²¹. In this way, the interaction of climatic variables and urban landscape is well accounted for in predicting energy needs.

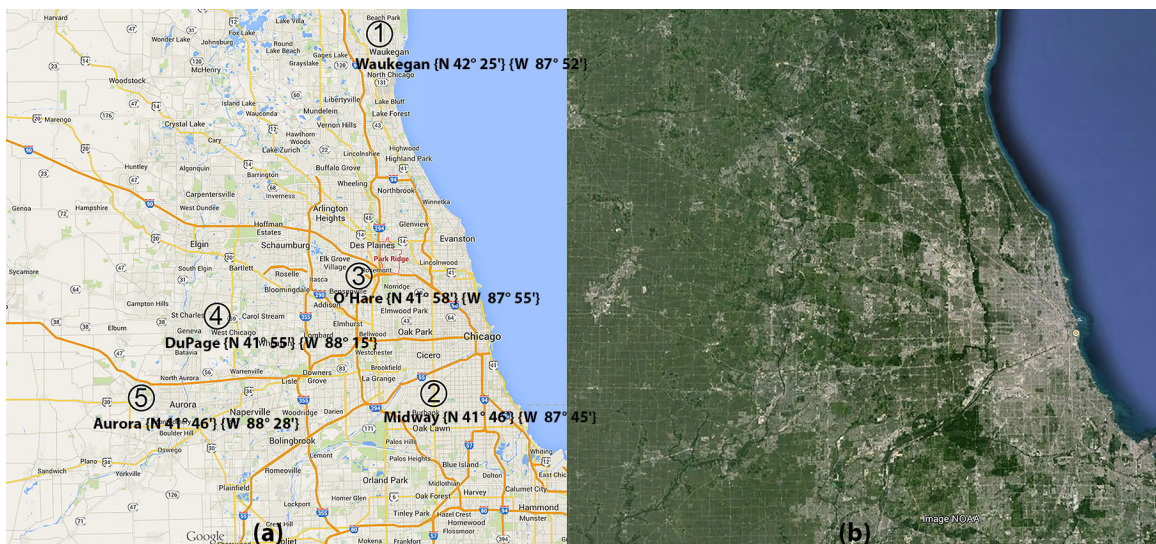


Figure 2: (a) Climatic data collection locations (Google Maps) and (b) LandSAT image of the Chicago metropolitan area showing urbanized to rural landscape pattern (Google Earth).

2.3 Physical Model Characteristics

A representative three-story, small-sized office building²² of 1366 square meters (14,700 square feet) is modeled per ASHRAE Standard 90.1-2013, Climatic Zone: 5A²³ and Appendix G requirements to estimate energy needs. The building footprint of 21.30 meters x 21.3 meters (70 feet x 70 feet) is chosen for orientation neutrality²⁴ in which 40 percent of the area is allotted for open office space, 30 percent for enclosed/private offices, 10 percent for corridors, and five percent for a conference room; remaining areas include a printing/photocopying room, a stairwell, and electric/mechanical rooms. The perimeter and core zoning pattern is adopted for energy-modeling purposes and perimeter zone depth is 3.65 meters (12 feet). The floor-to-floor height is 3.96 meters (13 feet) and clear floor-to-ceiling space is 2.74m (9 feet). The floor-to-floor glazing of 40 percent (27 percent for floor-to-ceiling) is equally distributed on all sides and includes internal blinds that are 20 percent closed during occupied hours and 80 percent closed when unoccupied. The opaque building constructions in the small- and medium-sized office prototype include mass walls, a flat roof with insulation above the deck, and slab-on-grade floors. Windows are defined as manufactured windows in punch-style openings. These envelope constructions are common for small-office buildings in the United States^{22,25} and are followed in the study. The building's operating hours are from 8 am to 5 pm Monday through Friday; it is closed on standard US holidays. Table 1 shows the building characteristics used for energy estimation purposes.

The baseline HVAC system for this building type and size and this climatic zone (5A) adopts ASHRAE 90.1-2013 Appendix G's suggestion on use of a (System3: PSZ-AC) constant volume packaged rooftop air conditioner. The space is conditioned by a packaged single-zone DX system with furnace. The efficiency of the packaged unit, EER, is 10 and the minimum efficiency of the furnace is 80 percent. Also, the natural gas nonresidential domestic hot-water system is modeled at 80 percent efficiency. The HVAC system maintains a 23.8°C (75°F) cooling set point and 21.11°C (70°F) heating set point during occupied hours. During off hours, the thermostat set point is 27.77°C (82°F) for cooling and 17.77°C (64°F) for heating. The economizer is set to maximum dry bulb temperature 70°F.

2.4 Comparison Method

The distance from Lake Michigan and from downtown are significant factors for intra-urban microclimatic variation. Among the selected locations, Waukegan is less urbanized, less populated, and closer to the lake. It is far north of downtown and is not influenced by the UHI. The West Side developments, where summertime UHI influences are significant, host other study locations. The variations in UHI and related building heating and cooling energy needs on the West Side locations are compared here with the Waukegan location.

Climatic changes. The temperature influences of UHI among the selected locations are compared seasonally, particularly during the extremely hot week identified by the NCDC. The summer months are particularly cru-

Table 1: Office building characteristics.

Envelope		Lighting (w/ft²)	
Roof	R-30ci (albedo 0.4, light)	Office (open/enclosed)	0.98 /1.11
Walls	R13+R10ci	Conference Room	1.23
Slab on Grade	R-15 for 24in	Restroom	0.98
Door	U-0.5	Corridor	0.66
Fenestration	U-0.42,	Mechanical	0.42
	SHGC-0.4	Copying Room	0.72
	VT-1	Plug Loads	0.75 ²⁶

cial due to an increase in cooling-related peak electric demand and energy. The summer months considered in this study are July through September; the winter months are January through March. The autumn and spring months are represented by October through December and April through June, respectively. The extremely hot week is from July 15 to 21 and the extremely cold week is from February 12 to 18. The average temperature of seasonal months is used to compare seasonal UHI. The average hourly temperature data is used to compare day and nighttime UHI. The day and nighttime hours are decided based on available global horizontal solar radiation, which is the sum of direct normal irradiance, diffuse horizontal irradiance, and ground-reflected radiation.

Annual energy use. A whole energy simulation program, eQUEST 3.65 (DOE, 2013), has been previously validated for its algorithm and published elsewhere, and is considered suitable for this study to estimate the energy performance of the small-office building, which was kept constant through the study. Keeping lighting, plug loads, and other energy needs constant throughout the study allowed the investigation to focus on shifting heating and cooling energy due to the changing climate. The weather files collected from the five stations in the Chicago metropolitan area were used to estimate intra-urban variations in energy use intensity (EUI), peak electric demand, and annual electric and heating energy use. The variations in intra-urban heating degree days (HDD) and cooling degree days (CDD) are also included in the study.

3.0 RESULTS AND ANALYSIS

The results and analysis of this investigation are presented in two sections: intra-urban climatic changes and building space conditioning energy needs. First, seasonal and diurnal temperature changes are discussed in relation to the lake effect and its impact on HDD and CDD. Second, microclimatic influences on energy use intensity (EUI), cooling energy, summertime peak demand, and heating energy are presented to inform decisions on energy efficiency of buildings.

3.1 Intra-Urban Climatic Changes

There is significant variation in average seasonal temperatures among all locations in Chicago metropolitan area. The average seasonal temperature includes hourly day and night temperatures for three months. The highest average temperature, 23.52°C, is observed during summer months at Midway; the lowest temperature, 20.6°C, is observed at Waukegan (Table 2). The temperature trends are opposite during winter months; DuPage (1.01°C) and Midway (-0.85°C) are warmer than Waukegan (-2.18°C). During spring months, DuPage (15.95°C) reports the highest temperature and Waukegan (13.42°C) is the lowest in the group. Although the average temperatures are lower at all locations during autumn, Midway reported the highest temperature at 7.13°C; Aurora showed the lowest among the group at -1.41°C. In general, average seasonal temperatures at Waukegan are lowest; thus it is a reasonable assumption for a baseline case when comparing intra-urban UHI.

Table 2: Seasonal UHI variation within the Chicago metropolitan area (°C).

	Waukegan	Midway	O'Hare	DuPage	Aurora
T (avg. summer)	20.60	23.52	21.34	20.54	21.44
ΔT (summer)		2.92	0.75	-0.05	0.85
T (avg. winter)	-2.18	-0.85	-1.11	1.01	-1.37
ΔT (winter)		1.33	1.07	3.19	0.81
T (avg. spring)	13.42	15.48	15.46	15.95	14.84
ΔT (spring)		2.06	2.04	2.53	1.42
T (avg. autumn)	3.37	7.13	4.00	3.89	1.96
ΔT (autumn)		3.76	0.63	0.52	-1.41

The highest seasonal intra-urban UHI variation among four locations is observed during autumn months and the lowest temperature variations are observed during spring months, ranging from 1.42°C at Aurora to 2.53°C at DuPage. When average temperatures are compared with those at Waukegan, the variation ranges from 3.76°C at Midway to -1.41°C at Aurora (Figure 3(a)). The negative temperature difference represents a cool island effect. This variation is consistent with its distance from the Lake Michigan as well as from the downtown area (Figure 3(b)). Thus, average wind direction and speed was analyzed at these locations. The average wind direction at Midway, O'Hare, DuPage, and Aurora is from southwest to northwest. The combined influence of wind direction and speed seems to minimize temperature gradient across the east-west axis, although industrial land use and a high percentage of paved areas exists in the West Side developments^{20,27}. Based on this observation, it is expected that the downtown area will remain warmer during autumn months, although further evidences will be helpful.

The summertime UHI intensity of 2.92°C is highest at Midway, while the West Side locations, DuPage and Aurora, show marginal differences of -0.05°C and 0.85°C when compared with Waukegan (Table 2). When com-

pared with Midway, the temperatures at O'Hare, DuPage, and Aurora are cooler by 2.18°C, 2.98°C, and 2.08°C. The lowest average summer temperature at DuPage is the most surprising result, as this location is on the West Side and closest to the center of the heat island reported by Gray and Finster²⁰. These summertime temperature trends, like autumn observations, do not follow previously published trends of warmer climate in the West Side developments. One of the significant influences is that the prevailing west-southwest wind, which averages 13.2 km/h, transporting in warm, humid air from the central and southern plains¹⁸, does not support the UHI phenomenon presented in Figure 1(b). In addition, while the major water body can provide summertime cooling, the distance of study areas from the lake may lessen its effect as evident in Figure 3(b). The lake's cooling influence also wanes in late summer when water temperature can reach as high as 26.7°C. The UHI effect is reported during day as well as night. Table 3 summarizes day and night average temperatures. The maximum seasonal day and night temperature difference (1.95°C) is observed at Aurora during summer, followed by spring (1.14°C), autumn (1.48°C), and winter (0.61°C). DuPage, O'Hare, and Midway follow a similar pattern, showing the lowest changes. Waukegan shows minimal change during the winter

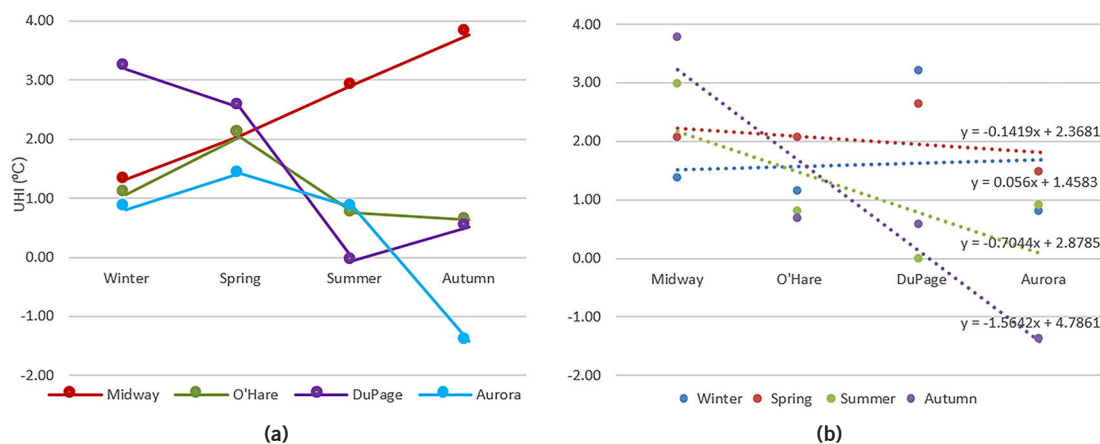


Figure 3: (a) Seasonal UHI intensities within Chicago metropolitan area and (b) UHI intensities in relation to the distance from the lake.

and autumn months (1.91 to 2.1°C), while the spring and summer months show temperature differences in the range of 3.44°C to 3.76°C, respectively. Table 2 and Table 3 provide the average temperature differences of the seasons. In order to investigate non-averaged temperature differences, this study delves into an extremely hot week.

The extreme summer week varies by location, so an overlapping period of two weeks, from July 13 to 26, is considered for this analysis as seen in Figure 4. During this time, the maximum daytime temperature (40.0°C) was recorded at Midway on July 24 (with standard deviation of 12.81°C). The peak demand for the office building is observed on the same day at the Midway location. Similarly, high daytime temperature increases peak electric demand, although dates vary among the selected locations. The highest day and night temperature difference is observed at Aurora (19.00°C) followed by Waukegan (15.20°C), Midway (14.00°C), O'Hare (13.30°C), and DuPage (13.00°C). The weekly average day and night temperature difference is highest at Aurora (13.00°C), followed by O'Hare (10.64°C), DuPage (10.31°C), Midway (9.21°C), and Waukegan (9.06°C). The higher nighttime temperature, which minimizes day and night differences, is an indication of nighttime

UHI. When compared with Waukegan, Midway shows high nighttime UHI and Aurora shows minimum nighttime UHI. Kolokotroni et al.¹⁶ suggest that warm nighttime temperatures can improve nighttime ventilation opportunities in office buildings in a warming climate. The warm nighttime urban temperature may potentially increase use of air conditioners during evening hours, especially in residential buildings. However, spring and autumn might provide the most opportunities to benefit from natural ventilation as an energy-saving strategy. Since the small-office building under study is operating during the day (8 am to 5 pm), this discussion focuses on daytime hours. The following section explores the UHI influences on predicted energy needs.

The variation in intra-urban climatic conditions is changing annual heating and cooling degree days for each location as shown in Table 4. Midway location represents the most modified urban climate and it is observed in highest CDD (691) and lowest HDD (3106) among other locations. In comparison to Waukegan, Midway has 70 percent higher CDD and 17 percent lower HDD. While CDD and HDD are representative of climatic zone and does not account for specific building condition that may have unique indoor climatic conditions, the building cooling and heating hours vary

Table 3: Average day and night UHI variation.

	Waukegan	Midway	O'Hare	DuPage	Aurora
T (summer day-night)	3.76	3.02	4.20	4.54	5.71
ΔT^* (summer day-night)		-0.74	0.44	0.78	1.95
T (winter day-night)	2.10	1.64	2.16	2.45	2.71
ΔT (winter day-night)		-0.47	0.06	0.35	0.61
T (spring day-night)	3.44	2.70	4.41	4.30	4.58
ΔT (spring day-night)		-0.74	0.44	0.78	1.95
T (autumn day-night)	1.91	2.06	2.47	3.38	3.39
ΔT (autumn day-night)		0.15	0.56	1.47	1.48

ΔT^* is estimated in comparison to Waukegan

significantly. The small-office building investigated in this study, shows 21 percent increase in building cooling hours and 22 percent decrease in building heating hours for Midway location. These changes are mainly due to external and internal gains. It is important to note that improved energy efficiency criteria of ASHARE 90.1-2013 allows for less building cooling hours (21 percent), however, it needs further study.

3.2 Building Heating and Cooling Energy Use

Energy Use Intensity (EUI). The annual building energy needs (gas, electric, and peak demand) of a three-story office building for selected locations in Chicago metropolitan area are discussed. For quality checks, the EUI at O'Hare location was compared with CBECS (2013) data for small buildings and then with EUI published by Pacific Northwest National Laboratory (PNNL) study on a small office building²⁴ that used a similar weather file. The EUI estimated at O'Hare in this study (26.75 KBTu/

ft²) is lower than in the published PNNL study (27.40 KBTu/ft²), which applied advanced energy-saving strategies. This change makes sense for small office buildings because the PNNL study adopted ASHRAE 90.1-2004 and applied the version of Advanced Energy Design Guide for Small Office Buildings available at that time. The highest EUI (6.863 kWh/ft²-yr) is observed for Midway, the lowest EUI (6.559 kWh/ft²-yr) at Waukegan. The simulation results for EUI at O'Hare (6.781 kWh/ft²-yr) and Aurora (6.796 kWh/ft²-yr) are very similar, whereas EUI (6.825 kWh/ft²-yr) at DuPage is slightly higher, similar to Midway. The annual electric energy needs shown in Figure 5(a) follow a similar trend. The energy consumption categories are lights, miscellaneous equipment (plug loads), space cooling, pumps and auxiliary, and ventilation fans. The building energy consumption at Midway is highest at 100,879kWh, compared to Waukegan at 96,424kWh. O'Hare and Aurora show similar results at 99,682kWh and 99,899kWh, respectively.

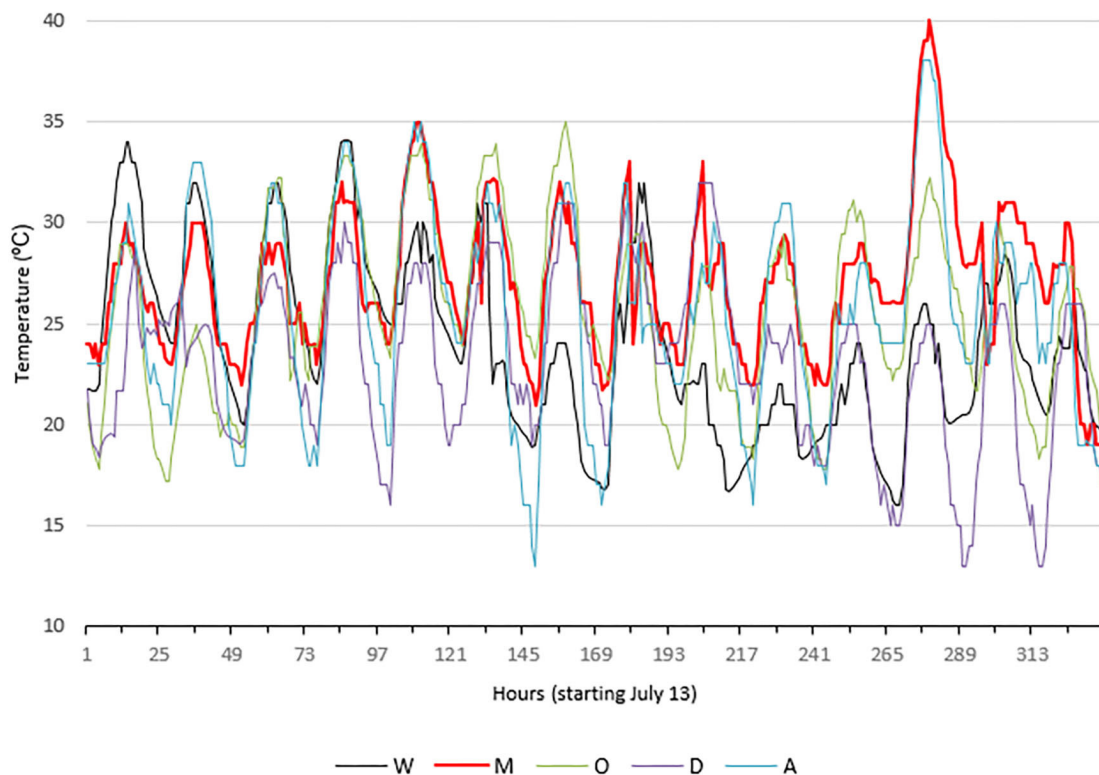


Figure 4: Day and night temperature variations during extreme summer week, July 13-26.

Cooling Energy. Cooling energy (kWh) needs are 34 to 37 percent of the total electric needs of the building. When annual cooling energy needs among Midway, O'Hare, DuPage, and Aurora are compared with Waukegan (Figure 5(a)), the energy needs are higher and cooling energy needs emerge as the most fluctuating energy category. In this category, the small office building at Aurora (28 percent) consumes the most energy, followed by Midway (27 percent), DuPage (24 percent), and O'Hare (19 percent). These variations are significant and affect overall EUI. Also, it is surprising to note that the Aurora location consumes more cooling energy than Midway. The main reason for such fluctuations is warm daytime starting conditions due to nighttime UHI as well as daytime UHI that is influenced by wind speed and direction in the metropolitan area. Furthermore, cloud cover plays an important role in the amount of global solar radiation received at these locations. Figure 6(a) shows the average hourly global horizontal solar radiation received at selected locations throughout the

year. Aurora receives the most solar radiation (386 w/m²), whereas Midway (200 w/m²) receives almost half that amount because of high cloud cover. This affects external heat gain at Midway compared to Aurora, while internal heat gain remains constant for all locations.

Peak Demand. Cooling-related peak electric demand is significant for all intra-urban locations. Annually, it constitutes 41 to 44 percent of total electric demand, except for Waukegan (38 percent). This contribution increases to 52 to 56 percent during summer months and 46 to 51 percent, and 39 to 44 percent during spring and autumn months, respectively. Midway location requires 56 percent of the peak demand for cooling during summer, which is not very different from Aurora (55 percent), DuPage (54 percent), or even O'Hare (52 percent). This data clearly indicates the relationship between temperature and peak demand: higher temperature increases peak demand, which can test the susceptibility of power infrastructure to extreme heat

Table 4: Annual heating and cooling degree days.

	Waukegan	Midway	O'Hare	DuPage	Aurora
CDD (18°C baseline)	407	691	506	523	444
Increase in CDD*		284 (70%)	99 (24%)	116 (29%)	37 (9%)
Building Cooling Hours	877	1065	1098	1097	1072
Increase in Building Cooling Hours		188 (21%)	221 (25%)	220 (25%)	195 (22%)
HDD (18°C baseline)	3747	3106	3430	3300	3629
Decrease in HDD*		-641 (-17%)	-317 (-8%)	-447 (-12%)	-118 (-3%)
Building Heating Hours	1329	1042	1188	1137	1133
Decrease in Building Heating Hours		-287 (-22%)	-141 (-11%)	-192 (-14%)	-196 (-15%)

* Changes in CDD and HDD are in relation to Waukegan location

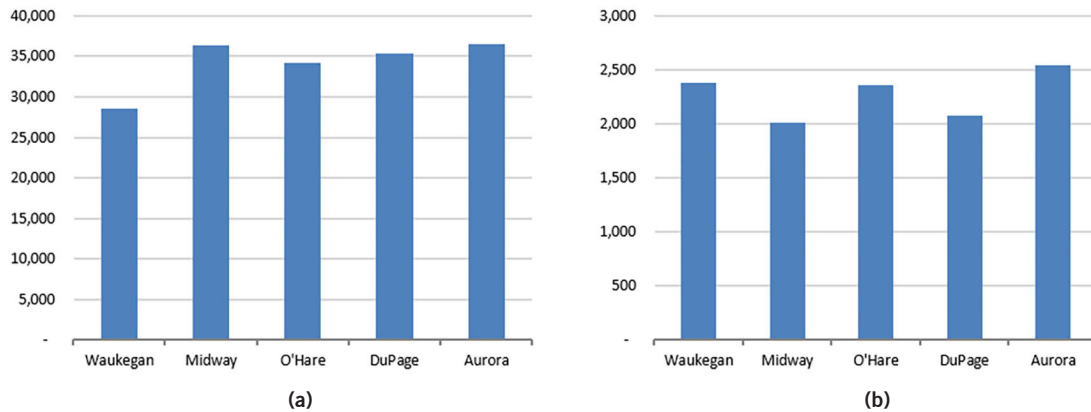


Figure 5: (a) Annual cooling energy (kWh) and (b) Annual heating energy (Therms).

events. One of the major influences of climate change in the built environment is increased extreme hot-weather (and cold-weather) events. Extreme hot-weather events are observed during the spring and autumn months as well: early heat waves are reported in April, late heat waves in October. Thus, early warming trends in spring show significant cooling-related peak demand. Aurora and O'Hare locations need 51 percent peak demand for cooling; Midway and DuPage are at 49 percent and 46 percent respectively. During the autumn months, the Midway location shows the highest cooling-energy contribution to peak demand.

Heating Energy. High heating-energy needs at Waukegan (2382 Therms) are not surprising because of the location's proximity to Lake Michigan. The lake tends to increase cloudiness and suppress summer precipitation in the area. Winter precipitation is enhanced by lake-effect snow that occurs when winds blow from the north or northeast. These winds allow air to pass over the relatively warm lake, boosting storm-system energy and water content and leading to increased snowfall. Similarly, the far West Side location of Aurora shows high (2539 Therms) heating-energy needs, as north or northeast winds do not seem to be influenced by the UHIs (i.e., the combination of land use, land cover, and anthropogenic heat sources) that are decreasing heating-energy needs at the Midway and DuPage locations.

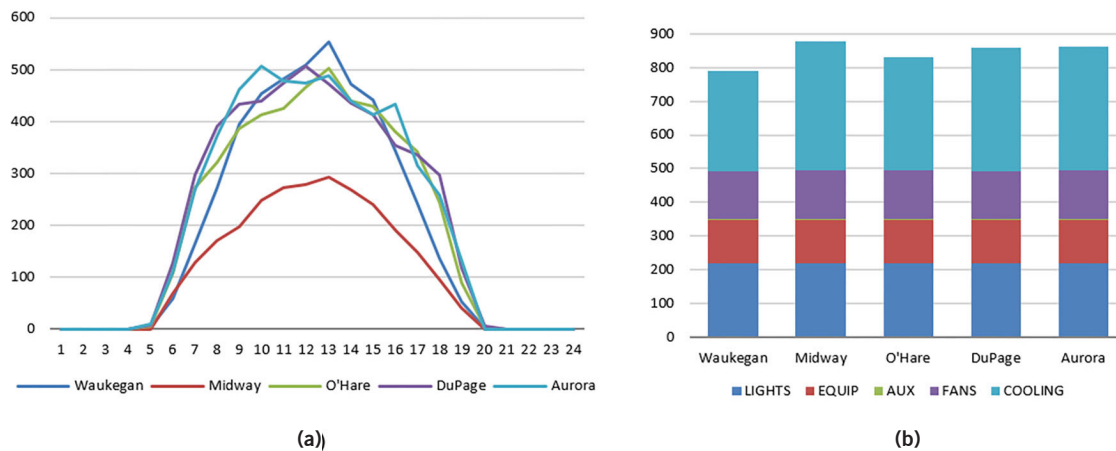


Figure 6: (a) Average hourly global solar radiation (w/m²) and (b) Annual Peak Demand (kW) distribution by major categories.

4.0 CONCLUSION

This article investigates two research questions, focusing on intra-urban climatic change and its impact on building space conditioning energy demand in the Chicago metropolitan area. Four intra-urban locations (Midway, O'Hare, DuPage, and Aurora) are compared with the baseline location, Waukegan. The average climatic data over a 30-year period (1980-2010) recorded in Typical Meteorological Year-3 format is used for this purpose and to help estimate building energy demand. There are prominent intra-urban microclimatic zones within the Chicago metropolitan area; UHI intensity varies by location, season, and on a day-night basis. Overall, average intra-urban temperature is warmer through the year. These following conditions are summarized:

- The highest UHI intensity was reported at the Midway location during the autumn (3.76°C) and summer (2.92°C) months.
- The highest UHI intensity during the winter (3.19°C) and spring (2.53°C) months was reported at the DuPage location.
- The distance of study locations from the lake, wind pattern, cloud cover, and solar radiation are influencing UHI through the year. A linear relationship of distance from the lake and UHI is particularly significant during autumn and summer months.
- The highest day-night UHI variation (19°C) during the extreme summer week was observed at Aurora location.

These intra-urban climatic changes modified CDD (18°C baseline) and HDD (18°C baseline):

- The highest increase in CDD (70 percent) was observed at Midway in comparison to Waukegan. O'Hare, DuPage, and Aurora also showed an increase in CDD by 24 percent, 29 percent, and 9 percent, respectively.
- The highest reduction in HDD (22 percent) was observed at Midway. O'Hare, DuPage, and Aurora also reported decreased HDD by 11 percent, 14 percent, and 15 percent, respectively.

The changes in CDD and HDD modified building energy use:

- Annual cooling-energy needs increased by 27 percent, 19 percent, 24 percent, and 28 percent at Midway, O'Hare, DuPage, and Aurora, respectively.
- Cooling-related peak energy demand increased by 20.62 percent, 1.69 percent, 5.12 percent, and 14.24 percent at Midway, O'Hare, DuPage, and Aurora, respectively.

- In contrast, heating-energy needs decreased by 16 percent, 1 percent, 13 percent, and 8 percent at Midway, O'Hare, DuPage, and Aurora, respectively.
- Cooling energy is significantly affected by microclimatic variation during summer and it can reach up to 52 to 56 percent of total building energy.

The most significant finding of this investigation is the introduction of less widely known key climatic factors: wind speed, cloud cover, and solar radiation and the lake effect as a powerful influence on energy demand and energy efficiency.

Failing to account for urban-microclimatic temperature differences may lead to errors that are too large to overlook. Further, certification of the performance of the buildings within the framework of a building energy-rating scheme like LEED certification be affected if local climate modifications are not accounted.

By providing evidence on existing intra-urban climatic change and its influence on changing energy needs, this study is useful for making informed design decisions while selecting energy-efficient passive and active design strategies for new and existing construction projects. This study provides insights for other lakeside cities and is useful for deciding on climate-responsive strategies that will safeguard the energy efficiency of future buildings.

This study can be advanced by testing passive and active design strategies suggested for the urban area's climatic zone. Its impact on various building types and scales will help evaluate energy efficiency in urban microclimatic conditions.

REFERENCES

- [1] Arnfield, A. J., (2003). "Two Decades of Urban Climate Research: A Review of Turbulence, Exchanges of Energy and Water, and The Urban Heat Island", *International Journal of Climatology*, Vol. 23, No. 1, pp. 1-26.
- [2] Lo, C. P., Quattrochi, D. A., and Luvall, J.C., (1997). "Application of High-Resolution Thermal Infrared Remote Sensing and GIS to Assess the Urban Heat Island Effect", *International Journal of Remote Sensing*, Vol. 18, No. 2, pp. 287-304.

- [3] Oke, T.R., (1988). "Street Design and Urban Canopy Layer Climate", *Energy and Buildings*, Vol. 11, pp. 103-113.
- [4] Erell, E., Pearlmutter, D., and Williamson, T.J., (2011). *Urban Microclimate: Designing the Spaces between Buildings*, Washington, DC: Earthscan.
- [5] Oke, T.R., (1987). *Boundary Layer Climate*, Vol. 2, New York, NY: Routledge.
- [6] Stone, B., Hess, J. J., and Frumkin, H., (2010). "Urban Form and Extreme Heat Events: Are Sprawling Cities More Vulnerable to Climate Change than Compact Cities?", *Environmental Health Perspectives*, Vol. 118, No. 10, pp. 1425-1428.
- [7] Sailor, D. J., (2011). "A Review of Methods for Estimating Anthropogenic Heat and Moisture Emissions in the Urban Environment", *International Journal of Climatology*, Vol. 31, No. 2, p. 189.
- [8] Hankey, S., Marshall, J. D., and Brauer, M., (2012). "Health Impacts of the Built Environment: Within-Urban Variability in Physical Inactivity, Air Pollution, and Ischemic Heart Disease Mortality", *Environmental Health Perspectives*, Vol. 120, No. 2, pp. 247-253.
- [9] McMichael, A. J., Woodruff, R. E., and Hales, S., (2006). "Climate Change and Human Health: Present and Future Risks", *Lancet*, Vol. 367, No. 9513, pp. 859-869.
- [10] Bobb, J. F., et al., (2014). "Heat-Related Mortality and Adaptation to Heat in the United States", *Environmental Health Perspectives*, Vol. 122, No. 8, pp. 811-816.
- [11] O'Neill, M. S., (2005). "Disparities by Race in Heat-Related Mortality in Four US Cities: The Role of Air Conditioning Prevalence", *Journal of Urban Health*, Vol. 82, No. 2, pp. 191-197.
- [12] Davis, R. E., et al., (2003). "Changing Heat-Related Mortality in the United States", *Environmental Health Perspectives*, Vol. 111, No. 14, pp. 1712-1718.
- [13] Akbari, H. and Konopacki, S., (2005). "Calculating Energy-Saving Potentials of Heat-Island Reduction Strategies", *Energy Policy*, Vol. 33, No. 6, pp. 721-756.
- [14] Kapsomenakis, J., et al., (2013). "Forty Years Increase of the Air Ambient Temperature in Greece: The Impact on Buildings", *Energy Conversion and Management*, No. 74, pp. 353-365.
- [15] Bhiwapurkar, P., (2007). Urban Heat Island Phenomenon, Urban Morphology, and Building Energy Use: The Case of Chicago, Chicago, IL: Illinois Institute of Technology.
- [16] Kolokotroni, M., et al., (2012). "London's Urban Heat Island: Impact on Current and Future Energy Consumption in Office Buildings", *Energy and Buildings*, No. 47, pp. 302-311.
- [17] Coseo, P. and Larsen, L., (2014). "How Factors of Land Use/Land Cover, Building Configuration, and Adjacent Heat Sources and Sinks Explain Urban Heat Islands in Chicago", *Landscape and Urban Planning*, Vol. 125, p. 117-129.
- [18] Angel, J., (2009). "Climate of Chicago - Description and Normals", Illinois State Water Survey, Retrieved on 11/20/2014 from <http://www.isws.illinois.edu/atmos/statecli/general/chicago-climate-narrative.htm>.
- [19] Weinstein, M. P., and Turner, R. E., eds., (2012). *Sustainability Science: The Emerging Paradigm and the Urban Environment*, New York, NY: Springer.
- [20] Gray, K., and Finster, M. E., (2004). The Urban Heat Island, Photochemical Smog, and Chicago: Local Features of the Problem and Solutions, Environmental Protection Agency.
- [21] Wilcox, S., and Marion, W., (2009). Users' Manual for TMY3 Data Sets, Golden, CO: National Renewable Energy Laboratory.
- [22] CBECS, (2012). Commercial Buildings Energy Consumption Survey 2012, Retrieved on 11/12/2014 from <http://www.eia.gov/consumption/commercial/reports/2012/preliminary/index.cfm>.
- [23] ASHRAE, (2013). ANSI/ASHRAE/IES Standard 90.1-2013 — Energy Standard for Buildings Except Low-Rise Residential Buildings, Atlanta, GA: ASHRAE.
- [24] Thornton, B., et al., (2010). Technical Support Document: 50% Energy Savings for Small Office Buildings, Richland, WA: Pacific Northwest National Laboratory.

[25] Richman, E. E., et al., (2008). National Commercial Construction Characteristics and Compliance with Building Energy Codes: 1999-2007, Richland, WA: Pacific Northwest National Laboratory.

[26] Mercier, C., and Moorefield, L.,(2011). Commercial Office Plus Load Savings and Assessment, California Energy Commission.

[27] Konopacki, S., and Akbari, H., (2002). Energy Savings of Heat-Island Reduction Strategies in Chicago and Houston, Berkeley, CA: Lawrence Berkeley National Laboratory, Environmental Energy Technologies Division.

05.

APPLES TO ORANGES:

Comparing Building Materials Data

Liane Hancock, Louisiana Tech University, lianeh@latech.edu

ABSTRACT

Why does no digital platform attempt to present all performance and sustainability characteristics for building materials in a way that side by side comparison is possible? Is the breadth of data too difficult to model? If the data could be visualized, what would it reveal? This article describes a digital platform with criteria that represents: look and feel; performance criteria; sustainability metrics; ecolabels and LEED points; access to materials safety data sheets, health product declarations, and environmental product declarations. With more than two hundred criteria, this populated model produces information at the scale of big data. Visual analysis of an initial input of data is most surprising in the area of sustainability, revealing significant voids in data and emerging patterns of disclosure.

KEYWORDS: materials, big data, sustainability, performance

1.0 INTRODUCTION

The building industry relies on the materials sector, which consists of a highly distributed network of companies that are loosely affiliated. Unlike the airline industry, the building materials sector cannot depend upon big manufacturers for standardization in publication of data. Ranging in size from boutique companies to architectural divisions within large multi-national conglomerates, each manufacturer approaches their communications differently and comparison between products is nearly impossible.

This article begins by investigating the specific issues that make the comparisons of sustainability and performance metrics problematic. It discusses the isolation of industries with regards to report of data and the range of terminology that results. This article then asks two questions. Could a single model map all the sustainability criteria being used within the building materials sector? What would visualization of the data reveal about the sector? To assemble the model, we analyzed a range of materials sustainability standards, isolating and listing their criteria. Analysis of individual materials allowed for the real time input of additional criteria, producing a

model that dynamically adjusts to changes in the sector. We populated the database with an initial set of seventy building materials to show the quantities of data published publicly by manufacturers. Selected across industries, this data represents both interior and exterior materials in an effort to mirror the sector. Visualizing this data reveals a landscape of big data fraught with substantial voids in information, interlaced with portions of the sector embracing publication of data and harmonization.

2.0 DATA DIALECTS

The data that manufacturers present on their materials is tailored specifically to their individual industry, such as the carpet or glass industry. The terminology and distribution of information isolates these industries from users and from each other. Each industry speaks its own dialect, and there is no infrastructure that gathers and presents these varying terms in a single platform. While this article emphasizes sustainability criteria, the database also includes performance attributes. A discussion of these attributes provides a good illustration of this variation in terminology. The terms used to describe performance attributes are highly specific, but the

words themselves are barely distinguishable. Color fast, fade resistant, lightfastness, and UV resistance relate to degradation of materials by the sun. The carpet industry and the upholstery industry differentiate the terms because of the specific effects upon their products, but, this vocabulary is nearly homogenous to anyone else. The healthcare industry distinguishes between antibacterial, bacteria resistant, and bacteriostatic; necessary

differentiation, but confusing to the uninitiated. For fire resistance, materials bear the label Class 1, 2 or Class A, B, C depending on level of flame spread. The numeric system applies to materials like gypsum board, plywood, and carpet while the alphabetical system applies to roofs, ceiling tiles, some countertops, and wall-covering. Figure 1 provides a list of all performance attributes cataloged during this study.

PERFORMANCE ATTRIBUTES






PERFORMANCE	 Moisture	Absorbent Porous Wicking Treated/Sealed Water Resistant	Waterproof Impervious Moisture Resistant
	 Acoustic	Sound Reflecting Sound Diffusing Sound Absorbing Sound Deadening	
	 Fire	Fireproof Fire Retardant Fire Resistant Flame Retardant Flame Resistant Heat Resistant	Smoke Resistant Self Extinguishing Fire Suppression Class A, Class B, Class C Class 1, Class 2
	 UV (SUN)	UV Resistant Fade Resistant Color Fast Lightfastness	
	 Durability & Resistance	SURFACE RESISTANCE Bulletproof Puncture Resistant Impact Resistant Scratch Resistant Sag Resistant Wear Resistant Stain Resistant Soil Resistant ANTISTATIC Anti-Static Static Control FRICTION Skip Resistant Skid Resistant Slip Resistant	CHEMICAL Anti-Corrosive Chemical Resistant Bleach Resistant Acid Resistant BACTERIA Antibacterial Bacteria Resistant Bacteriostatic Bactericidal Non-Porous Mildew/Mold Resistant Antimicrobial Anti-Allergenic

Figure 1: Performance criteria cataloged during this study.

2.1 Categorizing Sustainability Attributes

Sustainability attributes describe a wide, yet precise range of criteria. Because the language that describes these attributes is similar, it is difficult to distinguish each attribute from the others. To organize the attributes, we categorized and differentiated them based upon: environmental impacts adopted by existing standards and databases; attributes across life cycle phases; and a method for representing different levels of implementation, from qualitative statements to quantitative metrics.

Across existing materials sustainability standards and materials databases, environmental impacts typically divide into six categories: resource use, energy use, human health and toxicity, emissions, water use, and social accountability. We adopted this logic of categorization for the model. Each environmental impact divides into subcategories. The terminology within these subcategories is particular; but it is also similar enough that it becomes difficult for the layman to distinguish unless seen side by side. For example, materials may present data on resource impacts such as recycled content and reclaimed content, or, in another example, biologically based content and rapidly renewable content. The differences between these attributes are significant, but the language is similar enough to cause confusion. The model also considers environmental impacts across stages of lifecycle: acquisition, manufacturing and construction, use and maintenance, and end of life. All stages pertain to some categories, while other categories limit their application to only certain stages. For instance, energy use generates criteria across all stages, whereas resource use primarily produces criteria across acquisition and disposal.

Different industries and their products use widely different resources, and at different stages. Some require

large amounts of raw materials, others are energy intensive, and still others significantly impact water resources. Criteria that do not impact an industry are retained in this model, not deleted. Recording the lack of impact is significant in creating a complete picture for each industry, and providing the opportunity for comparison across industries.

The model also characterizes criteria based upon measurability: disclosure such as published audits and materials formulation; qualitative attributes such as policy or goal based criteria; relative metrics such as reduction in terms of numeric percentage, for instance reduction in energy use over a stated period of time; and quantitative metrics such as specific numeric limits or bans.

With regard to toxicity and human health, and emissions impacts, this method translates industry recognized benchmarks into the following levels¹: disclosure, reduction, and ban across red lists, chemical families, and specific chemicals. Existing lists include Living Building Challenge, EPA, LEED, and Perkins+Will Precautionary List. Individual chemicals and chemical families are currently listed in the model as building materials are input. At a later date, the expectation is that a list of chemicals will be input into the database. Crowd sourced research projects, such as Tox21 by the National Institutes of Health and Environmental Protection Agency, seek to test the toxicology of chemicals used in manufacturing processes. Eighteen hundred reports were released in 2014². The goal is to release data on ten thousand chemicals, a number easily accommodated by the database discussed in this article.

Figure 2 provides a list of all sustainability attributes included in the model.

SUSTAINABILITY ATTRIBUTES

SUSTAINABILITY ATTRIBUTES	 <p>Resource Use</p>	<p>Recycled Content: Post Industrial, Post Consumer Reclaimed/Reused Content Biologically Based Content Rapidly Renewable Content Wood Sourcing Verification Biodegradability/Compostability</p>	<p>Designed for Disassembly Dematerialization Recovery Program: Material, Product, Waste LCI Reductions Raw Material Extraction Impact Study Publicly Disclosed Material Inventory</p>
	 <p>Energy</p>	<p>Energy Use: Reduction, Limits Embodied Energy Renewable Energy Offsets Energy Recovery</p>	<p>LCI Reductions: Energy Efficiency Publicly Disclosed Strategy Energy Use Publicly Disclosed Energy Audit</p>
	 <p>Toxicity Human Health</p>	<p>Public Disclosure of Toxins, Reduction of Toxins, Ban of Toxins: Through Red Lists, Chemical Families, Specific Chemicals</p>	<p>LCI Reductions Publicly Disclosed Material Formula Third Party Toxicology Assessment</p>
	 <p>Toxicity Media Pollutants</p>	<p>Public Disclosure of Emissions, Reduction of Emissions, Ban of Emissions: Through Red Lists, Chemical Families, Specific Chemicals</p>	<p>Embodied Carbon LCI Reductions: Climate Change Emissions</p>
	 <p>Water Use</p>	<p>Water Consumption: Public Disclosure, Reductions, Limits Net-Zero Water Waterfootprint Water Recycling</p>	<p>Waste Water Quality Body of Water Protection LCI Reduction: Eutrophication LCI Reduction: Water Use Reduction</p>
	 <p>Social Accountability</p>	<p>ISO Compliant Environmental Management System ISO Compliant Quality Management System Employee Training for Ethics</p>	<p>US Labor Practices Adopted at All Global Facilities Supplier Assessment and Verifications Public Statement of on Non-Discrimination Labor Force Metrics Reported</p>
CERTIFICATIONS	<div> <div> ABNT Ecolabel Austrian Ecolabel Blue Angel China Environmental Label Cradle 2 Cradle Eco Logo EU Ecolabel GECA German TUV Green Circle Green Seal Green Squared Green Tag Certified Greener Product Certification Seal GSA Advantage Environmental Products ICC-ES Save Level Natureplus New Zealand Environmental Choice Nordic Swan </div> <div> NSF 140, 332, 336 SCS Environmentally Preferable Product SMaRT ULE Sustainable Product UN Global Compact EnerGuide Energy Star Energy Guide BASTA eco-INSTITUT Eurofins Indoor Air Comfort FloorScore Green Label Greenguard Air Quality Hazardous Substance Free Mark Indoor Advantage Sustainable Choice AUB-Zertifkat BRE Certified Environmental Profile Ecomark India, Japan </div> <div> Green Tick NSF Environmental Claims Verification USDA Biobased Product USDA Biopreferred Carbon Free Certified Carbon Reduction Label Cleaner and Green Certification Climate Cool Climatop BPI Compostable OK Compost Smart Watermark WaterSense WaterWise American Tree Farm System CSA Sustainable Forest Management FSC Chain of Custody Certification PEFC Sustainable Forestry Initiative </div> </div>		
USGBC LEED	<p>Sustainable Sites Water Efficiency Materials and Resources Indoor Air Quality Innovation in Design Regional Priority</p>		
DOCUMENTATION	<p>Health Product Declaration Environmental Product Declaration Life Cycle Assessment Material Safety Data Sheet</p>		

Figure 2: Sustainability criteria included in the model.

2.2 Standards and Certifications

To create value for a manufacturer's environmentally sustainable efforts, many companies seek certification for their products. There are dozens of standards organizations that issue certifications: Cradle2Cradle, GreenGuard, Nordic Swan, EU Ecolabel, and FSC are just a few. The number and variety of certifications creates confusion. In addition, the standards organizations and their certifications have non-descriptive and indistinguishable names, insignia, and seals, and often these names and graphics are tangentially related to what is being evaluated. With the exception of Energy Star and FSC, standards organizations and their certifications bear little name recognition, except within their specific sector. In 2014, UL Environment published the white article "Claiming Green", which asserts "Not all certifications marks are created equal. Some are actually difficult to decipher, either because the name doesn't explicitly convey the meaning or because they don't include qualifying language that specifies the exact environmental benefit they measure"³.

Standards organizations certify only a small percentage of market-share across products. Evaluating SMaRT, and Cradle2Cradle, both multi-attribute standards that certify a wide variety of materials, and NSF 140, a multi-attribute standard pertaining to the carpet industry, as of 2015: SMaRT had 65 certified products (29 pertaining to furniture, 31 manufacturers, and last updated November, 2012)⁴; Cradle2Cradle had more than 2000 certified products, of which 130 were building materials and supplies, and 120 were interior design materials and furniture, making a total of 250 materials related to the building industry⁵; and NSF140 had 28 carpet product platforms⁶.

Manufacturers choose which criteria they fulfill to achieve the threshold of certification, and then both certifiers and manufacturers do not reveal this information publicly. Many standards award certification at levels, silver, gold, platinum, but these levels of evaluation do not transfer across certifications, adding to opaqueness. Unlike certifications that focus only on a building product, BREEAM and USGBC LEED are different: they certify an entire building. For example, LEED criteria emphasize how materials, products, and systems behave in a building once they are installed, with a small number of criteria focusing upon the sourcing of building materials. Across the 110 criteria Material & Resources environmental product declaration, sourcing of raw materials, and material ingredients, and Indoor Environmental Quality Credit low emitting materials are

the main credits that pertain to materials⁷. This is like trying to define manufacturers' efforts on sustainability through a language of nine words.

2.3 Differentiating this Platform from Other Building Material Databases

Materials databases such as MaterialConnexion, materia.nl, and the UT Austin materials lab provide data on material look, feel, and performance, but are largely silent on sustainability. EcoScorecard offers a database of more than 30,000 materials, but limits sustainability information to LEED points. BEES and Pharos go into great detail evaluating the toxicity of materials, but are silent on other environmental impact categories. Databases that link to building information modeling provide life cycle assessment data that is numeric, calculable, and intended for comparison. However, such tools do not represent qualitative attributes including manufacturer led goal-based initiatives or percentage reductions in environmental impacts over time; nor do they provide data across all environmental impacts. Paula Melton states, "What's typically referred to as a 'whole-building LCA' is in fact nothing of the kind; the term is used loosely to describe a variety of assembly- and building-level analyses that may or may not include typical LCA impact categories... and may in fact only look at the construction phase of the building"⁸.

Our model is not a standard; it is a database. Each entry presents information published by manufacturers on sustainability attributes for a building material. The format organizes the data for a material on a single page; it also allows for comparison between materials. Users can evaluate the sustainability of different materials for the same product application. For instance, it can simultaneously provide data for a perforated metal panel system, a wood louver system, and a terracotta rain screen. The platform can also be used to investigate the sustainable attributes of different industries that have similar processes. For example, a user can compare reported data on energy usage during the manufacturing process for ceramic and glass products.

3.0 RESEARCH METHODS

In order to fully describe the range of building materials attributes, it was necessary to design a model for the data that presented: look and feel; performance attributes; sustainability metrics; ecolabels and LEED points; and access to material safety data sheets, health product declarations, and environmental product declarations.

3.1 Creating a Dynamic Environment and Listing Criteria

To design the database, the team at Louisiana Tech University developed a traditional, static, hierarchical taxonomy for attributes such as material makeup, translucency, texture, and finish. When describing performance and sustainability criteria, however, a heuristic method became necessary. While a selection of specifications and standards provided the bulk of the criteria, no one source of information provided all the possible terms. Plus, additional terms became apparent with the individual entry of materials. If the database was implemented as a static tool, the attributes would be limited to what existed at the time that the database was initially modeled. Instead, the model is a dynamic environment. Attributes can be added in real time, and made available to all materials already existing in the database.

To build the sustainability portion of the database, we aggregated sustainability criteria from eight materials sustainability standards: Cradle2Cradle, SMarT, EU Flower, Good Environmental Choice Australia, Nordic Swan, NSF/ANSI 140, BIFMA, and NSF/ANSI 336. This selection of standards was based on a study completed at Washington University in St. Louis, in 2011, in which the author was a participant. These certifications broadly represented the material sustainability certification landscape, and criteria focused upon the stages of resource extraction, manufacturing, and end of life phases. These standards were analyzed, isolating the criteria required to achieve certification. Each criterion for the standard was listed, establishing sub-categories within the six environmental impacts categories. The model also included: ecolabel and certification; LEED criteria; and criteria emphasizing sustainability during the use and maintenance stage of lifecycle assessment.


3.2 Design of Data Management

The innovation in the design of the database is that the platform accommodates so many types of information. The team recognized that each sustainable attribute can be described with the same four characteristics: a unique name for each attribute, which is common across all building material entries; whether the attribute is measureable; if it is measureable, one or more data entries; and a list of unit(s) associated with the attribute, so that the user can select the appropriate unit of measure for the specific data entry. In addition, each attribute is categorized as an ecolabel/certification, environmental impact based on life cycle stage, or LEED criterion.

Depending upon the type of attribute, the database provides different subsets from the master unit list. For Post-Consumer Recycled Content, a percentage as unit is appropriate. For Dematerialization, a percentage (of decrease in material) and numeric entry of start date to end date, in years, is appropriate. For Embodied Energy, the unit is energy unit/product unit, so for example btu/ft². In the case of this example units include: energy unit/linear dimension, energy unit/area, and energy unit/volume such as btu/linear foot, btu/ft², btu/ga; including both Imperial and Metric units. By providing an array of units tailored to the specific attribute, data entry is greatly simplified. In addition, a user may select a specific unit type and the database can automatically recalculate and display within that system (Imperial to Metric and Metric to Imperial), facilitating comparison between materials (Figure 3). Exceptions from this structure are toxicity and emissions. In such cases each named attribute requires selection from a drop down menu of emissions terms, redlist(s), chemical family (or families), or individual chemical(s), with each subsequent selection allowing further numeric entry and choice of corresponding unit (Figure 4).

3.3 Design Selection and Populating the Database

The initial dataset of 70 building materials represents both interior and exterior applications. Application, such as exterior cladding or glazing serves as a way to group materials with a range of manufacturers representing each application. The initial dataset included at most one material per manufacturer. Only the data represented on the manufacturer's website in conjunction with environmental product declaration, life cycle analysis, health product declaration, and material safety data sheet furnished information for the model. No assumptions about data were made. For instance, even though silica is locally sourced by the glass industry, glass manufacturers' websites do not mention regional priority; therefore that data was not included. In an effort to represent the range of data that manufacturers publish on sustainability, our selection incorporated a preponderance of manufacturers considered leaders in sustainability. Approximately 17 percent of the 70 materials entered carry a health product declaration, environmental product declaration, and/or life cycle assessment.



plug into the hub.

HOME MAIN SITE MY ACCOUNT MATERIALS LOGOUT

SUSTAINABILITY FOR: CF FLUTED

SUSTAINABILITY: CERTIFICATIONS »

SUSTAINABILITY: PRODUCT DECLARATION »

SUSTAINABILITY: EXTRACTION, MANUFACTURING, USE, END OF LIFE »

RESOURCE USE

☐ Recycled - Post Industrial

☐ Recycled - Post Consumer Content

☐ Reclaimed/Reused Content

☐ Rapidly Renewable Content

☐ Biological Material Content

☐ Wood Sourcing Verification

☒ Biodegradability/Compostability

Enter a Value

%

▼

Start Date

TO

End Date

☒ Recyclability/Designed for Disassembly

64

%

▼

☐ De-Materialization

☐ Material Recovery Program

☐ Product Recovery/Reuse Program

☐ Waste Recovery

☐ LCI Reductions

☒ Raw Material Extraction Impact Mitigation Study

Yes

▼

☐ Publicly Disclosed Material Inventory

☐ Waste Reduction

☐ Abundant Materials

ENERGY USE

☐ Energy Consumption Limits

☐ Reduction: Energy Consumption

☒ Renewable Energy

6

%

▼

Figure 3: Data entry screen for Resource Use Impact Category. Data is for specific insulated metal panels.

TOXICITY - MEDIA POLLUTANTS			
<input type="checkbox"/>	Ban of Emissions		
<input type="checkbox"/>	Ban of Formulation/Emissions: Red Lists		
<input type="checkbox"/>	Emission Limits		
<input type="checkbox"/>	Reduction: Total Toxic Air Emissions		
<input checked="" type="checkbox"/>	Public Disclosure Emissions Reporting	<input checked="" type="checkbox"/> Abiotic Depletion Potential .00032 kg/m2	
		<input checked="" type="checkbox"/> Acidification Potential (SO2) .1722 g/m2	
		<input type="checkbox"/> Embodied Carbon (CO2) Enter a Value g/m2	
		<input checked="" type="checkbox"/> Eutrophication Potential .0182 kg/m2	
		<input checked="" type="checkbox"/> Global Warming Potential 882.6 kg/m2	
		<input type="checkbox"/> Nitritification Potential (PO4) Enter a Value g/m2	oz/oz
		<input type="checkbox"/> Ozone Creation Potential (C2H4) Enter a Value g/m2	lb/qt
<input checked="" type="checkbox"/>	Reduction of Toxins: Specific Chemicals	<input type="checkbox"/> 1,2-dichlorobenzene Enter a Value % Start Date TO End Date	lb/ga
		<input type="checkbox"/> 1,1,1,2-tetrafluoroethane (R-134a) Enter a Value % Start Date TO End Date	lb/ft2
		<input type="checkbox"/> acrolein Enter a Value % Start Date TO End Date	lb/ft3
		<input type="checkbox"/> Acrylonitrile Enter a Value % Start Date TO End Date	lb/lb
		<input type="checkbox"/> aluminum hydroxide Enter a Value % Start Date TO End Date	lb/ton
		<input type="checkbox"/> antimony Enter a Value % Start Date TO End Date	ton/ton
		<input type="checkbox"/> asbestos Enter a Value % Start Date TO End Date	mg/cm2
			mg/cm3
			mg/m2
			mg/m3
			g/m2
			g/m3
			kg/m2
			kg/m3
			kg/l
			kg/kg
			kg/mt
<input type="checkbox"/>	Limits on Toxins: Red Lists		
<input checked="" type="checkbox"/>	Limits on Toxins: Chemical Family	<input type="checkbox"/> Aldehydes Enter a Value g/m2	mt/mt
		<input type="checkbox"/> alkylphenol ethoxylates Enter a Value g/m2	ppm
		<input type="checkbox"/> carbon monoxide Enter a Value g/m2	mol H+ / m2
		<input type="checkbox"/> cfc Enter a Value g/m2	mol H+ / ft2
		<input type="checkbox"/> halogenated organic solvents Enter a Value g/m2	mol H+ / ga
			mol H+ / ton

Figure 4: Data entry screen for Toxicity Media Pollutants. Data is for specific insulated metal panels.

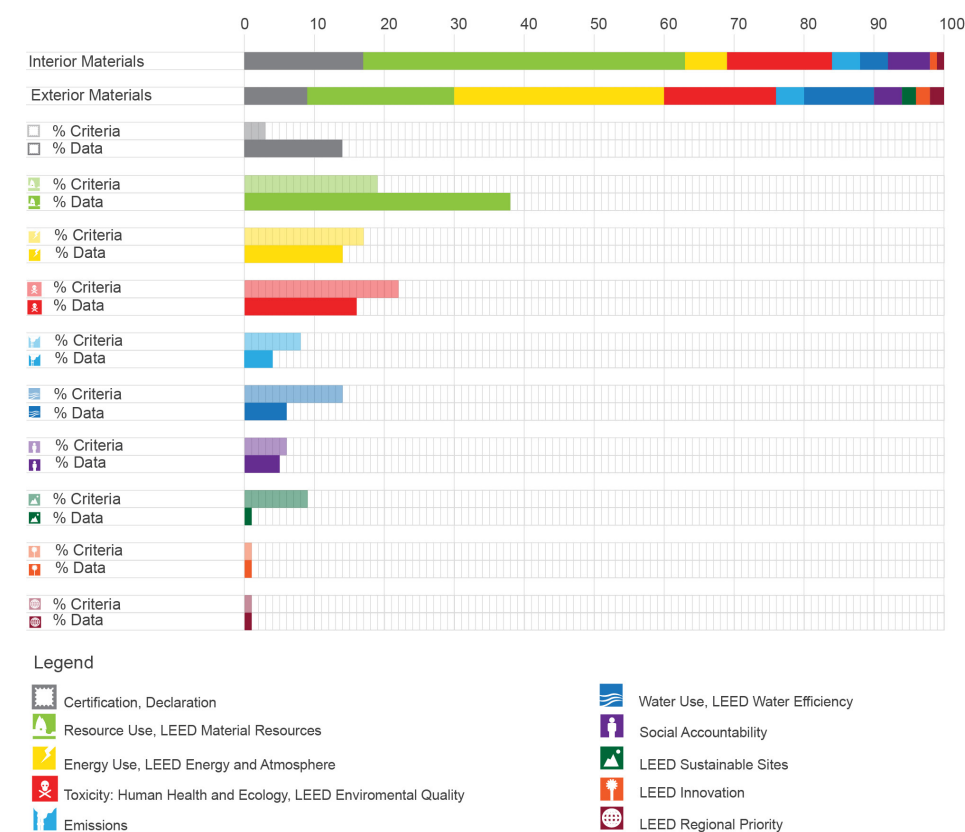
4.0 BIG DATA AND THE GREAT VOID

With more than 150 criteria focusing upon sustainability, the database represents the breadth of sustainability criteria that exist in the sector today (Figure 2). With so many possibilities, the model produces information at the scale of big data. Visualization of the initial dataset of 70 materials in tables demonstrates where manufacturers are reporting data across the sector, allowing comparison. This visualization reveals significant voids in information and emerging patterns of disclosure. For example, even though the initial dataset includes a range of manufacturers who are considered leaders in sustainability, no individual material presents data on more than 22 sustainability criteria, equivalent to 14 percent of possible criteria. That material is a specific type of insulating metal panels.

While manufacturers release data in efforts to increase transparency, there is still great hesitancy to reveal information on material makeup and processing. Under the shield of trade secrets, companies shroud toxic materials and processes that they are uninterested in revealing, leaving a void within the human health and toxicity impact category. Additional concerns now revolve around where liability resides with manufacturers' choices to disclose chemical makeup.

Looking across the data, it also seems that manufacturers predominantly focus upon what data their direct competitors reveal, and lack a broader understanding of the range of metrics that might be studied. For example, the production of glass is an energy intensive process, and so it is understandable that companies do not publish information on their energy usage. However, they are also silent on water use, social accountability, energy recovery, and regional priority for their resources.

Table 1: Distribution of both criteria and initial input data in percentages.



4.1 Environmental Impact Categories

The largest disclosure of data is in the resource use impact category for interior finishes. This is consistent with the fact that the public is most likely to be involved in material selection. They have the greatest awareness of this impact category; and are therefore most likely to ask for a manufacturer's metrics in this area and to respond to marketing on the subject. This impact category is also one of two places that LEED awards points for the selection of building materials (Table 1).

Most companies whose products have a biologically-based makeup focus their sustainability efforts in the resource use impact category; conversely, materials with significant petroleum-based content downplay that content by presenting a broader range of data across impact categories. This seems true of the plastics industry and may partially explain the breadth of data that the carpet industry publishes.

With regard to exterior materials, the greatest focus is upon sustainability through energy performance.

Human Health and Toxicity presents some of the oldest metrics, many of which are established through legislation. Taking Human Health and Toxicity together with LEED Environmental Quality, 22 percent of the criteria are dedicated to this environmental impact category – the greatest percentage among environmental impact categories. It is interesting to note Certifications, and Resource Use each hold a smaller percentage of criteria, but our analysis shows a larger percent of data falling within those criteria in comparison to Human Health and Toxicity. This is testament to their popularity.

Water is one of the most recently implemented impact categories, and has relatively few criteria. Across the initial dataset, the ceramic tile industry and the carpet industry provide the most data reporting on water. Social Accountability holds a relatively small percentage of criteria and data with most of the criteria being rooted in application of US legislation abroad (Table 1).

4.2 Visualization of the Initial Dataset and Disclosure

In Tables 2 and 3, visualization of the data for the seventy materials shows every sustainability attribute for each material and whether the criterion's value is null (blank) or whether data has been entered (colored block). Colored blocks organize according to: certification/ecolabel/declaration; environmental impact category across Life Cycle stages; and LEED categories.

Analysis of the initial dataset indicates significant differences in disclosure across individual industries. For example, the carpet industry shows consistency, reporting data across nearly all impact categories. In contrast, wallcovering and upholstery companies deliver almost no information on sustainability initiatives. One would expect that since both industries employ woven goods, they should publish similar data. This difference may be based on widely different supply chain management.

With regard to size, it seems that large manufacturers have the financial resources to test for a broad range of criteria, producing data across all sustainable impact categories. On the opposite end of the scale, a number of small companies embrace collecting data on sustainability as a way to differentiate themselves from larger firms. In a few cases the data reveals direct competition between firms that have nearly indistinguishable products.

Table 2: Visualization of input data for 26 exterior materials.

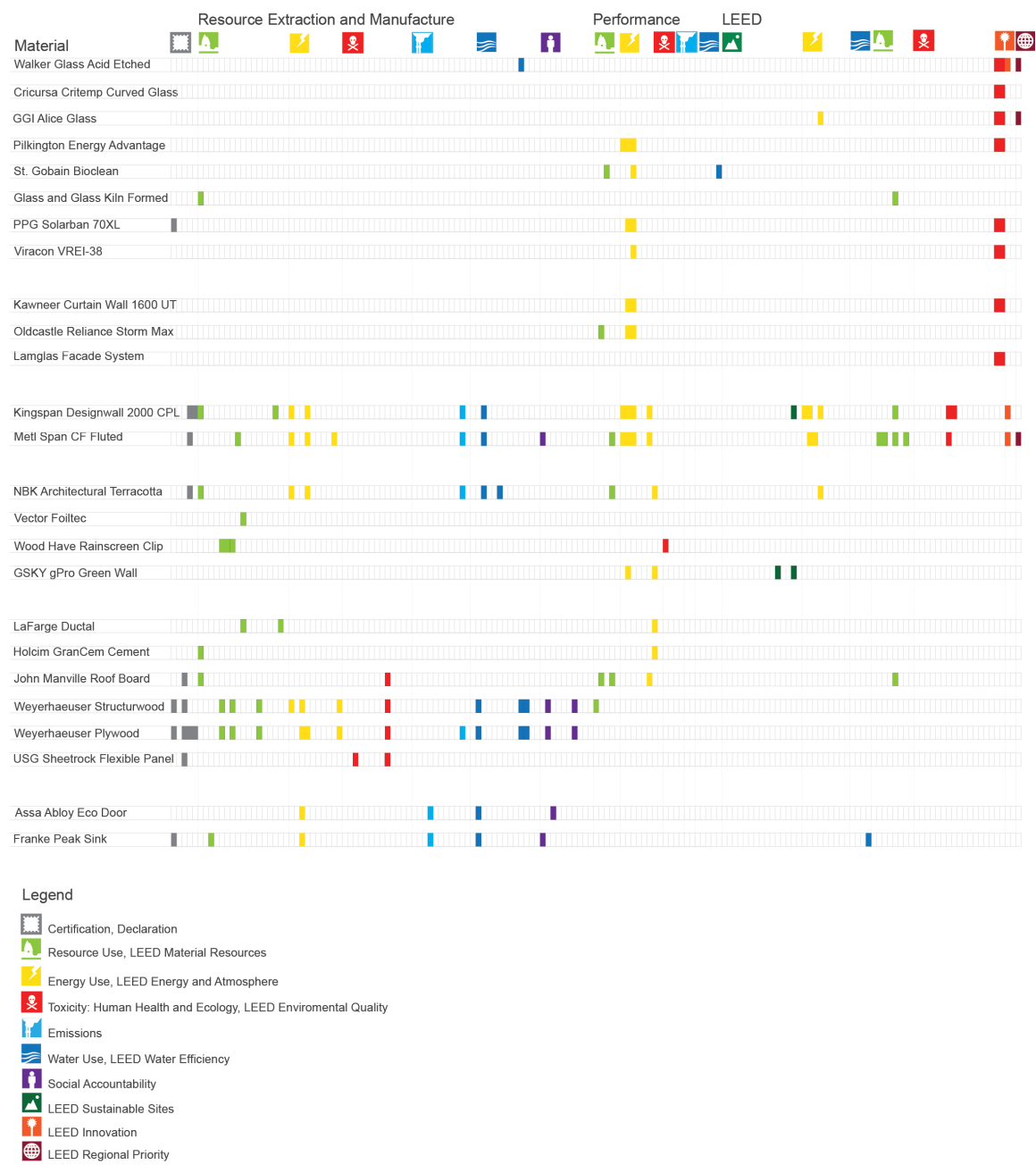
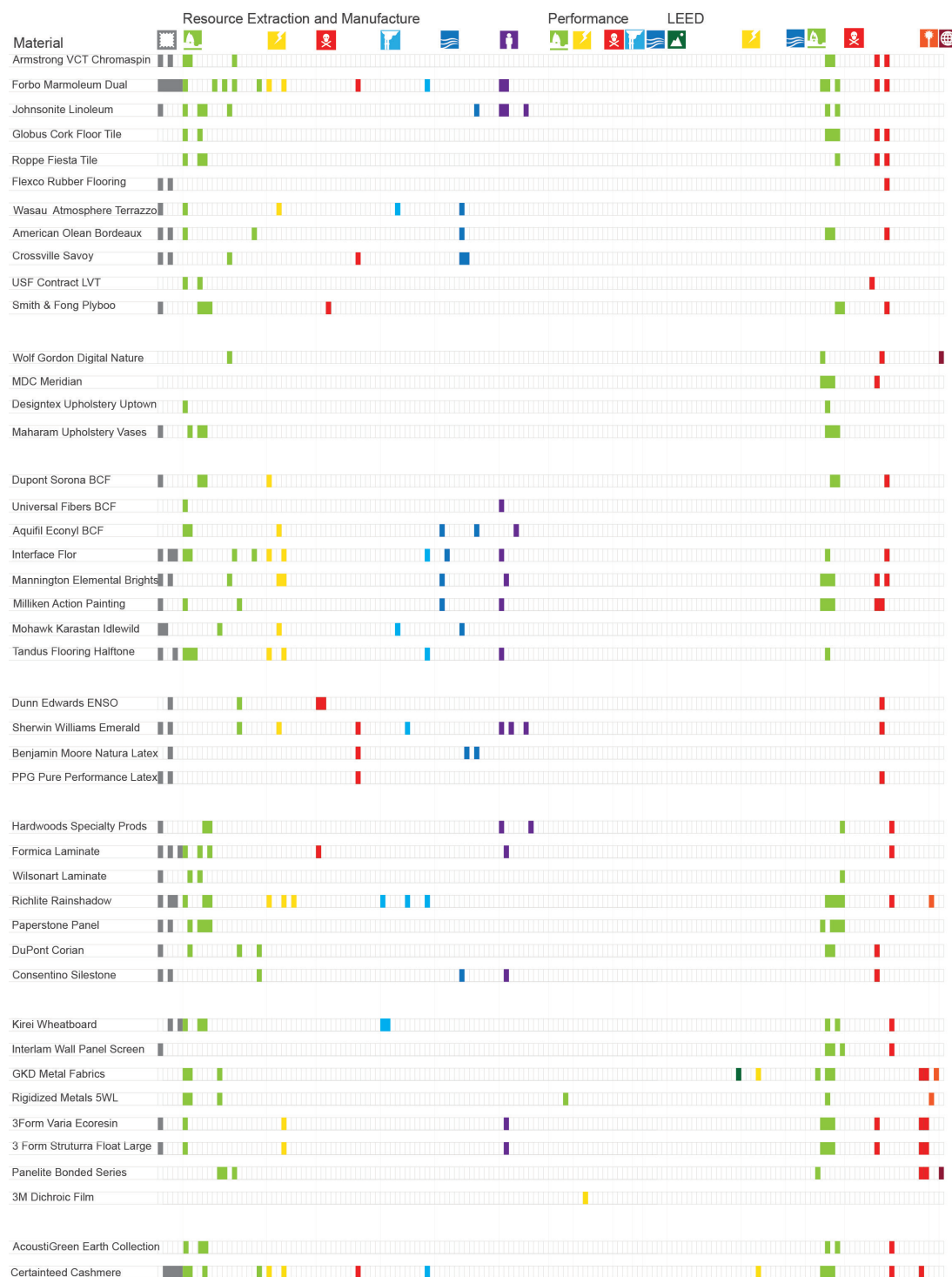


Table 3: Visualization of input data for 44 exterior materials.



5.0 CONCLUSION

This study establishes a database that includes the breadth of sustainability criteria across the building materials sector. Instead of simplifying information, we have created a dynamic network of data that provides a snapshot of the current landscape of sustainability criteria for building materials. To accomplish this, the team designed a simple data structure that accommodates the range of criteria used by manufacturers and material sustainability standards, from qualitative attributes to numerical metrics. Additionally, the design of the data structure enables categorization of these attributes across environmental impacts and lifecycle stages.

An initial attempt to compare materials across industries appears to reveal industries that are too specific; where variation in data reporting is too large; and that attempts to compare products across industries will be apples to oranges. Additionally, with so many sustainability attributes to evaluate, simultaneous consideration seems certain to result in confusion.

However, when we widen the frame and visualize the data across all the attributes, the voids become as important as the data itself. Industries are not disclosing different data, instead the data is episodic across the range of possible attributes, and the individual disclosures do not align. Once the voids become part of the data, then it is possible to compare products across industries. The simultaneous consideration of all the sustainability attributes does not cause confusion because the populated database results in hardly any information. Analysis reveals disclosure of data at several scales, and through discrete strategies: across individual environmental impacts; within specific industries; and at the scale of direct competition between corporations. As a result, visualization of the populated database accurately exhibits the atomized approach by which the sector discloses data across sustainability attributes today.

Acknowledgments

The development of the building materials database was funded by a grant awarded from the U.S. Economic Development awarded to Louisiana Tech University and managed by Dr. Dave Norris. Our interdisciplinary team drew from the fields of architecture, computer science, and graphic design. The team included: the author, as principal investigator; Dr. Sumeet Dua, Upchurch En-

dowed Professor of Computer Science and Cyber Engineering, College of Engineering and Science; Patrick Miller, Associate Professor and Coordinator Graphic Design, School of Design; and a total of six students who were enrolled in undergraduate and graduate programs in architecture, computer science, and graphic design. The team was assisted by Hannah Rae Roth, Lecturer, Washington University in St. Louis, and Kim Mitchell, of Sutton Mitchell Beebe and Babin in Shreveport, LA. The coordination and effort that all team members devoted to this project made its success.

The analysis of the initial eight material sustainability standards occurred through a study completed at Washington University in St. Louis in 2011. Principal Investigator: Charles McManis, Thomas and Karole Green Professor of Law, Washington University in St. Louis, Project Director: Hannah Rae Roth, Washington University in St. Louis. Other participants included: Dr. Charles Ebinger, Senior Fellow and Director, Brookings Institution; George Contreras, Associate Professor, American University; Liane Hancock, Assistant Professor, Louisiana Tech University; and a team of graduate and undergraduate research assistants. This research was funded by a joint grant from the Brookings Institution and Washington University in St. Louis.

REFERENCES

- [1] Rossi, M., Peele, C., and Thorpe, B., (2012). The Guide to Safer Chemicals. BizNGO/Clean Production Action, Retrieved from http://www.bizngo.org/static/ee_images/uploads/resources/guide_safer-chemicals_full.pdf.
- [2] Environmental Protection Agency, (2014). "ToxCast Chemical Data Challenges and Release", Retrieved from <http://www.epa.gov/comptox/challenges.html>.
- [3] Shelton Group, UL Environment, (2014). "Claiming Green", Retrieved from <http://environment.ul.com/wp-content/upload/2014/10/ULEClaimingGreenReport.pdf>.
- [4] The Institute for Market Transformation to Sustainability, (2015). List of SMaRT Certified Materials, Retrieved from <http://mts.sustainableproducts.com/SMaRT Certified.html>.
- [5] Cradle2Cradle, (2015). Product Registry, Retrieved from <http://www.c2ccertified.org/products/registry>.

[6] The Carpet and Rug Institute, (2015). NSF/ANSI 140 Standard Sustainable Product Platforms, Retrieved from <http://www.carpet-rug.org/Carpet-for-Business/Green-Building-and-The-Environment/NSF-ANSI-140-Standard/Sustainable-Carpet-Product-Platforms.aspx>.

[7] USGBC, (2015). LEED for New Construction and Major Renovations (V4), Retrived from <http://www.usgbc.org/credits/new-construction/v4>.

[8] Melton, P., (2013), "Whole-Building Life-Cycle Assessment: Taking the Measure of a Green Building," Environmental Building News, Retrieved from <http://www2.buildinggreen.com/article/whole-building-life-cycle-assessment-taking-measure-green-building>.

Kais Al-Rawi
Architectural Association

Dr. Antonieta Angulo
Ball State University

Dr. Pravin Bhiwapurkar
University of Cincinnati

Terri Boake
University of Waterloo

Dr. Mark Clayton
Texas A&M University

Heidi Creighton
BuroHappold Engineering

Diane Kaufman Fredette
Fredette Architects

PEER REVIEWERS

Daniel Faoro
Lawrence Technological University

David Green
Perkins+Will

Walter Grondzik
Ball State University

Mo Harmon
Synthesis Design + Architecture

Dr. Azza Kamal
University of Texas at San Antonio

Rashida Ng
Temple University

Edward Orlowski
Lawrence Technological University

Dr. Ash Ragheb
Lawrence Technological University

AUTHORS

01.



MICHAEL GIBSON

Michael Gibson is an Assistant Professor in the Department of Architecture at Kansas State University. Michael earned his M.Arch at Harvard University and has professional experience in architectural offices in Boston and Baltimore. Previously Michael taught at Ball State University. His research addresses thermal performance and energy issues in building envelopes and has involved advanced manufacturing, computer simulation, experimentation with full-scale prototypes, and collaborations with major industry partners.

02.



CHRISTOPHER BOON

Christopher Boon is a recent graduate of the M.Arch program at Portland State University. He was awarded the ARCC King Medal for Excellence in Architectural and Environmental Design Research for the research presented in this article. His Master's thesis focused on how architectural form contribute to the re-creation of riparian habitat on Portland's post-industrial waterfront. He is also a professional chef and artist that specializes in encaustic painting.

02.



COREY GRIFFIN

With graduate degrees in architecture and structural engineering, Corey Griffin is an Associate Professor in the School of Architecture at Portland State University. His research focuses on the intersections of structural systems and green buildings with an emphasis on integrated design, multi-performance structures, and building longevity. Professor Griffin is the director of BUILT – the Building Science Lab to Advance Teaching - as well as the interim director of the Green Building Research Lab at Portland State University.

02.



NICHOLAS PAPAETHIMIOU

Nicholas Papaefthimiou is an associate at ZGF Architects LLP and an adjunct faculty member at the University of Oregon. He leads research efforts within ZGF's Portland office and focuses on healthcare design. ZGF is a member of the Research-based Design Initiative at Portland State University, a partnership between the academy and practice focused on generating translational building science research.

02.



JONAH ROSS

Jonah Ross is an associate at ZGF Architects LLP. He is a 3D technical artist who focuses on rendering, architectural illustration, program and phasing animation, visualization, scripting, parametric modeling, iterative energy modeling, researching and developing Rhino/Grasshopper parametric models for form finding, design exploration, and analysis.

KIP STOREY

Kip Storey is a principal at ZGF Architects LLP and has 25 years of professional experience managing healthcare, corporate, and higher education projects in all phases of development. He has been responsible for project management, design feasibility studies, and extensive coordination with consultants, contractors, and clients. He has also played an integral role in multiple Integrated Project Delivery efforts for large-scale projects.



02.

MING TANG

Ming Tang is an Assistant Professor at the University of Cincinnati, a registered architect, and founding partner of TYA Design. He has won numerous design awards, including first place in d3 Natural System Competition, IAAC self-sufficient housing contest, and Chichen Itza lodge museum design competition. His research includes parametric design, digital fabrication, building information modeling, virtual reality, human-computer interaction (HCI), and performance-driven design. His book, *Parametric Building Design with Autodesk Maya* was published by Routledge in 2014.



03.

PRAVIN BHIWAPURKAR

Dr. Pravin Bhiwapurkar is as an Assistant Professor in the School of Architecture and Interior Design at the University of Cincinnati. His research and teaching interests are integrated design development, high performance buildings, environmental technologies in design, urban climate change and the built environment, climate responsive building design, net zero energy buildings, daylighting, social and health impacts of climate change, technology transfer and human-technology interaction.



04.

LIANE HANCOCK

Liane Hancock is an Assistant Professor of architecture at Louisiana Tech University, and serves as foundation coordinator for architecture within the School of Design. Her primary area of research is on materials, construction methods, and labor. For this project, she led a cross-disciplinary, inter-institutional effort to develop an online building materials database funded by a grant from the Federal Economic Development Administration Office of Innovation and Entrepreneurship. Liane holds degrees in architecture from MIT and Columbia University.



05.

MOHAWK windpower 

This piece is printed on Mohawk sustainable paper which is manufactured entirely with Green-e certificate wind-generated electricity.

Through its "Green Initiative" Program, Phase 3 Media offers recycled and windpowered paper stocks, recycles all of its own post-production waste, emails all client invoices, and uses environmentally friendly, non-toxic cleaning supplies, additionally Phase 3 Media donates 5% of all sales from its recycled product lines to Trees Atlanta.

PERKINS+WILL

© 2015 Perkins+Will All Rights Reserved

For more information, please send an email to pwresearch@perkinswill.com

